

RESTRICTED INVESTIGATION REPORT 1743R

CSIRO

INSTITUTE OF MINERALS, ENERGY AND CONSTRUCTION

DIVISION OF EXPLORATION GEOSCIENCE

**MAGNETIC PROPERTIES, MAGNETIC STRATIGRAPHY AND
MAGNETIC FABRIC OF ROCKS FROM THE NORTHERN
LEASES, THE REDAN/FARMCOTE AREA, THE RISE
AND SHINE AREA AND THE RUPEE TREND,
BROKEN HILL BLOCK**

**(AMIRA PROJECT 78/P96B: APPLICATIONS
OF ROCK MAGNETISM)**

D.A. Clark

P.O. Box 136

North Ryde, NSW

Australia 2113

JULY, 1988

DISTRIBUTION LIST

Copy No.

AMIRA

1-18

CSIRO Division of Exploration Geoscience

D.A. Clark

19

P.W. Schmidt

20

B.J.J. Embleton

21

A.A. Green

22

CSIRO IMEC Records

23

This is copy number of 23.

TABLE OF CONTENTS

| | Page |
|--|------|
| 1. Introduction | 1 |
| 2. Geology of the Broken Hill Area | 1 |
| 3. Magnetic Petrophysics of the Northern Leases Area | 3 |
| 4. Magnetic Petrophysics of the Redan/Farmcote Area | 6 |
| 5. Magnetic Petrophysics of the Rise and Shine Area | 8 |
| 6. Magnetic Petrophysics of the Rupee Trend Area | 17 |
| 7. Magnetic Stratigraphy | 21 |
| 8. Summary and Conclusions | 27 |
| 9. Acknowledgements | 30 |
| 10. References | 30 |

LIST OF FIGURES

- Fig. 1. Geology and sampling localities in the Northern Leases.
- Fig. 2. Magnetic fabric of sites 1-4. Major susceptibility axes (magnetic lineations) are represented by squares, intermediate axes are represented by triangles (sometimes omitted for clarity) and minor susceptibility axes are represented by dots. Estimated schistosity planes, their corresponding poles (represented by asterisks), mesoscopic lineations and fold axis plunges are also indicated.
- Fig. 3. Magnetic fabric of sites 5-9. Symbols as for Fig.2.
- Fig. 4. Magnetic fabric of sites 10-18. Magnetic lineations from specimens with prolate susceptibility ellipsoids and magnetic foliations from specimens with oblate ellipsoids are plotted. Symbols as for Fig.2.
- Fig. 5. Magnetic fabric of site 19. Symbols as for Fig.2.
- Fig. 6. Magnetic fabric of site 20. Symbols as for Fig.2.
- Fig. 7. Magnetic fabric of site 21. Symbols as for Fig.2.
- Fig. 8. Magnetic fabric of all specimens from site 22. Symbols as for Fig.2.
- Fig. 9. Magnetic lineations of specimens with $L > 1.02$, magnetic foliation poles of specimens with $F > 1.02$ (site 22). Symbols as for Fig.2.
- Fig.10. Geology and sampling localities of the Rise and Shine area.
- Fig.11. Peppertree Prospect (Rise and Shine) - geology and magnetics.
- Fig.12. Magnetic fabric of the Peppertree Prospect DDH PT1 samples. Symbols as for Fig.2.
- Fig.13. Magnetic fabric of the Traverse IV samples. Symbols as for Fig.2.
- Fig.14. Magnetic fabric of the Traverse V samples. Symbols as for Fig.2.
- Fig.15. Magnetic fabric of the Traverse VI samples. Symbols as for Fig.2.
- Fig.16. Magnetic fabric of the Traverse VII samples. Symbols as for Fig.2.
- Fig.17. Simplified 1:25000 geology and sampling localities, northern Rupee Trend area (back pocket).
- Fig.18. Structural and stratigraphic interpretation, northern Rupee Trend area (back pocket).

- Fig.19. Magnetic profile, geology and susceptibility along Traverse VIII (10800N, Rupee grid).
- Fig.20. Magnetic fabric of sites 98-107 (Purnamoota Subgroup), Traverse VIII. Symbols as for Fig.2.
- Fig.21. Magnetic fabric of sites 108-117 (Sundown Group), Traverse VIII. Symbols as for Fig.2.
- Fig.22. Magnetic fabric of sites 118-130 (Broken Hill Group), Traverse VIII. Symbols as for Fig.2.
- Fig.23. Magnetic fabric of sites 131-135 (Cues Formation), Traverse VIII. Symbols as for Fig.2.
- Fig.24. Magnetic stratigraphy of the Rise and Shine and northern Rupee Trend areas.

LIST OF TABLES

- TABLE 1. SUSCEPTIBILITIES AND KOENIGSBERGER RATIOS OF NORTHERN LEASES SAMPLES
- TABLE 2. NRM VECTORS AND MAGNETIC FABRICS OF NORTHERN LEASES SAMPLES
- TABLE 3. BASIC MAGNETIC PROPERTIES OF REDAN AREA SAMPLES
- TABLE 4. SUSCEPTIBILITIES AND KOENIGSBERGER RATIOS OF TRAVERSE III AND DDH PT1 SAMPLES
- TABLE 5. MEAN NRM VECTORS OF TRAVERSE III AND DDH PT1 SAMPLES
- TABLE 6. SUSCEPTIBILITIES AND KOENIGSBERGER RATIOS OF TRAVERSE IV SAMPLES
- TABLE 7. MEAN NRM VECTORS OF TRAVERSE IV SAMPLES
- TABLE 8. SUSCEPTIBILITIES AND KOENIGSBERGER RATIOS OF TRAVERSE V SAMPLES
- TABLE 9. MEAN NRM VECTORS OF TRAVERSE V SAMPLES
- TABLE 10. SUSCEPTIBILITIES AND KOENIGSBERGER RATIOS OF TRAVERSE VI SAMPLES
- TABLE 11. MEAN NRM VECTORS OF TRAVERSE VI SAMPLES
- TABLE 12. SUSCEPTIBILITIES AND KOENIGSBERGER RATIOS OF TRAVERSE VII SAMPLES
- TABLE 13. MEAN NRM VECTORS OF TRAVERSE VII SAMPLES
- TABLE 14. SUSCEPTIBILITIES AND KOENIGSBERGER RATIOS OF TRAVERSE VIII SAMPLES
- TABLE 15. MEAN NRM VECTORS OF TRAVERSE VIII SAMPLES
- TABLE 16. SUSCEPTIBILITIES AND KOENIGSBERGER RATIOS OF TRAVERSE IX SAMPLES
- TABLE 17. MEAN NRM VECTORS OF TRAVERSE IX SAMPLES
- TABLE 18. SUSCEPTIBILITIES AND KOENIGSBERGER RATIOS FOR DDH NR1, DDH BMX1 AND DDH TH2 SAMPLES
- TABLE 19. MEAN NRM VECTORS OF DDH NR1, DDH BMX1 AND DDH TH2 SAMPLES

LIST OF APPENDICES

- APPENDIX I - SAMPLES COLLECTED FROM THE BROKEN HILL AREA
- APPENDIX II - STRATIGRAPHIC INDEX (ABRIDGED)
- APPENDIX III - LITHOLOGICAL/MINERALOGICAL INDEX

1. INTRODUCTION

The work described in this report was carried out as part of the AMIRA project 78/P96B (Applications of Rock Magnetism). The Rock Magnetism Group of the CSIRO Division of Exploration Geoscience has conducted three sampling programs in the Broken Hill area: a magnetic petrophysical study of the Redan/Farmcote area for North Broken Hill Ltd (July 1979); a magnetic fabric study in the Northern Leases, also for NBH Ltd (March 1981); and extensive sampling in the Rise and Shine area (Aberfoyle Ltd) and in the northern Rupee Trend area (Billiton Ltd), carried out in October 1985. Details of the samples collected for these studies are given in Appendix I. The stratigraphic units (with their mnemonic symbols) from which the samples have been collected are defined in Appendix II and an index of definitions and symbols for sampled rock types and some of their constituent minerals is given in Appendix III.

Most samples were collected from outcrops using a portable drill and were oriented using a sun compass as well as a magnetic compass. Some oriented drill core samples were also supplied by sponsors. Core samples were sliced into standard 25mm diameter x 22mm height cylinders for measurement of magnetic properties. Natural Remanent Magnetisations (NRMs) and susceptibility anisotropies were measured using the Digico-type fluxgate spinner magnetometer and anisotropy delineator, interfaced to an Olivetti PC, respectively.

2. GEOLOGY OF THE BROKEN HILL AREA

There is a voluminous literature on Broken Hill and only the briefest summary of the geology will be given here, together with citations of particularly pertinent references. The stratigraphy of the Willyama Supergroup has been described in detail by Stevens et al (1982) and Willis et al (1983). The geology of individual 1:25000 map sheet areas is discussed in articles in Stevens (1980) and a systematic description of the rock types characteristic of the Broken Hill Block is given by Stevens and Stroud (1983). An alternative interpretation of the quartzofeldspathic gneisses of the mine sequence as clastic sediments rather than metamorphosed acid volcanics has been published recently by Haydon and McConachy (1987) and Wright et al (1987). Marjoribanks et al (1980) described the complex structural and tectonic evolution of the Broken Hill region. Stevens (1986) has reviewed the post depositional history of the Willyama Supergroup and Harrison and McDougall (1981) have published an analysis of the prolonged thermal history of the region, based on Ar40/Ar39 age spectra.

Deposition of the Willyama Supergroup commenced in the Lower Proterozoic at about 1820 Ma. A thick marine (?) sequence of terrigenous and volcanic clastics with intercalated felsic and basic volcanics and occasional chemical sediments was metamorphosed to amphibolite-granulite facies and deformed twice at about 1660 Ma, in the Olarian Orogeny. A third

deformation, accompanied by retrograde metamorphism, occurred soon after. Retrograde schist zones formed before 1570 Ma and emplacement of Mundi Mundi type granites took place at about 1490 Ma. Uplift of the deeply buried (13-20 km) rocks to near surface levels between 1490 Ma and about 1100 Ma was followed by deposition of Adelaidean sediments. Intrusion of alkaline ultramafic plugs and dykes at 560 Ma was followed at 520 Ma by the thermal pulse and folding associated with the Delamerian Orogeny. Temperatures of the presently exposed rocks dropped below 100 C as late as 280 Ma.

The basal exposed unit in the Broken Hill Block consists of migmatites (the Clevedale Migmatite) and is overlain by feldspathic metasedimentary composite gneisses (Thorndale Composite Gneiss). The overlying Thackaringa Group comprises quartzofeldspathic gneisses and sodic plagioclase-quartz rocks. The overlying Broken Hill Group reflects a shift to well-bedded, predominantly pelitic metasediments and is subdivided into a basal metasedimentary unit (Allendale Metasediments), overlain by the Purnamoota Subgroup which contains basic gneiss, garnet-bearing quartzofeldspathic gneisses and "lode horizon" rocks as well as metasediments. The Broken Hill Group is in turn overlain by the predominantly pelitic metasediments of the Sundown Group in which basic and felsic gneisses are absent. The top exposed unit is the Paragon Group, which comprises carbonaceous pelitic and fine-grained psammitic metasediments.

Structural interpretation in the Broken Hill Block has always been very controversial, due to the great complexity which reflects the prolonged history of intense metamorphism and deformation. In this Report structure will be discussed in the context of the model developed by workers from Adelaide University (Laing et al, 1978; Marjoribanks et al, 1980). The first deformational event is interpreted to have been accompanied by syntectonic metamorphism to granulite facies and to have produced flat-lying gravity nappes. This event is believed to have inverted the Broken Hill orebody. The first deformation was accompanied by development of a high-grade schistosity (S1) which is generally parallel to bedding. A prominent lineation (L1) within S1 is defined by orientation of sillimanite and fibrolite in pelitic metasediments. The second generation deformation is also associated with high grade metamorphism and produced a prominent schistosity (S2) which is axial planar to F2 folds. In places a high grade mineral lineation within S2 can be observed that typically plunges to the southwest, parallel to adjacent F2 axes, although more complex relationships occur in one of the sampled areas, around the North mine. The major macroscopic structures of the Broken Hill mines area are interpreted to be second generation. The third generation schistosity (S3) is associated with retrograde metamorphism and is characteristically a vertical schistosity axial plane to moderately open F3 folds. Within retrograde schist zones there is a retrograde schistosity which has strike parallel to the zone boundaries. In the NE-trending set this schistosity is usually parallel to S3 in adjacent rocks. There is often a steeply

plunging lineation within retrograde schist zones.

3. MAGNETIC PETROPHYSICS OF THE NORTHERN LEASES AREA

Sampling localities within the Northern Leases area are shown in Fig.1. The aim of the original study of this area was to examine the correlation between magnetic fabric and geological structure in the relatively well-understood Northern Leases area and to evaluate the applicability of magnetic fabric studies as an aid to structural mapping in other parts of the Broken Hill Block where the structure is not so well known. The magnetic fabric study was reported by Clark (1981). Principles of the magnetic fabric method have been described by Clark and Embleton (1980), Clark (1981) and Clark et al (1987).

Susceptibilities and Koenigsberger ratios of the Northern Leases samples are given in Table 1 and the mean NRM vectors and magnetic fabric elements are listed in Table 2. Traverse I extended from the hinge of the Mine Antiform to the NW limb in Potosi Gneiss. Sites 1-4 are moderately magnetic with a mean susceptibility of 650 microgauss/Oersted and a vector mean NRM intensity of 1200 microgauss. The relatively high Koenigsberger ratio (3.2) suggests that remanence dominates the magnetisation of this magnetic portion of the Potosi Gneiss unit. However the NRM directions are quite scattered within and between sites and the effective remanence on a large scale (tens to hundreds of metres) may be greatly reduced by cancellation arising from near random scattering of remanence vectors. This conclusion is reinforced by the general observation in the Broken Hill Block that the form of most magnetic anomalies is consistent with magnetisation by induction and that dips interpreted assuming magnetisation parallel to the present field are consistent with mapped dips (McIntyre, 1979; Isles, 1983; Tucker, 1983) and by the fact that the extensive sampling around Broken Hill has failed to indicate any well-defined characteristic remanence directions.

The samples from sites 1-4 have a pronounced susceptibility anisotropy associated with a well-developed magnetic fabric. The susceptibility axes of specimens from sites 1-4 are plotted in Fig.2, together with mesoscopic structural elements. Minor susceptibility axes (magnetic foliation poles) cluster around the mean S2 pole, implying that the magnetic foliation, which reflects the preferred dimensional orientation of magnetite in these samples, corresponds to the S2 schistosity. Major susceptibility axes (magnetic lineations) are grouped around the local F2 fold axis.

The less magnetic Potosi Gneiss samples from sites 5-9 exhibit a streaking of magnetic foliation poles between the poles to the axial plane S2 schistosity and the bedding-parallel S1 schistosity (Fig.3). The magnetic lineations are again parallel to the F2 axis. The magnetic fabric of sites 5-9 has lower symmetry (monoclinic) than the simpler (orthorhombic) fabric of sites 1-4. This may reflect more intense development of S2 at sites 1-4 (where S1 was not observed) due to proximity to

the fold hinge. However it is also probably significant that the lower symmetry fabric corresponds to low susceptibilities which are influenced, or even dominated by, paramagnetism of silicate minerals such as biotite and garnet. The streaking of minor axes between the poles to the two schistosity may therefore reflect superimposition of an orthorhombic (S2,F2) magnetite fabric onto a paramagnetic fabric, which reflects preferred crystallographic orientation of Fe-bearing silicates. The symmetry of the paramagnetic fabric may be orthorhombic (S1,F2) or, more probably, monoclinic (S1-S2,F2), i.e. reflecting variable overprinting of S1 by S2. Thus, although the symmetry of the magnetic fabric of an individual specimen can be no lower than that of a triaxial ellipsoid (i.e. orthorhombic), more complex petrofabrics can be studied by examining the magnetic fabric of a group of specimens with varying properties. In the case of sites 1-9, the variable overprinting of S1 by S2 is apparent from Figs.2-3 and the approximate orientations of the schistosity poles can be estimated from the end points of the streaked distribution of minor susceptibility axes. The utility of the magnetic lineations for determining fold axes is also obvious.

The Lord's Hill Granite Gneiss is very weakly magnetic and has negligible remanence because the susceptibility is almost entirely due to paramagnetic silicate minerals, which carry no remanence. Because of the low susceptibility and the weak anisotropy of paramagnetic minerals, the measurements were affected by noise and the susceptibility axes are consequently somewhat scattered. However the overall pattern is very similar to that of Fig.3. The scatter of magnetic lineations is reduced if only specimens with prolate (lineation dominant) ellipsoids are considered. Minor susceptibility axes are streaked between the S1 and S2 poles, but the minor axes of specimens with oblate (foliation dominant) ellipsoids are mostly clustered around the S2 pole (see Fig.4). Paramagnetic and ferromagnetic fabrics of rocks have been discussed in detail by Rochette (1987).

Sites 1-18 lie within the structural subarea 3 of Laing et al (1978), for which F2 plunges NE parallel to L1. There is no visible L2 at sites 1-9, but L2 is observed to plunge SW, oblique to F2, around sites 10-18. Some of the scatter of susceptibility axes for sites 10-18 may reflect partial overprinting of lineations as well as foliations. There is an indication of streaking of magnetic lineations towards L2 for some of the less lineated specimens. The overall appearance of Figs.2-4 bears a striking resemblance to the structural element orientation diagrams shown for subarea 3 by Laing et al (1978).

Site 19 lies in a basic granulite unit of the Cues Formation on the SE limb of the Round Hill Synform, which is within subarea 5 of Laing et al (1978). In this subarea S2 poles cluster about an ESE direction with moderate inclination, S0/S1 poles are streaked along a girdle which dips steeply NE and F2 axes have shallow SW plunges, parallel to L2 but oblique to L1. The magnetic fabric elements for site 19 are shown in Fig.5. The magnetic lineations are clustered around the F2 fold axis at the

site. S2 was the only visible schistosity at site 19 but the magnetic foliation poles are streaked along a girdle, which corresponds to the mapped distribution of S1 poles in the subarea, even within samples. Thus the magnetic foliations reflect variable overprinting of S1 by S2, even though this was not apparent in the visible mesoscopic fabric. This is another illustration of the sensitivity of the magnetic fabric technique, where susceptibility anisotropy reflects petrofabrics which are too weakly developed to be readily observable. Again, the fold axis plunge could have been satisfactorily estimated from the magnetic lineations. The bulk susceptibility of the samples from site 19 is probably due to magnetite and paramagnetic silicates (hornblende and pyroxene) in about equal measures. The measured Koenigsberger ratio is very high and is probably due to lightning. This conclusion is supported by the great scatter in NRM directions of individual samples.

The psammopelitic metasediment samples from sites 20-21, within the Sundown Group, exhibit well-grouped minor susceptibility axes centered on the poles to S1 and S2, which are subparallel (Figs.6-7). These sites fall within subarea 6 of Laing et al (1978). There is no clearly defined magnetic lineation for these sites but the major susceptibility axes fall on a WNW-dipping girdle which conforms to the overall distribution of F2 axes in this subarea. The magnetic properties of these samples are dominated by paramagnetism.

The magnetic fabric elements of the retrograde schist samples from site 22 are shown in Figs.8-9. The samples are only weakly magnetic but the magnetic fabric is well-defined and easily measurable, reflecting the strong preferred orientation of paramagnetic micas. Site 22 lies within the Globe-Vauxhall Shear Zone, adjacent to subareas 5 and 7 of Laing et al (1978). The minor susceptibility axes, particularly those of specimens with pronounced foliation ($F > 1.02$), cluster around the pole to the visible S3 schistosity which is also parallel to the S3 developed within subarea 7. The magnetic lineations are tightly clustered about a steeply plunging mean direction which corresponds to the lineation parallel to steeply plunging intrafolial folds within retrograde schist zones (Marjoribanks et al, 1980). The interchange of the intermediate and major axes of some of the specimens (Fig.8) suggests overprinting of a subhorizontal lineation by the characteristic steep retrograde lineation. The most highly lineated specimens all have steeply plunging magnetic lineations, indicating full development of L3 (Fig.9).

The bif unit from the Parnell Formation which was sampled at site 23, SE of Imperial Ridge, lies within subarea 6 of Laing et al (1978). Within this zone F2 axes are streaked along a west-dipping girdle but mainly have shallow to moderate plunges to the WSW, parallel to L1-2. The sampled outcrop exhibited mesoscopic folding. Although the attitude of S0 (bedding) varied for one sample, the orientation of the magnetic foliation was consistent for all samples. The mean foliation pole is $\text{dec}=128, \text{inc}=+54$, which is parallel to the bedding pole of most samples and also to the majority of S0/S1 poles and to the well-grouped S2 poles of

subarea 6. It appears, somewhat surprisingly, that the magnetic fabric of these bif samples is not simply a textural anisotropy arising from concentration of magnetite into strongly magnetic bands, but reflects preferred dimensional orientation of individual magnetite grains as well. The measured anisotropy ($A=1.21$) is in fact much lower than that of most bifs which exhibit mainly textural anisotropy. The magnetic fabric of the site 23 samples appears to represent a foliation developed parallel to S1-2 which is often, but not always, parallel to bedding. There is also a well-developed magnetic lineation with shallow plunge to the WSW, parallel to the predominant fold axis direction.

Overall there is strikingly good agreement between the magnetic fabric data and the mapped structural elements throughout the Northern Leases area. Susceptibility anisotropy is confirmed as a sensitive indicator of preferred orientation of minerals which reflects the deformational history and provides a useful indication of structure. Overprinting of fabrics (e.g. an axial plane S2 superimposed on a bedding-parallel S1) is detectable by examining a suite of specimens. Fabrics of low symmetry can be studied, particularly when distinct paramagnetic and ferromagnetic fabrics are present within samples. The ease and rapidity of the magnetic fabric method makes it an attractive technique for structural analysis, particularly when complemented by mapping of mesoscopic fabrics and by microscopic examination. The magnetic property measurements confirm the conclusions of McIntyre (1979) and Isles (1983) that magnetic units in the Broken Hill Block rarely correspond exactly to mapped lithological units, but generally represent approximately conformable narrow bands, often of limited strike extent, within mapped units. This is exemplified by the Potosi Gneiss unit (sites 1-9), which is only magnetic near the fold hinge (sites 1-4).

4. MAGNETIC PETROPHYSICS OF THE REDAN/FARMCOTE AREA

A number of rock units associated with prominent magnetic anomalies in the Redan/Farmcote area were sampled in July 1979. The basic magnetic properties of these samples are given in Table 3. With the exception of site 24-5, the samples are thought to come from units which can be correlated with the Thackaringa Group elsewhere in the Broken Hill Block (Willis et al, 1983). The Thackaringa Group was formerly known as the Quartzofeldspathic rock suite or Suite 3 (Stevens et al, 1980), and consists mainly of quartz-feldspar-biotite gneisses and leucocratic plagioclase-quartz rocks plus metasedimentary composite gneisses. Amphibolites are locally abundant and quartz-magnetite and quartz-garnet rocks are common. In aeromagnetic maps the Thackaringa Group is characterised by high amplitude anomalies (often >500 nT) which are generally conformable and quite persistent along strike (strike lengths are typically 10-20 km).

The most magnetic rocks sampled in the Redan/Farmcote area

were the relatively unweathered quartz-magnetites at sites 24-3 and 24-7. As well as having high susceptibilities, reflecting the magnetite content, these samples exhibited very intense NRMs and exceptionally high Q values. These samples came from prominently exposed outcrops (e.g. The Tors) and could be expected to have suffered lightning strikes. The Koenigsberger ratios are unreasonably high for magnetite-bearing rocks and the intense NRMs are therefore attributed to lightning and are not considered representative of the magnetisation at depth.

The oxidised equivalents of the quartz-magnetite rocks (quartz-secondary iron oxide rocks and ferruginous gossans) are significantly less magnetic than the quartz-magnetites, but again have very high Q values which are probably not representative. AF and thermal demagnetisation of specimens from sites 24-1 and 24-3 shows that the remanence carried by these samples is essentially monocomponent. AF cleaning of specimens from site 24-7, on the other hand, removes a soft SW horizontal component, isolating a hard component which is directed W and shallow down. This direction is closer to the directions from the other qm/qf sites, but there is still a large scatter for the cleaned directions. No characteristic remanence component can be defined for these samples on the basis of demagnetisation data. Thus the possible existence of remanence which makes a substantial contribution to observed magnetic anomalies cannot be definitively addressed. There is an indication from the aeromagnetics over these localities that these qms and surrounding rocks tend to be associated with magnetic lows. Because of the high magnetite content of these rocks the negative anomalies are not simply due to a lower susceptibility than the surrounding rocks, suggesting that remanent magnetisation must be the cause.

The magnetite-bearing sodic plagioclase-quartz-K-feldspar rock ("magnetic Redan Gneiss") from site 24-4 has a moderate susceptibility and an intense NRM which corresponds to a Koenigsberger ratio of 75, which again is inordinately high for a remanence carried by magnetite. The NRM directions from individual specimens are quite scattered and the scatter is not reduced by AF or thermal demagnetisation. The form and amplitude of the aeromagnetic anomaly is consistent with magnetisation by induction. The intense remanence of the outcrop samples is again attributable to lightning. The sodic plagioclase-quartz-K-feldspar rock ("non-magnetic Redan Gneiss") from site 24-9 has very low susceptibility. The weak remanence is directed steep downward and is monocomponent, but is quite soft to AF cleaning and may not be representative.

The amphibolite unit sampled at site 24-5 is tentatively assigned to the Thorndale Composite Gneiss (tg). The only good exposure was of relatively weakly magnetic amphibolite outcropping parallel to poorly exposed magnetic amphibolite associated with a prominent ground and aeromagnetic anomaly. The measured Koenigsberger ratios are reasonable for a rock containing fine-grained magnetite and the NRM directions are quite stable to AF and thermal demagnetisation. The observed

anomaly is consistent with a normally polarised unit with a strong magnetisation about 10 times as strong as the sampled rocks. The steep upward directed remanence of these samples may also characterise the magnetisation of the parallel magnetic amphibolite unit.

The ferricretes sampled at sites 24-6 and 24-8 appear to be amenable to palaeomagnetic dating of the precipitation of iron oxides. The haematite ferricrete sampled at site 24-6 is weakly magnetic, but carries a very hard monocomponent remanence which is stable to thermal demagnetisation up to the Curie point of haematite (670 C), and which is unaffected by AF demagnetisation up to 1000 Oe. The mean direction corresponds to a palaeopole position of 70S,111E, which indicates an age of around 35 Ma. However the large error on the pole position, which is due to the small number of samples rather than an inherently large scatter, makes this estimate very uncertain. In fact, the meagre data from this site only constrain the palaeomagnetic age to be less than about 100 Ma.

The NRM directions of the maghaemite ferricrete samples from site 24-8 reflect a soft component which overprints a steep hard component of normal polarity (dec=0,inc=-75). The soft component, which has a shallow south direction, appears to be palaeomagnetic noise rather than a geologically meaningful component. The palaeopole corresponding to the AF cleaned direction is lat=60S, long=142E, which indicates an age of about 90 Ma for formation of the ferricrete. Again there is a large error on this estimate due to the limited number of samples, but the indications are very favorable that palaeomagnetism could be usefully applied to dating the event which produced precipitation of the iron oxides.

The susceptibility anisotropies of the samples from the Redan/Farmcote area are weak to moderate ($A = 1.01-1.21$), except for the quartz-magnetites from site 24-7 which have anisotropies of about 120% ($A = 2.2$). The magnetic foliations of the quartz-magnetites are invariably parallel to any visible banding and can be interpreted as representing bedding in samples where the mesoscopic fabric is indistinct. Magnetic lineations vary from very steeply plunging to shallow NW-plunging, and appear to represent axes of small scale folding within the quartz-magnetites. The majority of the Redan/Farmcote sites have magnetic foliations striking approximately NE and dipping steeply NW. NW plunges predominate for the magnetic lineations. An exception is provided by the maghaemite ferricrete from site 24-8, which has a horizontal magnetic foliation suggestive of layering, possibly produced by fluctuating ground water levels tending to concentrate the iron oxides into bands.

5. MAGNETIC PETROPHYSICS OF THE RISE AND SHINE AREA

A total of 73 oriented cores were collected along five traverses within the Rise and Shine EL 2071 (Aberfoyle) in October 1985. Aberfoyle also provided 18 drill core samples from

DDH PT1 (Peppertree Prospect), which were orientable from the drill hole survey and the visible schistosity. The simplified geology, based on Aberfoyle's mapping, and the locations of traverses III-VII and DDH PT1 are shown in Fig.10. Detailed geology, sample locations for traverse III and a ground magnetic profile across the Peppertree Prospect, adjacent to DDH PT1 are shown in Fig.11.

There is a fundamental problem of structural and stratigraphic interpretation for the Rise and Shine area, which lies within the western part of the Stephens Creek 1:25000 sheet. The geology of the Stephens Creek map sheet area has been described by Stroud (1978,1980). Within the Rise and Shine area two sequences containing lode horizon rocks, hereafter called the Eastern Lode and Western Lode, lying to the west of the Stephens Creek Granite Gneiss (Thackaringa Group) and separated by a thick monotonous sequence of metasediments, are recognised. The Eastern and Western Lodes have been interpreted by the NSW Geological Survey to represent the Parnell Formation and Hores Gneiss respectively, separated by Freyers Metasediments. The entire sequence is thus considered to consist of Broken Hill Group rocks, younging to the west. Aberfoyle geologists, on the other hand, have interpreted upper lode horizons of both Eastern and Western Lodes to represent Hores Gneiss, separated by Sundown Group metasediments which form the core of a major synform. On this interpretation the younging direction is eastwards for the Western Lode.

One problem for the Aberfoyle interpretation is the rarity of quartz-feldspar-biotite-garnet ("Potosi") gneiss in the Eastern Lode. This rock type is generally characteristic of the Hores Gneiss and is abundant in the Western Lode, near the interpreted top of the Broken Hill Group. The absence of substantial units of Potosi Gneiss from the Eastern Lode may possibly be due to an interpreted shear, between the Sundown Group and the Broken Hill Group of the Eastern Lode, which is inferred to have removed the uppermost Hores Gneiss and the calc-silicate ellipsoid-bearing lowermost horizon of the Sundown Group. In support of the assignment of the thick metasedimentary sequence to the Sundown Group, the aeromagnetic signatures of the rocks resemble more closely anomalies associated with the Sundown Group elsewhere in the Broken Hill Block than the generally very subdued response over Freyers Metasediments.

Further support for the Aberfoyle model is provided by detailed mapping which reveals that within both the Eastern and Western Lodes the lode horizon rocks actually occur within two parallel stratigraphic intervals which can be interpreted as Hores Gneiss and Parnell Formation respectively. The structure and stratigraphy of the Rise and Shine area will hereafter be discussed on the basis of the Aberfoyle interpretation (the Synclinal Structure model). It should be borne in mind, however, that this interpretation is tentative and the alternative model cannot be ruled out on the basis of the available information.

A major aeromagnetic feature is associated with the metasedimentary sequence (interpreted Sundown Group) between the Western and Eastern Lodes. This feature corresponds to anomaly PE of Isles (1983) and anomaly A of McIntyre (1979). One aim of the current study was to determine if the magnetic rock types, and hence the noisy magnetic signatures, extended from the Sundown Group into the uppermost Broken Hill Group of the Western Lode. The anomaly extends parallel to the NNE general geological strike direction for a distance of 15 km and is consistent with a parallel-sided source dipping 70W. This requires the inferred syncline to be isoclinal with a west-dipping axial plane.

The susceptibilities and Koenigsberger ratios of the traverse III and DDH PT1 samples are given in Table 4 and the NRM vectors are listed in Table 5. This traverse and drill hole covered most of the Broken Hill Group sequence that is interpreted to be present within the Eastern Succession. The metasediments sampled at the surface are all weakly magnetic and carry negligible remanence. The majority of the subsurface samples are also weakly magnetic, but two samples (FSMg from 120 m and FSE from 250 m) have susceptibilities greater than 0.0002 G/Oe.

The ground magnetic profile also indicates that magnetic units are absent within and immediately adjacent to the lode horizon, and for at least 300 m to the west. A broad positive anomaly, with superimposed narrow spikes, flanked to the (grid) east by a smaller low, is located to the east of the lode horizon, mainly beyond the zone intersected by the drill hole and lying largely over an area of poor outcrop. The total amplitude of the main broad anomaly is about 75 nT and its full-width at half-maximum is approximately 150 m (see Fig.11). It should be noted that a linear regional anomaly has been removed from the raw ground magnetic data before plotting in Fig.11. Because of the smooth nature of the magnetic field either side of the magnetic horizon, estimation of the base level and regional trend is quite unambiguous. This anomaly is also reflected in the detailed aeromagnetic survey of the area, which shows a coincident 75 nT anomaly with a width of about 170 m and a similar linear regional trend.

The anomaly over the Peppertree Prospect is a relatively minor feature, representing a magnetic interval of limited strike extent within the lower half of the Broken Hill Group of the Eastern Lode, compared to the major broad (800 m), high amplitude (up to 1500 nT) and continuous (strike extent 15 km) anomaly associated with the Sundown Group, which was discussed above. The form of the Peppertree Prospect anomaly is consistent with a tabular body, magnetised parallel to the present field, dipping very steeply to the NW (note the obliquity of grid and magnetic north in Fig.11).

The magnetic properties of the DDH PT1 samples indicate that the top of the magnetic zone was penetrated by the drill hole but that the zone is very inhomogeneous and the magnetic

material is confined to thin bands separated by non-magnetic rocks. No magnetic material was found in the surface traverse. This might indicate that weathering has destroyed the magnetic minerals, but the paucity of outcrop within the magnetic zone and the distribution of magnetic material as thin horizons could also explain the apparent absence of magnetic rocks at the surface as simply due to sampling problems. Magnetic rocks have been found at the surface elsewhere in the Rise and Shine area and in the northern Rupee Trend area (see the next section) and it has been concluded on the basis of extensive sampling in the Broken Hill Block that if outcrop is present beneath short wavelength airborne and ground magnetic response, then fragments of outcrop will be magnetic at the surface, and that deep magnetic weathering is not prevalent (Tucker, 1983). Thus it appears from the surface sampling along traverse III that magnetic rocks are genuinely scarce, even within the general magnetic interval, implying that magnetite distribution is restricted to very thin horizons, which may also be laterally very discontinuous.

Sites 39 and 40 are respectively within amphibolite and bif units that are adjacent to the second, stratigraphically lower, lode horizon of the Eastern Lode, which lies south of DDH PT1. It is apparent from the aeromagnetic map that the 50 nT double-peaked anomaly associated with this magnetic interval is along strike from the ground magnetic anomaly of Fig. 11. The sampled garnet amphibolite is moderately magnetic, with a susceptibility of 0.00073 G/Oe which is significantly above the background value for the metasedimentary rocks and a substantial remanence which corresponds to a Koenigsberger ratio of 1.2. However the remanence, if representative, is directed subparallel to the strike and would not greatly enhance the effective magnetisation of the unit. The bif unit is strongly magnetic, with a susceptibility of 0.031 G/Oe and a Q value of almost 2, but is very thin and is therefore associated with a strong ground magnetic anomaly which drops off rapidly with height (as $1/h$ if the unit has great strike length and depth extent, and more rapidly otherwise). The NRM of the bif is directed SW horizontal, i.e. along strike, and would contribute very little to the magnetic response.

The aeromagnetic anomaly associated with the narrow stratigraphic interval containing the lower lode horizon (Parnell Formation?) probably arises from the generally elevated magnetite content of the rocks stratigraphically close to, and along strike from, the chemical sediments (bif and lode horizon rocks). The bif unit alone is incapable of producing the total amplitude of the anomaly which in any case is double-peaked, indicating that there are two main magnetic horizons within the magnetic zone. The ground magnetic anomaly adjacent to DDH PT1 (Fig. 11) shows that the magnetic zone is in fact even more complex and consists of many thin magnetic horizons.

Of the 7 surface sites and 12 subsurface samples collected from the magnetic zone only sites 39 and 40 and DDH PT1 samples 120 m, 200 m and 260 m were significantly more magnetic than the background. The ground and aeromagnetic anomalies indicate that

the magnetic zone is about 200 m wide and has an average magnetisation of about 50 microgauss, which corresponds to an effective susceptibility of about 90 microgauss/Oersted. This susceptibility is much lower than that of the more magnetic samples and confirms that the broad anomaly arises from many thin, closely spaced, magnetic layers within a much greater volume of weakly-magnetic material.

The susceptibility contrast between the magnetic and non-magnetic zones estimated from the drill core samples is 50 microgauss/Oersted. If the site 39 amphibolite is included as representative of the magnetic zone the calculated susceptibility contrast is 100 microgauss/Oersted (0.0001 G/Oe or 0.0013 SI). It is appropriate to include in the analysis the surface samples which come from the magnetic zone adjacent to DDH PT1, assuming that magnetic weathering is minimal. When this is done the calculated susceptibility contrast is 75 microgauss/Oersted. It is incorrect to include the bif unit in the calculated susceptibility of the magnetic zone without weighting against its high contribution, because of the thinness of this unit. The bif was in fact especially sought out for sampling and a genuinely random sampling scheme would probably have missed it. Overall the inferred susceptibility of the magnetic zone conforms quite well to the average value determined from the sampling.

The magnetic fabric of the DDH PT1 samples is shown in Fig.12. The magnetic fabric of the surface samples along Traverse III is similar, but the axes are somewhat more scattered. The minimum susceptibility axes mainly group about a NW-SE subhorizontal axis but are somewhat streaked along a NE-dipping girdle. From the distribution of schistosity poles, which are also plotted in Fig.12, it is apparent that the magnetic foliation poles (minimum axes) correspond closely in their distribution to the mapped S0 and S2 poles. The streaked distribution of minimum axes arises partly from variation in attitude of bedding and axial plane schistosity and partly from variable overprinting of bedding-parallel S1 by S2. Some of the elongation of the magnetic foliation poles along the girdle may also reflect partial overprinting by an S3 schistosity, which is well-developed within the NE-trending retrograde schist zone, as some of the samples are clearly retrogressed.

The magnetic lineations (maximum susceptibility axes) are somewhat scattered, but tend to cluster about a NE down mean direction. By analogy with the Northern Leases area, and many other deformed metamorphic terranes for which the magnetic fabric has been studied, the distribution of magnetic lineations indicates predominantly NE-plunging fold axes in this area. This is consistent with the mesoscopic F2 fold axes that have been mapped in the Peppertree Prospect (see Fig.12) and with NE-plunging structures which lie to the NE of the traverse. Some of the scatter in the susceptibility axes may reflect refolding of F2 structures by F3 folding as a SW-plunging F3 fold has been mapped adjacent to DDH PT1.

The magnetic fabric of the magnetic amphibolite unit at site 39 exhibits some streaking of minimum axes between E and SE shallow down directions. The foliation poles lie within the girdle containing poles to bedding and S2 schistosity in nearby units. This girdle dips shallowly to the NE, orthogonal to the inferred axis of folding, which therefore plunges steeply SW. The magnetic lineations are well-grouped about this F2 fold axis. Again the local structure is well-defined by the magnetic fabric. The magnetic foliation poles of the bif unit at site 40 are clustered close to the bedding pole as expected for a banded rock with textural anisotropy. The magnetic lineations are also well-grouped about a SW subhorizontal direction, which suggests a locally horizontal fold axis.

Traverse IV is interpreted to extend from the upper Broken Hill Group of the Western Lode into the highly magnetic zone of the Sundown Group. This area was sampled in order to ascertain whether the magnetic rocks were restricted to the Sundown Group or whether the uppermost Broken Hill Group was also magnetic. The susceptibilities and Koenigsberger ratios of the Traverse IV sites are given in Table 6 and the NRM vectors are listed in Table 7. Site 41 was at the westernmost end of this traverse and was found to lie within a very weakly magnetic leucocratic quartzofeldspathic gneiss which is interpreted to belong to the Hores Gneiss. Proceeding eastwards, samples from sites 42-44 were relatively strongly magnetic and consisted of metasedimentary composite gneiss, and two amphibolite units respectively. Continuing up the succession the rest of the samples were weakly magnetic, including the amphibolites at the top of the Hores Gneiss and pelitic/psammopelitic metasediments of the Sundown Group.

Although Traverse IV extended well into the general zone of noisy high amplitude aeromagnetic anomalies the samples from the eastern end of the traverse are clearly not representative of the rocks which are producing the anomalies. There is evidence from the stacked profiles that the major magnetic sources within the Sundown Group lie immediately to the east of Traverse IV, in an area of poor outcrop. There is a subsidiary, but nevertheless substantial, anomaly with an amplitude of 250 nT associated with the sampled magnetic zone within the upper Broken Hill Group. Thus the eastern end of traverse IV probably lies between two magnetic zones: the first within the upper Hores Gneiss and the second, major, one stratigraphically somewhat above the basal Sundown Group.

The thickness of the Hores Gneiss magnetic zone is estimated from the sampling to be about 40 m. The broad magnetic zone within the Sundown Group is about 500 m wide overall, but is revealed by the aeromagnetics to be a complex zone consisting generally of two parallel magnetic horizons, which persist over strike lengths of several hundred metres (up to about 2 km), then die out, to be replaced by other magnetic horizons at slightly different stratigraphic levels. This behaviour is quite typical of curvilinear anomalies in the Broken Hill Block, which are

generally found to be stratabound but do not consistently coincide with particular lithological units or stratigraphic horizons (McIntyre, 1979; Isles, 1983). Tucker (1983) states that many individual magnetic sources in the Willyama Supergroup, particularly in the Thackaringa and Broken Hill Groups, appear to approximate ellipsoids of dimensional ratios very roughly equal to 1:10:100 (stratigraphic thickness, dip extent, strike extent respectively). The geometry of sources within the Rise and Shine area may be, at least qualitatively, similar.

The magnetic fabric of the Traverse IV samples is shown in Fig. 13, where maximum and minimum susceptibility axes, calculated from the sample mean susceptibility tensors, have been plotted. The magnetic foliation poles tend to group close to, but consistently to one side of, the pole to the steep NW-dipping bedding plane. There is also some streaking of minimum axes along a NE-dipping girdle, suggesting overprinting of bedding-parallel S1 by S2. The orientation of this girdle indicates folding about predominantly SW-plunging axes in this area, if the above interpretation of the girdle distribution of minimum axes is correct. There is no consistent grouping of magnetic lineations. The maximum susceptibility axes have a girdle distribution, normal to the main group of minimum axes and the general bedding pole. It follows from the orthogonality of susceptibility axes and the overall geometry of Fig. 13, that those samples which appear to have strongly overprinted schistosity, as indicated by minimum axes displaced along the NE-dipping girdle away from the bedding pole, also have magnetic lineations in the SW down octant, whereas samples with bedding-parallel magnetic foliations tend to have broadly north-plunging magnetic lineations. Thus the magnetic fabrics which most clearly reflect folding, by indicating overprinting of bedding-parallel fabric by axial plane schistosity, suggest a preponderance of SW-plunging local fold axes.

Examination of the magnetic fabrics of individual specimens from Traverse IV samples and subdivision of the samples on the basis of lithology and bulk susceptibility augments somewhat the interpretable information on petrofabric. The ferromagnetic fabric of the strongest samples is indistinguishable from the purely paramagnetic fabric of the very weak leucocratic gneisses and the hybrid fabric of Broken Hill Group rocks of intermediate susceptibility, indicating that the symmetry of the total (ferromagnetic plus paramagnetic) magnetic fabric of the Broken Hill Group samples is essentially axially symmetric, with foliation pole close to the bedding pole and an almost uniform scatter of lineations along the orthogonal girdle. The Sundown Group samples, on the other hand, exhibit magnetic fabrics of lower symmetry, with a girdle distribution of foliation poles and predominantly SW down lineations. Thus the indication from magnetic fabric of SW-plunging fold axes is confined to the Sundown Group samples.

Traverse V started close to the base of the Broken Hill Group of the Western Lode and finished within the Hores Gneiss,

but did not reach the top of the Broken Hill Group. The susceptibilities and Koenigsberger ratios of the Traverse V samples are given in Table 8 and the NRM vectors are given in Table 9. The samples are all quite weakly magnetic, except for site 61, which lies within an intrusive granite and which has a slightly elevated susceptibility and a relatively intense remanence and which appears to be associated with a 25 nT anomaly on one flight line. Other prominent anomalies are associated with Broken Hill Group rocks which are stratigraphically equivalent to the sampling sites but these anomalies are very discontinuous, usually being confined to one (200 m spaced) line but which sometimes appear to recur along strike, close to the same stratigraphic position, after dropping out for several hundred metres. The traverse stopped just short of the main magnetic zone, associated with the Sundown Group, which is generally poorly exposed compared to the Broken Hill Group in the Rise and Shine area.

The magnetic fabric of the Traverse V samples is shown in Fig.14. The minimum susceptibility axes tend to cluster about a SE direction with very shallow inclination, but are significantly streaked along a subhorizontal girdle. Magnetic lineations tend to plunge very steeply or to the SW. At the western end of the traverse steep lineations predominate whereas around the central portion and towards the eastern end SW-plunging lineations are more common. Around the central and eastern portions of the traverse mapped parasitic folds are generally observed to be SW-plunging and bedding and S2 schistosity poles generally lie in the SE quadrant of a subhorizontal girdle. The overall disposition of mapped structures indicates some structural complexity in this area.

The aeromagnetic signatures, which show apparent truncation of individual magnetic horizons and sharp changes in trend, also suggest refolding of the steeply dipping units about steeply plunging axes. However the apparent continuity along strike of the lode horizon and amphibolite units which intersect the western half of Traverse V appears to rule out the large scale sinistral folding about a steep axis which is apparently indicated by the magnetic anomaly pattern. Thus the magnetic horizon near Traverse V is probably discordant and may indicate facies variation rather than a major structure.

The magnetic fabric is interpreted to indicate subvertical fold axes in the west and SW-plunging and steeply plunging axes, possibly of different generations, in the central and eastern parts of Traverse V. The scale of this folding is probably quite small. The granite from site 61 exhibits a well-defined sub-vertical lineation with magnetic foliation poles randomly scattered in the horizontal plane. This fabric shows no sign of the axial plane schistosity and is therefore post-deformational. The magnetic lineation is interpreted to represent a vertical flow direction during emplacement.

Traverse VI lies to the south of Traverse V and extends

from the upper Broken Hill Group, stratigraphically equivalent to the eastern end of Traverse V, into the lowermost Sundown Group. The Hores Gneiss contains a tourmaline schist horizon in this area. The susceptibilities and Koenigsberger ratios of the Traverse VI samples are given in Table 10 and the NRM vectors are listed in Table 11.

None of the samples is strongly magnetic, even though the traverse extends well into the magnetic zone of the Sundown Group. The difficulty in finding magnetic rocks again suggests that the magnetic material comprises only a very minor proportion of the stratigraphy. The subsidiary magnetic anomaly (within the Broken Hill Group of the Western Lode) at this locality lies near site 80 and appears to be associated with the lowermost Potosi Gneiss unit, unlike Traverse IV, where the magnetic horizon is stratigraphically above the Potosi Gneiss. This confirms that the upper Broken Hill Group anomaly is not strictly conformable.

The magnetic fabric of the Traverse VI samples is depicted in Fig.15. Minimum susceptibility axes are shallow and are concentrated in the SE quadrant, with some streaking of axes within a subhorizontal girdle. Thus the most characteristic orientation of magnetic foliation at this locality, as throughout the Rise and Shine area, is subvertical with NE strike. The maximum susceptibility axes tend to plunge steeply, generally to the west. The magnetic fabric again suggests that the local fold axes are usually steep.

Traverse VII lies within the northern part of the Rise and Shine EL and extends from the lower lode horizon (Parnell Formation?) of the Western Lode through a thick sequence of metasediments, interpreted as Freyers Metasediments, but does not reach the upper Broken Hill Group and Sundown Group magnetic zones, because of the lack of outcrop. Susceptibilities and Koenigsberger ratios are given in Table 12 and the NRM vectors are listed in Table 13. None of the samples are strongly magnetic, which is to be expected since the traverse lies within a magnetically quiet zone. The susceptibilities of the metasediments are very consistent and average 27 microgauss/Oersted. Q values are generally low, reflecting the near absence of ferromagnetic minerals from these rocks.

To the south of Traverse VII the upper Broken Hill Group anomaly appears to be associated with the major mapped Potosi Gneiss unit and the immediately overlying garnetiferous pelitic/psammopelitic unit, whilst the amphibolites in the upper Hores Gneiss appear to be non-magnetic. Again the magnetic horizon of the upper Broken Hill Group is stratigraphically somewhat displaced with respect to the central part (Traverse IV) and southern part (Traverse VI) of the EL.

The general geological strike swings around from the NE direction, which characterises most of the Rise and Shine area, towards the east in the northeasternmost part of the EL.

This change in trend is also apparent from the aeromagnetics. Considerable local variation of bedding attitude and mesoscopic fabric is observed within the Freyers Metasediments towards the eastern end of Traverse VII. The magnetic fabric of the Traverse VII samples is shown in Fig.16. Minimum susceptibility axes are generally subhorizontal, usually with NW declination, but there is wide dispersion of foliation poles within a horizontal girdle. Magnetic lineations are NE plunging at the western end of the traverse, close to the lode horizon, but are subvertical elsewhere, except for sites 92 and 95 which have NW-plunging lineations. The magnetic fabric again appears to reflect overprinting of schistosity and local folding about variable, usually steep axes.

6. MAGNETIC PETROPHYSICS OF THE RUPEE TREND AREA

A total of 46 oriented surface samples were collected along two traverses within the northern part of Billiton's Rupee Trend EL, which lies mostly within the western half of the Mt Gipps 1:25000 map sheet and extends onto the Pinnacles 1:25000 sheet. Billiton also supplied 12 orientable drill core samples from three diamond drill holes within the Rupee Trend. Simplified geology and structural/stratigraphic interpretation maps (based on the NSW Mines Department Mt Gipps 1:25000 sheet), with the sampling localities plotted, are in the back pocket (Fig.17 and Fig.18 respectively).

Traverse VIII starts in the lower Broken Hill Group, on the western limb of the Rupee Antiform, and extends across the Antiform, through the Sundown Group, back into the Broken Hill Group and continues into the underlying Thackaringa Group. A geological cross-section and the ground magnetic profile along 10800N (Rupee Grid), which is close to Traverse VIII, are shown in Fig.17, together with the measured susceptibilities of the Traverse VIII samples projected onto 10800N. The susceptibilities and Koenigsberger ratios of the Traverse VIII samples are given in Table 14 and the NRM vectors are listed in Table 15.

Strongly magnetic samples are confined to the Sundown Group and the Cues Formation of the Thackaringa Group, which both correspond to magnetic zones delineated by the ground magnetics. Within the relatively magnetically quiet Broken Hill Group, the samples were weakly to very weakly magnetic. A relationship between susceptibility and lithology, consistent with what is observed in the other areas discussed in this Report, was found within the magnetically quiet zones, from which magnetite is essentially absent. Leucocratic gneisses invariably have very low susceptibilities (usually 3-6 microgauss/Oersted), whereas amphibolites are consistently more magnetic (with susceptibilities generally in the range 60-120 microgauss/Oersted). Metasediments and non-leucocratic quartzofeldspathic gneisses have susceptibilities which are intermediate (commonly 20-40 microgauss/Oersted). These systematic differences can be attributed to the paramagnetic susceptibilities of the constituent minerals. In the leucocratic

phases the susceptibility of the minor component of Fe-bearing silicates is diluted, and partially cancelled, by the diamagnetism (very weak negative susceptibility) of the quartz and feldspars which make up most of the rock. On the other hand the amphibolites consist largely of mafic minerals (such as amphiboles, pyroxenes, garnet etc.) which have a relatively large paramagnetic susceptibility because of their iron content. The metasediments and quartzofeldspathic gneisses have lower mafic contents than the amphibolites and consequently have lower susceptibilities. Within the non-magnetite-bearing metasediments the pelites tend to have slightly higher susceptibilities than the psammites, because of their higher paramagnetic Fe contents.

Although the Sundown Group is associated with a prominent broad ground magnetic anomaly of amplitude 800 nT, only two of the ten sites within the Sundown Group were more magnetic than background. This observation and the occurrence of many narrow anomalies, with amplitudes of up to several hundred nT, superimposed on the broad anomaly suggest that the magnetic units are thin and constitute a minor component of the stratigraphy.

The major magnetic anomaly along Traverse VIII is associated with the Cues Formation, which consists largely of psammitic composite gneiss with numerous thin quartz-magnetite and quartz-secondary iron oxide rocks and minor garnet quartzites. Two of the five sites within the Cues Formation are significantly more magnetic than background, one of which is strongly magnetic. The magnetic samples are magnetite-bearing metasediments. It appears to be significant that these otherwise ordinary rocks which happen to contain magnetite, unlike similar lithologies within the magnetically quiet zones, are stratigraphically close to highly magnetic units such as quartz-magnetites. The background level of magnetite is elevated within "normal" rocks which are stratigraphic equivalents or near equivalents of magnetite-rich chemically deposited rocks.

The amplitude of the broad ground magnetic anomaly over the Cues Formation is about 1800 nT, but there are many superimposed spiky anomalies with amplitudes of up to 1200 nT. The magnetic pattern over the Thorndale Composite Gneiss, to the east of the traverse, is qualitatively similar, but has lower amplitude. The individual magnetic units, associated with very short wavelength anomalies, appear to be even thinner within the Cues Formation and Thorndale Composite Gneiss than within the Sundown Group, probably reflecting the different nature of the sources. The general form of the broad anomalies over the three magnetic zones is similar and is consistent with magnetisation parallel to the present field, given the consistent steep northwestward dip of the units. This observation, coupled with the inconsistency of NRM directions for the magnetic rocks, suggests that either the measured NRMs are contaminated by surface effects and are not representative, or that the in situ NRMs are randomly scattered on a mesoscopic scale and the effective remanence of the units is thereby greatly reduced.

Traverse IX lies to the west of the Barrier Highway, approximately along 12800N (Rupree Grid), within the Purnamoota Subgroup of the Broken Hill Group. This locality and the nearby DDH NR1 are near the nose of the Broken Hill Synform in the North Rupee Trend area. The susceptibilities and Koenigsberger ratios of the Traverse IX samples are listed in Table 16 and the NRM vectors are given in Table 17. Basic magnetic properties and NRM vectors of the samples from the three Rupee Trend drill holes are given in Tables 18 and 19 respectively.

Only one surface site is appreciably magnetic. Site 141 lies within retrograde schist, which may originally have been a leucocratic rock, and is strongly magnetic, with a susceptibility of 0.0075 G/Oe and an intense steep downward directed remanence which may not be representative of the bulk magnetisation of the rock. The magnetite in this rock may have been produced by retrograde reactions, but magnetite is not generally associated with retrogression in the Broken Hill Block (Isles, 1983).

The nose of the SW-plunging Broken Hill Synform is outlined by aeromagnetic anomalies, associated with the Parnell Formation, which overlie the eastern half of Traverse IX and DDH NR1. To the southwest of Traverse IX, on the NW limb of the Broken Hill Synform the Parnell Formation contains bif units and in DDH NR1 a thin bif, grading to Potosi Gneiss, was intersected around 92 m depth. This sample is quite strongly magnetic and a nearby metasedimentary sample (111 m) has a susceptibility elevated above background. Thus the Parnell Formation in the Broken Hill Synform is relatively magnetite-rich, probably due to the influence of chemical sedimentation. The high susceptibility of the retrograde schist at site 141 may therefore arise from pre-retrogressive magnetite which has survived the retrogression. To the south of Traverse IX, on the SE limb of the Broken Hill Synform, the magnetic horizon within the Purnamoota Subgroup is slightly transgressive. This magnetic zone, which is not as prominent as the Sundown Group and Cues Formation zones to the east, appears to be associated with the Freyers Metasediments, rather than the Parnell Formation, near Traverse VIII and further south. The ground magnetic profile of Fig. 19 indicates that the source of the low amplitude aeromagnetic anomaly is a very thin, highly magnetic horizon within the Purnamoota Subgroup, probably in the Freyers Metasediments.

Examination of Table 18 shows that the Q values of the magnetic DDH samples are all less than unity, whereas it is commonly found that magnetic surface samples have high Koenigsberger ratios. This tends to confirm the supposition that many surface samples are contaminated by palaeomagnetic noise, probably due to lightning. The magnetic samples from DDH BMX1 are mineralised quartz-magnetite rocks, grading to metasediments. In DDH TH2 the only magnetic sample is a pyrrhotite-bearing mineralised psammite. The susceptibility of this rock appears to be due to magnetite rather than pyrrhotite, based on thermal demagnetisation of the NRM. This is supported by the fact that

the other pyrrhotite-bearing samples from this hole are weakly magnetic, indicating that the pyrrhotite must be intermediate "hexagonal", rather than monoclinic 4C pyrrhotite. Palaeomagnetic cleaning of the DDH samples did not define any consistently oriented remanence components, although the demagnetisation behaviour of individual specimens defined apparently well-resolved remanence components. This confirms the general conclusion that the Broken Hill Block rocks appear to carry very complex multicomponent remanences, reflecting a very complicated thermal and chemical history, precluding their usefulness as palaeomagnetic recorders and tending to lead to macroscopic mutual cancellation of remanences which may have substantial intensities on a mesoscopic scale, but which have very scattered directions.

Magnetic fabric elements for the Traverse VIII samples are plotted in Figs.20-23. Fig.20 shows the magnetic foliation poles and magnetic lineations of the Purnamoota Subgroup samples on the NW limb of the Rupee Antiform (sites 98-107). Foliation poles are mainly clustered about a SE shallow down direction, consistent with the pole to the steeply NW-dipping S1-2 schistosity. Magnetic lineations are clustered into two groups: subvertical and NE-SW horizontal. Some apparent streaking of the minimum axes is also consistent with interchange of susceptibility axes, which can represent variable overprinting of magnetic fabrics. There appears to be little difference in magnetic fabric on the basis of lithology or bulk susceptibility.

The magnetic fabric of the Sundown Group samples is shown in Fig.21. The general pattern is similar to Fig.20, but the magnetic lineations tend to be streaked between the subvertical group and the shallow NE-SW group, but predominantly plunge to the SW. The Purnamoota Subgroup samples from the SE limb of the Rupee Antiform (sites 118-127) exhibit mainly moderately to steeply west plunging lineations (Fig.22). The amphibolites within the Allendale Metasediments (sites 128-130) exhibit lineations which are streaked within the steeply WNW-dipping magnetic foliation. The lineations of sites 131-135 within the Cues Formation are either subvertical or else plunge in the SW quadrant (Fig.23). Small-scale folds around Traverse VIII plunge fairly consistently to the WSW. This is reflected in the west to southwest plunging magnetic lineations which are common in these samples. The streaking of magnetic lineations towards the subvertical cluster may reflect genuine variation of plunges from shallow to very steep or it may reflect overprinting of fabrics. The petrofabric in this area appears from the mapped mesoscopic fabrics and structures to be of low symmetry, with the local fold axes oblique to the subparallel bedding and axial plane schistosity (S1-2). In some cases the subvertical magnetic lineations may reflect projection of an oblique lineation onto the schistosity plane, or it may represent the direction of maximum extension associated with production of the axial plane schistosity.

The magnetic fabric of the Traverse IX samples does not

show a consistent orientation. Magnetic foliation poles are very scattered, reflecting the structural complexity in this area which is near the nose of a major structure, but the average orientation defines a subvertical E-W foliation. Magnetic lineations vary from subvertical to NE or SE-plunging. The aeromagnetics over this locality also indicates structural thickening of the magnetic units within this zone. The magnetic fabric demonstrates that near traverse IX the local structures are much more variable than is evident from the gross disposition of mapped units or from the relatively few mapped mesoscopic structural elements in this area.

7. MAGNETIC STRATIGRAPHY

It has been found throughout the Broken Hill Block that most prominent curvilinear anomalies correspond to stratigraphic magnetite-bearing horizons. These horizons represent rocks which, apart from their higher magnetite contents, resemble non-magnetic rocks from the same area, but which commonly are stratigraphically equivalent to, or stratigraphically near, chemically precipitated magnetite-rich rocks such as quartz-magnetite and bif (McIntyre, 1979). Magnetic anomalies within the Broken Hill Block are in general associated with particular stratigraphic intervals, rather than being controlled by lithology.

The geological significance of magnetite in metamorphic terranes has been reviewed by McIntyre (1980). A major control on the production of magnetite during metamorphism of sediments is the oxidation state inherited from the depositional and diagenetic environments. A low ferric/ferrous iron ratio favours incorporation of iron into paramagnetic silicates during metamorphism. On the other hand a high ferric/ferrous iron ratio, representing very oxidised conditions, produces weakly magnetic (antiferromagnetic) haematite during metamorphism. Magnetite formation is maximised when the inherited oxidation state is intermediate. Thus in many cases magnetite-bearing horizons within metasedimentary sequences represent premetamorphic sedimentary environmental zones rather than lithological boundaries. The oxidation state in these zones may be controlled by the mineralising fluids that precipitate the chemical sediments, increasing the potential of the nearby rocks to generate metamorphic magnetite.

The association between magnetic rocks and chemical sediments may also simply reflect precipitation of magnetite, at lower levels than for adjacent chemical sediments, during deposition or diagenesis. The lower magnetite content of the magnetic marker horizons, which enclose or parallel the chemical sedimentary horizons, is then attributable to dilution by clastic material. This model accounts for the observation that almost any rock type can be locally magnetic in the Broken Hill Block (Tucker, 1983). There is also a relationship between the magnetite contents of basic and felsic gneisses and magnetite in adjacent, enclosing or stratigraphically equivalent clastic metasediments

and chemical sediments. Amphibolite units and quartzofeldspathic gneisses within generally magnetic stratigraphic intervals tend to be magnetic (e.g. the magnetic amphibolites adjacent to magnetic metasediments on Traverse IV, within the magnetic zone of the upper Hores Gneiss). Basic and felsic gneisses of the Willyama Supergroup are usually interpreted as metamorphosed, altered tholeiitic and rhyodacitic volcanics respectively (Willis et al, 1983). The correlation between their magnetite contents and that of associated sedimentary rocks suggests that the gneisses may originally have been volcanoclastic or have a substantial sedimentary component. Haydon and McConachy (1987) have suggested that the felsic gneisses were originally clastic sediments, with some immature volcanic component.

In the case of magnetic stratigraphic units which are not associated with chemical precipitates, such as the pelitic metasediments of the Sundown Group, the magnetite content is attributable to metamorphic processes and may reflect palaeoenvironmental conditions (an intermediate oxidation state), low quartz content, which decreases the stability field of fayalite relative to magnetite plus quartz, and the ability of pelitic rocks to generate magnetite from haematite and hydrous silicates such as chlorite and biotite by dehydration during metamorphism (McIntyre, 1980). Similar considerations apply to the Freyers Metasediments. The generally low magnetic response over the graphitic metasediments of the Paragon Group (Isles, 1983; Tucker, 1983) may be due to the inhibiting effect of carbon on magnetite production during metamorphism (McIntyre, 1980).

The generalised magnetic stratigraphy of the Broken Hill Block has been discussed by Isles (1983) and Tucker (1983). Tucker (1983) recognises up to 25 magnetic units within the stratigraphy of the Willyama Supergroup. The Clevedale Migmatite, which is only exposed in the Mt Darling Range, contains many short strike-length, contorted, narrow magnetic horizons. The magnetic character of the Thorndale Composite Gneiss is similar to that of the Clevedale Migmatite, although it is more heterogeneous. The Thackaringa Group is generally characterised by persistent, subparallel narrow curvilinear anomalies, often associated with quartz-magnetites and belts of magnetite-bearing amphibolites and metasediments. The Broken Hill Group exhibits mainly short strike-length, narrow curvilinear anomalies. Amphibolites and Potosi Gneiss associated with Pb/Zn mineralisation are variably magnetic. Magnetic horizons within the Broken Hill Group are recognised within the Hores Gneiss, Freyers Metasediments and Parnell Formation. The latter horizon appears to be the most persistent. The highest stratigraphic intervals associated with substantial anomalies lie within the Sundown Group, particularly within the lower Sundown Group but somewhat above the base. These horizons are quite persistent.

Isles (1983) and Tucker (1983) subdivided the Broken Hill Block into domains of different magnetic character, between which the magnetic stratigraphy may vary. The local magnetic

stratigraphy of the areas studied for this case history, based on magnetic properties and magnetic signatures, will now be discussed in some detail. Sites 1-4 in the Northern Leases represent a thin magnetic horizon of the Hores Gneiss. This horizon corresponds to only part of the sampled Potosi Gneiss unit and has short strike-length, but corresponds to a magnetic stratigraphic interval which is best developed in the Sundown/Broken Hill/Rockwell area of the Central Magnetic Domain. The bif from site 23 corresponds to a very persistent magnetic horizon, associated with chemical sediments, of the Parnell Formation in this magnetic domain. Although the sampled amphibolite unit from the Cues Formation (site 19) is not very magnetic, its susceptibility is significantly above the paramagnetic background value of about 80 microgauss/Oersted which typifies amphibolites without magnetite. This implies the presence of magnetite in this sample, which is significant because of the prevalence of chemically precipitated magnetite in the Cues Formation.

The assignment of samples from the Redan/Farmcote area to stratigraphic positions is tentative, but the magnetic properties of the samples and the observed anomaly patterns are consistent with the interpreted stratigraphic correlation. The "Redan Gneiss" samples and the quartz-iron oxide rocks are variably, but generally strongly, magnetic. The properties and magnetic signatures resemble those of Thackaringa Group rocks elsewhere in the Broken Hill Group. The magnetic amphibolite unit, adjacent to site 24-5, resembles typical sources within the Thorndale Composite Gneiss.

There is much more information on which to base a magnetic stratigraphy in the Rise and Shine and Rupee Trend areas. In the Rise and Shine EL there are some differences in magnetic signatures of horizons, interpreted to be stratigraphically equivalent, within the Eastern and Western Lodes. In the Eastern Lode the upper Hores Gneiss, including the Potosi Gneiss units, is absent and the lower Hores Gneiss, containing the upper lode horizon of the Eastern Lode, and the Freyers metasediments are non-magnetic. The magnetic interval within the Broken Hill Group of the Eastern Lode appears to be largely confined to the Parnell Formation, which contains the lower lode horizon, magnetic amphibolites and bifs, although to the SW of the DDH PT1 there is a magnetic horizon of very limited strike length which appears to lie within Hores Gneiss. The Allendale Metasediments are thin in this area and it is not clear from the magnetics if they contain magnetic horizons. However this formation is not generally magnetic (Tucker, 1983). The uppermost Thackaringa Group exposed in this area, represented by the Stephens Creek Granite Gneiss, is generally weakly magnetic, but contains some minor impersistent magnetic horizons.

In the Western Lode there is a relatively persistent magnetic horizon in the Hores Gneiss, which is slightly discordant. In the central part of the EL the magnetic horizon consists of magnetic amphibolites and metasediments which lie stratigraphically above the major Potosi Gneiss units overlying

the upper lode horizon of the Western Lode. In the southern part of the EL the upper Broken Hill Group anomaly is apparently associated with the lowermost Potosi Gneiss unit. Between these localities the anomaly dies out and reappears, but appears to be somewhat transgressive, particularly around Traverse V. Immediately to the north of Traverse V, the anomaly appears to overlie the upper Parnell Formation, stratigraphically just above the lower lode horizon of the Western Lode. This anomaly then appears to swing almost parallel to Traverse V and then resume its general trend, parallel to the geological strike, within the Hores Gneiss. However, on comparison with the northern and southern areas of the EL this impression is believed to be arise from lateral impersistence of magnetic horizons, with the Hores Gneiss anomaly dying out where the Parnell Formation anomaly happens to build up.

In the northern part of the EL the magnetic zone within the upper Broken Hill Group coincides with the thick Potosi Gneiss and the immediately overlying metasediments, i.e. the stratigraphic position of the magnetic interval lies between the positions in the central and southern areas. A minor, impersistent magnetic horizon appears to be associated with the upper Parnell Formation, just above the lode horizon, in the northern and central parts of the Rise and Shine EL, but apparently lies just below the lode horizon in the southernmost part of the EL. This horizon is best-developed in the central area, near Traverse V.

The dominant magnetic feature of the Rise and Shine area is the intense and persistent broad anomaly associated with the Sundown Group. This feature is revealed in the detailed aeromagnetics as a composite anomaly, made up of two or more parallel horizons which drop out and reappear along strike, often at a slightly different stratigraphic level. The magnetic horizons appear to occur mainly in the lower Sundown Group, but nevertheless above the boundary with the Broken Hill Group. This stratigraphic position of the magnetic horizons within the Sundown Group corresponds to other areas of the Broken Hill Block, but the anomalies are particularly large in the Rise and Shine area. Fig.24 provides a pictorial representation of the magnetic stratigraphy of the Rise and Shine area, compared to the Rupee Trend area, which is discussed below. The magnetic stratigraphy of the Rise and Shine area is also summarised in Table 20.

The detailed aeromagnetics over the Broken Hill Synform and the Rupee Antiform reveal a number of subparallel magnetic horizons which outline the Broken Hill Synform. By comparison with the mapped geology the main magnetic horizons are found to lie within the Sundown Group, with subsidiary but nevertheless quite persistent horizons within the Broken Hill Group (particularly in the Parnell Formation), which define the closure of the synform in the Rupee homestead area, and the Cues Formation of the Thackaringa Group, which outlines the core of the synform.

To the SW of the Rupee Antiform, in the Mt Darling Range, there is a very prominent magnetic zone associated with the Cues Formation and a more subdued, but still substantial response over the Thorndale Composite Gneiss, which outlines the Mt Darling Creek Antiform with non-magnetic Alma Gneiss in its core. Complex magnetic zones, reflecting ubiquity of moderately magnetic sources, are associated with the Clevedale Migmatite in the cores of the Clevedale and the Donsandel North Antiforms. The continuation of this characteristic magnetic pattern beneath overlying non-magnetic rocks of the Thorndale Composite Gneiss to the north of the Clevedale Antiform indicates a gentle northward plunge for this structure, whereas the sharp truncation of the pattern at the northern boundary of the Clevedale Migmatite of the Donsandel North Antiform indicates a steep plunge (Isles, 1983).

Examination of Fig.19 allows some refinement of the relationships inferred from the aeromagnetics. A very thin, but strongly magnetic, horizon occurs within the Purnamoota Subgroup, apparently over Freyers Metasediments. This horizon is also apparent in the aeromagnetics, but is greatly attenuated due to the increased sensor height/thickness ratio. From the aeromagnetics it appears that this anomaly is quite persistent along strike but is slightly transgressive to geological trends. Further to the north and around the nose of the Broken Hill Antiform the main magnetic horizon of the Broken Hill Group appears to be within the Parnell Formation.

The lowermost Sundown Group, immediately overlying the Broken Hill Group of the NW limb of the Rupee Antiform, appears to be weakly magnetic. The magnetic zone of the Sundown Group starts somewhat east of the Rupee Schist Zone and continues to the eastern boundary of the Sundown Group with the Broken Hill Group. Magnetic response over the Broken Hill Group on the SE limb of the Rupee Antiform is very subdued. The gradual rise of the magnetic intensity over the Allendale Metasediments, on the smooth NW flank of the major anomaly associated with the Cues Formation, is attributable to the NW dip of the magnetic horizon beneath the traverse, rather than to a gradually increasing susceptibility within the lower Broken Hill Group. Highly magnetic units within the Broken Hill Group, if present, would produce noisy ground magnetic anomalies similar to those observed over the other magnetic zones in Fig.19. The absence of short wavelength anomalies over the Broken Hill Group suggests that this stratigraphic interval is non-magnetic on the SE limb of the Rupee Antiform. Deep magnetic weathering is unlikely, but could also account for the smoothness of the profile over the Broken Hill Group.

The Cues Formation is seen from the ground magnetics to consist of many, closely spaced, thin magnetic units which produce the large spiky anomalies shown in Fig.19. Although many of these sharp anomalies are probably due to quartz-magnetites, there is a generally elevated level of magnetite in the Cues Formation and some individual anomalies are due to "normal" rocks, such as metasediments. This implies that some of the broad

feature evident in the ground profile and the aeromagnetic response over the Cues Formation is due to general dissemination of magnetite throughout the Formation, rather than simply representing the superposition of many short wavelength anomalies.

The generalised magnetic stratigraphy of the Rupee Trend area is summarised in Table 21 and Fig.24. The most prominent magnetic features throughout the Broken Hill Block arise from the distribution of magnetite which is often, but not always, readily interpretable in terms of stratigraphy. Almost any rock type can be magnetic in the Broken Hill Block, provided it lies within a stratigraphic interval which is generally magnetic in the area. The small, but systematic, lithology dependent differences in the susceptibilities of non-magnetite-bearing rocks revealed by this study raises the possibility that ground magnetics and high resolution aeromagnetics may be useful as mapping tools, not only in areas of high magnetic relief, but also within magnetically quiet domains.

The paramagnetic susceptibilities of different lithologies consistently show the relationships: amphibolites > metasediments /quartzofeldspathic gneisses > leucocratic quartzofeldspathic gneisses. Of the metasediments, pelites have higher paramagnetic susceptibilities than psammites. These relationships are readily explicable on the basis of the content of paramagnetic iron, which is mainly within the mafic minerals. The differences in susceptibility are sufficiently predictable, in the absence of magnetite, and are large enough to produce detectable anomalies, provided noise due to nearby strongly magnetic sources is minimal. The paramagnetic susceptibility of amphibolites of all types is typically about 80 microgauss/Oersted, compared to 30 microgauss/Oersted for metasediments and 5 microgauss/Oersted for leucocratic phases. The susceptibility contrast between an amphibolite unit and metasediments with these properties is sufficient to produce anomalies of up to 40 nT on ground profiles, provided the thickness of the unit is much greater than the sensor height ($t > 6$ m, say, for a subcropping unit), or an aeromagnetic anomaly of about $3t/h$ nT, where t is the thickness of the unit and h is the sensor height ($h > t$). Such aeromagnetic anomalies should be detectable by surveys with sub nT resolution, in favourable conditions, but detection with ground magnetics would be much easier.

Application of magnetic surveys in magnetically quiet areas, where paramagnetic susceptibility contrasts can be detected, could be useful for lithological mapping because the magnetic horizons defined by the survey should correspond closely to individual rock units. The information provided by the magnetic survey in this case may be more easily interpretable than for magnetically active zones, for which the magnetite-bearing magnetic horizons may be somewhat discordant.

8. SUMMARY AND CONCLUSIONS

(i) Extensive sampling within the Broken Hill Block has failed to find any characteristic remanence direction, even on a mesoscopic scale, although individual samples may have intense NRM and high Koenigsberger ratio. The form of both short and long wavelength features in ground and aeromagnetic surveys is almost always consistent with magnetisation parallel to the present geomagnetic field, suggesting that induced magnetisation dominates remanence on a macroscopic scale. Q values of magnetic subsurface samples are usually less than unity, suggesting that surface samples with high Koenigsberger ratios have been affected by lightning and that their NRMs are unrepresentative of the bulk of the rock unit. The inconsistency of raw and cleaned remanence directions in samples which are unaffected by palaeomagnetic noise is probably due to the prolonged complex thermal history of the Broken Hill Block. Although the bedrock lithologies do not appear to carry a useful palaeomagnetic signal, palaeomagnetic dating of ferricrete formation seems to be feasible.

(ii) Most lithologies present in the Broken Hill Block can be locally magnetic, but magnetic rocks represent only a minor component of the total volume. The magnetic mineral causing almost all substantial anomalies is magnetite. Prominent curvilinear anomalies are usually subparallel to geological boundaries, but are often slightly discordant. Magnetic horizons tend to be confined to particular stratigraphic intervals, within which individual magnetic units are sometimes very persistent but more often have short strike length. Within such magnetic zones individual anomalies tend to build up and attenuate along strike, dropping out altogether then reappearing at a slightly different stratigraphic level. A generalised magnetic lithostratigraphy can be devised for the Broken Hill Block. There are, however significant differences in magnetic character between different areas, which can be used to subdivide the Broken Hill Block into various magnetic domains.

(iii) Measurement of magnetic properties of samples collected from magnetic zones confirmed that otherwise "normal" rocks, including pelitic and psammitic metasediments and composite gneisses, quartzofeldspathic gneisses and amphibolites (all of which are generally weakly magnetic) often contain substantial amounts of magnetite and hence are magnetic. Such rocks are often adjacent to, or enclosing, or stratigraphically equivalent to, magnetite-rich chemical sediments such as quartz-magnetite rocks and bifs. Quartz-magnetites and bifs are invariably strongly magnetic, but are often very thin. Individual units of such rocks may therefore produce relatively small aeromagnetic anomalies, although the ground magnetic response over outcropping or subcropping units is spectacular. Much of the aeromagnetic response over stratigraphic intervals which contain these rocks arises from the generally elevated level of magnetite in the surrounding rocks. Individual magnetic units within magnetic zones are generally thin and may be impersistent, causing sampling problems. The paramagnetic susceptibilities of

amphibolites are consistently greater than those of metasediments and quartzofeldspathic gneisses, which in turn are greater than the paramagnetic susceptibilities of leucocratic quartzofeldspathic gneisses. The differences arise from the different proportions of mafic minerals in these rocks. It has been shown that in magnetically quiet areas, where magnetite is absent, rock units may be directly mappable using high resolution magnetic surveys to detect the low amplitude anomalies arising from the small, but systematic, susceptibility contrasts.

(iv) The magnetic fabric of samples from the Northern Leases area correlates very well with the mapped structures and mesoscopic fabrics. Except for the site within the Globe-Vauxhall Schist Zone, the magnetic foliations clearly reflect overprinting of bedding-parallel S1 by the axial plane schistosity of second generation folds (S2). Minor susceptibility axes either cluster near the pole to the dominant schistosity or are streaked between the S0/S1 and S2 poles, reflecting varying degrees of overprinting of schistositities. Magnetic lineations (major susceptibility axes) are parallel to the F2 fold axes. There is some evidence that paramagnetic and ferromagnetic fabrics are overprinted to different extents, indicating that petrofabrics of lower symmetry than orthorhombic could be studied from analysis of paramagnetic and ferromagnetic fabrics of individual specimens, as well as by examining total magnetic fabric data from suites of specimens. Retrograde schist samples have magnetic fabrics which reflect retrogression, with magnetic foliation parallel to S3 schistosity and magnetic lineation parallel to the petrofabric lineation. The correlation between magnetic fabric and structure obtains within all the structural subareas of Laing et al (1978) from which samples were collected.

(v) The magnetic fabric data from the Rise and Shine and Rupee Trend areas are not as straightforward as those obtained from the Northern Leases, but nevertheless often show a clear relationship with local structure. There is a fairly consistent NE subvertical mean magnetic foliation in the Rise and Shine area, parallel to the predominant S0 and S2 planes, except for the northeastern part of the EL where there is a change in geological strike. The magnetic foliation poles show some streaking (a partial girdle distribution) away from the dominant direction, reflecting variations in bedding/schistosity attitude and overprinting of schistositities. The magnetic lineations are generally orthogonal to this girdle and are interpreted to indicate fold axis plunges. Where plunges are mapped there is reasonable agreement between the magnetic lineations and fold axes. Local plunges are generally to the NE or SW and the magnetic fabric data suggest that steep plunges predominate. The scale of this folding appears to be quite small and the relationship between these local structures and the regional structure of this area is not clear. In the traverse across the Rupee Antiform the magnetic foliations are found to be NE subvertical, parallel to the predominant S0 and S2 planes. Magnetic lineations are subvertical, or else plunge in the SW quadrant parallel to the mapped axes of minor folds.

(vi) A refined magnetic stratigraphy, based on sampling and ground and aeromagnetic surveys, is proposed for the Rise and Shine and Rupee Trend areas. The dominant magnetic feature of the Rise and Shine area is the broad zone of high amplitude anomalies associated with the Sundown Group, which lies between interpreted Broken Hill Group of the Eastern and Western Lodes. This zone as a whole has great strike length, but consists of at least two magnetic horizons which persist typically for 1 km before dropping out. Other magnetic horizons appear at slightly different stratigraphic levels and disappear in turn. The magnetic zone appears to commence within the lower Sundown Group, but above the basal contact with the Broken Hill Group. There is a fairly persistent subsidiary magnetic horizon within the Hores Gneiss of the Western Lode. This horizon is slightly transgressive, but generally lies in the middle to upper Hores Gneiss, and does not continue up to the contact with the Sundown group. A minor, somewhat impersistent, magnetic horizon, which lies stratigraphically close to the main lode horizon, is also associated with the Parnell Formation of the Western Lode. The Thackaringa Group to the west of the Western Lode is also associated with substantial anomalies. To the east of the Eastern Lode, however, the upper exposed Thackaringa Group rocks, represented by the Stephens Creek Granite Gneiss, are generally weakly magnetic. In the Eastern Lode the upper Hores Gneiss is absent and the only persistent magnetic horizon lies within the Parnell Formation.

(vii) In the Rupee Trend area there are a number of very persistent magnetic zones which define approximate stratigraphic intervals. The largest anomalies are associated with the Cues Formation of the Thackaringa Group which contains quartz-magnetites and lode horizon rocks. Other formations from the Thackaringa Group that are represented in this area (Rasp Ridge Gneiss, Alma Gneiss) are non-magnetic. A prominent, continuous magnetic feature is also associated with the Sundown Group. The general magnetic character of the Thorndale Composite Gneiss qualitatively resembles that of the Cues Formation, but with much lower amplitude anomalies. The Clevedale Migmatite exhibits a noisy magnetic response, associated with a multiplicity of moderately to strongly magnetic sources. Within the Broken Hill Group, the Parnell Formation is associated with a magnetic anomaly which persists from the nose of the Broken Hill Synform along the NW limb. The Freyers Metasediments exhibit a relatively minor anomaly, which arises from a very narrow, strongly magnetic, horizon on the SE limb of the Broken Hill Synform, which continues around the nose of the structure and builds up along the NW limb. On the SE limb of the Rupee Antiform this magnetic horizon is absent from the Purnamoota Subgroup of the Broken Hill Group.

9. ACKNOWLEDGEMENTS

Wolf Leyh (NBH Ltd), Chris Bain and Ian Freytag (Aberfoyle Ltd) and Peter Elliott (Billiton Ltd) assisted with field work and information. I would particularly like to thank Neil Raphael of the NSW Geological Survey, who helped with lithological identification of the samples and stratigraphic interpretation of the sampling localities.

10. REFERENCES

- Clark, D.A., 1981. Relationship between magnetic fabric and geological structure in the Northern Leases area, Broken Hill. CSIRO Restricted Investigation Report 1237R.
- Clark, D.A. and B.J.J. Embleton, 1980. Applications of rock magnetism. CSIRO Restricted Investigation Report 1193R.
- Clark, D.A., D.W. Emerson and T. Kerr, 1987. The use of electrical conductivity and magnetic susceptibility tensors in rock fabric studies. *Explor. Geophys.*, 19, 244-248.
- Harrison, T.M. and I. McDougall, 1981. Excess Ar40 in metamorphic rocks from Broken Hill, New South Wales: implications for Ar40/Ar39 age spectra and the thermal history of the region. *Earth Planet. Sci. Lett.*, 55, 123-149.
- Haydon, R.C. and G.W. McConachy, 1987. The stratigraphic setting of the Pb-Zn-Ag mineralization at Broken Hill. *Econ. Geol.*, 82, 826-856.c
- Isles, D.J., 1983. A regional geophysical study of the Broken Hill Block, N.S.W., Australia. PhD thesis, University of Adelaide.
- Laing, W.P., R. W. Marjoribanks and R.W. Rutland, 1978. Structure of the Broken Hill mine area and its significance for the genesis of the orebodies. *Econ. Geol.*, 73, 1112-1136.
- Marjoribanks, R.W., R.W.R. Rutland, R.A. Glen and W.P. Laing, 1980. The structure and tectonic evolution of the Broken Hill Region, Australia. *Precambrian Research*, 13, 209-240.
- McIntyre, J.I., 1979. Aeromagnetism - an effective geological mapping aid for the Willyama Complex? *Bull. Aust. Soc. Explor. Geophys.*, 10, 42-53.
- McIntyre, J.I., 1980. Geological significance of magnetic patterns related to magnetite in sediments and metasediments - a review. *Bull. Aust. Soc. Explor. Geophys.*, 11, 19-33.
- Rochette, P., 1987. Magnetic susceptibility of the rock matrix related to magnetic fabric studies. *J. Struct. Geol.*, 9, 1015-1020.

Stevens, B.P.J., 1980 (ed). A guide to the stratigraphy and mineralization of the Broken Hill Block, New South Wales. NSW Geol. Surv. Rec., 20, Part 1, 153 pp.

Stevens, B.P.J., 1986. Post-depositional history of the Willyama Supergroup in the Broken Hill Block, NSW. Aust. J. Earth Sci., 33, 73-98.

Stevens, B.P.J. and W.J. Stroud, 1983 (eds). Rocks of the Broken Hill Block: their nature, stratigraphic distribution, and origin. NSW Geol. Surv. Rec., 21, Part 1, 323 pp.

Stroud, W.J., 1978. Geology of the Stephens Creek 1:25000 sheet, Broken Hill, New South Wales. NSW Geol. Surv. Rpt, GS1978/060.

Stroud, W.J., 1980. Stratigraphic interpretation of the Stephens Creek 1:25000 sheet area. NSW Geol. Surv. Rec., 20(1), 97-101.

Tucker, D.H., 1983. The characteristics and interpretation of regional magnetic and gravity fields in the Broken Hill district. Proceedings of the Aus. I.M.M. Broken Hill Conference, 81-114.

Willis, I.L., R.E. Brown, W.J. Stroud and B.P.J. Stevens, 1983. The Early Proterozoic Willyama Supergroup: stratigraphic subdivision and interpretation of high to low-grade metamorphic rocks in the Broken Hill Block, New South Wales. J. Geol. Soc. Australia, 30, 195-224.

Wright, J.V., R.C. Haydon and G.W. McConachy, 1987. Sedimentary model for the Broken Hill Pb-Zn deposit, Australia. Geology, 15, 598-602.

TABLE 1
 SUSCEPTIBILITIES AND KOENIGSBERGER RATIOS OF
 NORTHERN LEASES SAMPLES

| Site | Lithology | Stratigraphic Position | k ($\mu\text{G}/\text{Oe}$) | Q |
|-------|-----------------|---------------------------|----------------------------------|------|
| 1-4 | BG ₁ | Bh | 650 | 3.2 |
| 5-9 | BG ₁ | Bh | 48 | 0.05 |
| 10-18 | BG ₂ | Tr | 18 | 0.05 |
| 19 | ax | Tc | 170 | 21 |
| 20-21 | M+FM | S | 40 | 0.01 |
| 22 | rm | B? | 28 | 0.11 |
| 23 | bif | Bp | 18,000 | 1.5 |

k = cgs (emu) susceptibility $\times 10^6$

Q = J/kF , where J = NRM intensity in μG and F = geomagnetic field intensity = 0.58 Oe

TABLE 2

NRM VECTORS AND MAGNETIC FABRICS OF NORTHERN LEASES SAMPLES

| Site | NRM | Lineation | Foliation pole | A | P |
|-------|--------------------|---------------------|---------------------|------|------|
| 1-4 | (1200;265°,-06°) | (84°,21°) (16°) | (178°,20°) (12°) | 1.24 | 0.95 |
| 5-9 | (41;285°, +20°) | (72°,55°) (15°) | - | 1.03 | 1.00 |
| 10-18 | (1.4;358°,-09°) | (65°,49°) (16°) | (164°,03°) (18°) | 1.10 | 1.01 |
| 19 | (2050;351°, +50°) | (213°,33°) (10°) | - | 1.06 | 1.00 |
| 20-21 | (0.2;040°,-70°) | - | (128°,33°) (9°) | 1.06 | 1.01 |
| 22 | (1.8;092°,-29°) | (328°,69°) (8°) | (124°,19°) (5°) | 1.11 | 0.94 |
| 23 | (15700;025°, +41°) | (250°,20°) (46°) | (128°,54°) (20°) | 1.21 | 0.96 |

NRMs are expressed in the form: (Intensity (μ G); dec, inc) where declination is positive clockwise from TN and inclination is positive downwards

Mean magnetic lineation and foliation pole directions are expressed as: (dec, inc) (α_{95}) where α_{95} is the half-angle of the 95% cone of confidence about the mean direction.

A = anisotropy magnitude = k_1/k_3 ; P = prolateness of susceptibility ellipsoid = $k_1k_3/(k_2)^2$

TABLE 3
BASIC MAGNETIC PROPERTIES OF REDAN AREA SAMPLES

| Site | Lithology | k | NRM | Q |
|------|-----------|--------|-----------------------|-----|
| 24-1 | qf | 1560 | (30,200;303°,-30°) | 33 |
| 24-2 | qf-fe | 1810 | (14,400;066°,+02°) | 14 |
| 24-3 | qm | 14,800 | (350,000;313°,+59°) | 41 |
| 24-4 | Pl(+ mt) | 700 | (30,500;261°,-47°) | 75 |
| 24-5 | a | 75 | (310,;022°,-77°) | 7 |
| 24-6 | Czf (hm) | 35 | (70;015°,-66°) | 3.5 |
| 24-7 | qm | 74,000 | (3,600,000;231°,+04°) | 84 |
| 24-8 | Czf (mhm) | 4600 | (4470;199°,-22°) | 1.7 |
| 24-9 | Pl | 15 | (19;296°,+78°) | 2.2 |

NRMs are given in the form: (Int (μ G); dec, inc)

TABLE 4
 SUSCEPTIBILITIES AND KOENIGSBERGER RATIOS OF TRAVERSE III
 AND DDH PT1 SAMPLES

| Site | Lithology | Stratigraphic position | k | Q |
|-------|-----------|------------------------|--------|------|
| 25 | FE | Bh? S?? | 22 | 0.12 |
| 26 | FE | Bh? S?? | 23 | 0.03 |
| 27 | M | Bh? S?? | 25 | 0.21 |
| 28 | EM | Bh? S?? | 21 | 0.22 |
| 29 | M | Bh? | 24 | 0.01 |
| 30 | rm | Bh? | 35 | 0.09 |
| 31 | E | Bf? | 19 | 1.31 |
| 32 | M | Bf? | 18 | 0.25 |
| 33 | E | Bf? | 25 | 0.16 |
| 34 | S-M | Bf? | 15 | 0.71 |
| 35 | E | Bf? | 32 | 0.04 |
| 36 | ES | Bf? Bp? | 25 | 0.03 |
| 37 | EM-Lf? | Bf? Bp? | 21 | 0.13 |
| 38 | E | Bh? S?? | 26 | 0.13 |
| 25-38 | - | Bs? | 24 | 0.17 |
| 39 | ag | Bp? | 730 | 1.2 |
| 40 | bif | Bp? | 30,800 | 1.8 |

| | | | | |
|--------------|-----------------|---------|-----|------|
| PT1-10 m | BG ₂ | Bh? | 26 | 0.10 |
| PT1-17 m | P-FEM | Bh? | 22 | 0.82 |
| PT1-47 m | rm | Bh? | 8 | 0.09 |
| PT1-74 m | FEMg | Bf? | 22 | 0.02 |
| PT1-90 m | FEMg | Bf? | 32 | 0.30 |
| PT1-100 m | FEMg | Bf? | 15 | 0.06 |
| PT1-120 m | FSMg | Bf? | 220 | 0.85 |
| PT1-125 m | E-SE | Bf? | 36 | 0.24 |
| PT1-130 m | E-SE | Bf? | 27 | 0.00 |
| PT1-140 m | EM | Bf? | 28 | 0.02 |
| PT1-155 m | SE-E | Bf? | 38 | 0.03 |
| PT1-175 m | SE-E | Bf? | 30 | 0.01 |
| PT1-200 m | (F)EMg | Bf? | 91 | 1.08 |
| PT1-230 m | SE | Bf? | 67 | 0.11 |
| PT1-245 m | SE | Bf? | 15 | 0.00 |
| PT1-260 m | FSE | Bf? Bp? | 250 | 4.12 |
| PT1-272 m | ag | Bp? | 32 | 0.01 |
| PT1--290 m | rEM | Bp? Ba? | 25 | 0.00 |
| <hr/> | | | | |
| PT1 combined | - | Bs? | 55 | 1.3 |
| <hr/> | | | | |

TABLE 5

MEAN NRM VECTORS OF TRAVERSE III AND DDH PT1 SAMPLES

| Site/DDH depth | Intensity (microgauss) | Declination | Inclination |
|----------------|---------------------------|-------------|-------------|
| 25 | 1.5 | 033 | -59 |
| 26 | 0.5 | 317 | -66 |
| 27 | 3.0 | 039 | +29 |
| 28 | 2.7 | 009 | -26 |
| 29 | 0.2 | 176 | +87 |
| 30 | 1.8 | 343 | -60 |
| 31 | 14.5 | 008 | -73 |
| 32 | 2.6 | 035 | -36 |
| 33 | 2.3 | 069 | -55 |
| 34 | 6.2 | 014 | -62 |
| 35 | 0.7 | 246 | -51 |
| 36 | 0.5 | 305 | -60 |
| 37 | 1.6 | 000 | -70 |
| 38 | 2.0 | 187 | -27 |
| 25-38 | 2.3 | 020 | -63 |
| 39 | 508 | 359 | -12 |
| 40 | 32340 | 227 | +02 |
| 10 m | 1.5 | 274 | -47 |
| 17 m | 10.4 | 049 | +43 |
| 47 m | 0.4 | 253 | +30 |
| 74 m | 0.3 | 043 | +06 |
| 90 m | 5.6 | 071 | -07 |
| 100 m | 0.5 | 310 | -55 |
| 120 m | 108 | 245 | +68 |

| MEAN NRM VECTORS OF TRAVERSE III AND DDH PT1 SAMPLES (continued) | | | | |
|---|---------------------------|-------------|-------------|--|
| Site/DDH depth | Intensity (microgauss) | Declination | Inclination | |
| 125 m | 5.1 | 264 | +02 | |
| 130 m | 0.04 | 282 | -80 | |
| 140 m | 0.3 | 167 | +40 | |
| 155 m | 0.6 | 332 | -07 | |
| 175 m | 0.1 | 161 | -44 | |
| 200 m | 57 | 098 | +63 | |
| 230 m | 4.2 | 127 | +61 | |
| 245 m | 0.01 | 074 | -67 | |
| 260 m | 598 | 097 | +65 | |
| 272 m | 0.2 | 346 | +25 | |
| 290 m | 0.03 | 263 | +18 | |
| PT1 combined | 41 | 101 | +70 | |

TABLE 6
 SUSCEPTIBILITIES AND KOENIGSBERGER RATIOS OF TRAVERSE IV SAMPLES

| Site | Lithology | Stratigraphic position | k | Q |
|------|-----------|------------------------|------|------|
| 41 | Lf | Bh? | 6 | 0.23 |
| 42 | FM-FS | Bh? | 4900 | 0.47 |
| 43 | a | Bh? | 1960 | 4.4 |
| 44 | a | Bh? | 6610 | 1.3 |
| 45 | a | Bh? | 98 | 0.34 |
| 46 | rE | Bh? | 18 | 0.13 |
| 47 | a | Bh? | 82 | 0.00 |
| 48 | M | S? | 16 | 0.01 |
| 49 | E-M | S? | 27 | 0.03 |
| 50 | E | S? | 25 | 0.00 |
| 51 | M | S? | 32 | 0.01 |
| 52 | M | S? | 16 | 0.04 |
| 53 | Lq | Bh? | 4 | 0.20 |

TABLE 7

MEAN NRM VECTORS OF TRAVERSE IV SAMPLES

| Site/DDH depth | Intensity (microgauss) | Declination | Inclination |
|----------------|---------------------------|-------------|-------------|
| 41 | 0.8 | 210 | +53 |
| 42 | 1330 | 355 | +06 |
| 43 | 5050 | 352 | -03 |
| 44 | 4960 | 135 | +25 |
| 45 | 19 | 273 | +40 |
| 46 | 1.4 | 141 | -81 |
| 47 | 0.2 | 205 | +65 |
| 48 | 0.05 | 325 | -01 |
| 49 | 0.5 | 249 | +69 |
| 50 | 0.07 | 252 | -54 |
| 51 | 0.2 | 013 | -74 |
| 52 | 0.3 | 045 | -31 |
| 53 | 0.5 | 354 | -53 |

TABLE 8
 SUSCEPTIBILITIES AND KOENIGSBERGER RATIOS OF TRAVERSE V SAMPLES

| Site | Lithology | Stratigraphic position | k | Q |
|------|-----------|------------------------|----|------|
| 54 | M | Ba? | 24 | 0.09 |
| 55 | M | Ba? | 29 | 0.03 |
| 56 | M | Ba? Bs? | 25 | 0.11 |
| 57 | FE | Bs? | 30 | 0.16 |
| 58 | M-E | Bs? | 22 | 0.41 |
| 59 | E | Bs? | 20 | 0.90 |
| 60 | E | Bs? | 22 | 0.73 |
| 61 | G | - | 69 | 23 |
| 62 | M | Bs? | 25 | 0.36 |
| 63 | EM | Bs? | 24 | 0.12 |
| 64 | Lf | Bs? | 8 | 0.09 |
| 65 | E | S? | 23 | 0.05 |
| 66 | E | S? | 24 | 0.23 |
| 67 | S-M | S? | 23 | 0.06 |
| 68 | EM | S? | 32 | 0.05 |
| 69 | E | S? | 21 | 0.03 |
| 70 | E | S? | 13 | 0.05 |
| 71 | rm | S? | 32 | 0.47 |
| 72 | BG? Lq? | Bh? | 38 | 0.00 |
| 73 | M | Bh? | 32 | 0.08 |
| 74 | FM-M | Bh? | 24 | 0.03 |
| 75 | FM-M | Bh? | 33 | 0.01 |
| 76 | FM-M | Bh? | 32 | 0.04 |

TABLE 9

MEAN NRM VECTORS OF TRAVERSE V SAMPLES

| Site/DDH depth | Intensity (microgauss) | Declination | Inclination |
|----------------|---------------------------|-------------|-------------|
| 54 | 1.2 | 030 | -56 |
| 55 | 0.5 | 322 | -59 |
| 56 | 1.5 | 296 | -10 |
| 57 | 2.7 | 349 | -59 |
| 58 | 5.2 | 011 | -63 |
| 59 | 11.5 | 010 | -61 |
| 60 | 9.4 | 020 | -61 |
| 61 | 905 | 322 | -33 |
| 62 | 5.2 | 357 | -56 |
| 63 | 1.7 | 351 | -70 |
| 64 | 0.4 | 007 | -43 |
| 65 | 0.6 | 022 | -50 |
| 66 | 3.2 | 022 | -61 |
| 67 | 0.7 | 356 | -57 |
| 68 | 1.0 | 347 | -61 |
| 69 | 0.3 | 056 | -85 |
| 70 | 4.4 | 155 | +33 |
| 71 | 8.8 | 018 | -59 |
| 72 | 0.09 | 333 | +30 |
| 73 | 1.4 | 012 | -68 |
| 74 | 0.3 | 033 | -59 |
| 75 | 1.0 | 172 | +45 |
| 76 | 0.8 | 341 | -44 |

TABLE 10
 SUSCEPTIBILITIES AND KOENIGSBERGER RATIOS OF TRAVERSE VI SAMPLES

| Site | Lithology | Stratigraphic position | k | Q |
|------|-----------|------------------------|-----|------|
| 77 | M | Bh? | 30 | 1.2 |
| 78 | Lf | Bh? | 3 | 0.41 |
| 79 | ae | Bh? | 120 | 0.00 |
| 80 | rFE | Bh? | 26 | 0.17 |
| 81 | FMg | Bh? | 22 | 0.27 |
| 82 | (F)M | Bh? S? | 46 | 0.16 |
| 83 | M(g) | S? | 19 | 0.01 |
| 84 | (F)EMg | S? | 31 | 0.01 |
| 85 | (F)M | S? | 11 | 0.03 |

TABLE 11

MEAN NRM VECTORS OF TRAVERSE VI SAMPLES

| Site/DDH depth | Intensity (microgauss) | Declination | Inclination |
|----------------|---------------------------|-------------|-------------|
| 77 | 2.1 | 333 | -29 |
| 78 | 0.7 | 186 | +63 |
| 79 | 0.1 | 074 | +06 |
| 80 | 2.5 | 071 | -69 |
| 81 | 3.5 | 088 | -51 |
| 82 | 4.2 | 020 | -55 |
| 83 | 0.2 | 312 | +28 |
| 84 | 0.1 | 356 | -10 |
| 85 | 0.2 | 088 | +34 |

TABLE 12
 SUSCEPTIBILITIES AND KOENIGSBERGER RATIOS OF TRAVERSE VII SAMPLES

| Site | Lithology | Stratigraphic position | k | Q |
|-------|-----------|------------------------|----|------|
| 86 | rM | Bp? | 28 | 0.10 |
| 87 | E | Bp? | 29 | 0.37 |
| 88 | rE-rM | Bp? | 29 | 0.02 |
| 89 | E-M | Bp? | 32 | 0.00 |
| 90 | M | Bf? | 30 | 0.05 |
| 91 | M | Bf? | 23 | 0.01 |
| 92 | E | Bf? | 23 | 1.6 |
| 93 | S | Bf? | 33 | 0.25 |
| 94 | M | Bf? | 30 | 0.06 |
| 95 | E-M | Bf? | 25 | 0.74 |
| 96 | rE-rM | Bf? | 24 | 0.17 |
| 97 | S | Bf? | 20 | 4.5 |
| 86-97 | - | Bs? | 27 | 0.25 |

TABLE 13

MEAN NRM VECTORS OF TRAVERSE VII SAMPLES

| Site/DDH depth | Intensity (microgauss) | Declination | Inclination |
|----------------|---------------------------|-------------|-------------|
| 86 | 1.7 | 004 | -70 |
| 87 | 6.3 | 295 | -26 |
| 88 | 0.3 | 327 | -17 |
| 89 | 0.03 | 169 | +56 |
| 90 | 0.9 | 359 | -58 |
| 91 | 0.2 | 040 | +33 |
| 92 | 22 | 025 | -64 |
| 93 | 4.8 | 270 | +33 |
| 94 | 1.1 | 205 | +26 |
| 95 | 11 | 010 | -60 |
| 96 | 2.3 | 302 | +69 |
| 97 | 53 | 081 | +29 |

TABLE 14
 SUSCEPTIBILITIES AND KOENIGSBERGER RATIO OF TRAVERSE VIII SAMPLES

| Site | Lithology | Stratigraphic position | k | Q |
|------|-----------|------------------------|-----|------|
| 98 | E | Bp? | 32 | 0.32 |
| 99 | a | Bp? Bf? | 90 | 0.01 |
| 100 | Lf | Bf | 4 | 0.19 |
| 101 | Lf | Bf | 4 | 0.04 |
| 102 | BG | Bh | 21 | 0.05 |
| 103 | Lf | Bh | 3 | 0.14 |
| 104 | S | Bh | 9 | 0.02 |
| 105 | S | Bh | 12 | 0.16 |
| 106 | M | Bh | 29 | 0.03 |
| 107 | BG | Bh | 24 | 0.03 |
| 108 | E | S | 40 | 0.05 |
| 109 | E | S | 24 | 0.05 |
| 110 | rm | S | | |
| 111 | M | S | 29 | 0.29 |
| 112 | E(M) | S | 22 | 0.04 |
| 113 | M | S | 850 | 1.0 |
| 114 | S | S | 28 | 0.03 |
| 115 | E | S | 27 | 0.89 |
| 116 | M-E | s | 21 | 0.07 |
| 117 | EM | S | 940 | 8.8 |
| 118 | M | Bs | 24 | 2.0 |
| 119 | E | Bs | 19 | 4.0 |
| 120 | E | Bs | | |
| 121 | BG | Bs | 30 | 0.56 |
| 122 | BG | Bs | 29 | 0.29 |
| 123 | BG | Bs | 21 | 0.09 |
| 124 | BG | Bs | 36 | 0.02 |
| 125 | a | Bs | 63 | 0.20 |
| 126 | ag | Bs | 58 | 0.03 |
| 127 | Lf | Bs | 4 | 0.06 |

| | | | | |
|-----|------|----|------|------|
| 128 | a | Ba | 94 | 0.27 |
| 129 | a-ax | Ba | 56 | 0.02 |
| 130 | a | Ba | 85 | 0.01 |
| 131 | qf | Tc | 22 | 2.4 |
| 132 | rM | Tc | 230 | 0.80 |
| 133 | E | Tc | 3130 | 5.1 |
| 134 | Lq | Tc | 21 | 0.08 |
| 135 | qf | Tc | 45 | 5.2 |
| 136 | a | Ba | 71 | 0.00 |

| | | | | |
|--------|---|----|----|------|
| 98-107 | - | Bs | 23 | 0.05 |
|--------|---|----|----|------|

| | | | | |
|---------|---|---|-----|-----|
| 108-117 | - | S | 160 | 5.2 |
|---------|---|---|-----|-----|

| | | | | |
|---------|---|----|----|------|
| 118-127 | - | Bs | 32 | 0.39 |
|---------|---|----|----|------|

| | | | | |
|-------------|---|----|----|------|
| 128-130,136 | a | Ba | 78 | 0.08 |
|-------------|---|----|----|------|

| | | | | |
|---------|---|----|-----|-----|
| 131-135 | - | Tc | 690 | 4.7 |
|---------|---|----|-----|-----|

TABLE 15

MEAN NRM VECTORS OF TRAVERSE VIII SAMPLES

| Site/DDH depth | Intensity (microgauss) | Declination | Inclination |
|----------------|---------------------------|-------------|-------------|
| 98 | 6.0 | 102 | -35 |
| 99 | 0.4 | 344 | -64 |
| 100 | 0.4 | 333 | +04 |
| 101 | 0.09 | 030 | -32 |
| 102 | 0.6 | 055 | -74 |
| 103 | 0.2 | 136 | -26 |
| 104 | 0.1 | 119 | +47 |
| 105 | 1.1 | 063 | +55 |
| 106 | 0.6 | 337 | -52 |
| 107 | 0.4 | 285 | +30 |
| 108 | 1.2 | 039 | +33 |
| 109 | 0.7 | 009 | -51 |
| 111 | 4.9 | 029 | -61 |
| 112 | 0.5 | 018 | -52 |
| 113 | 492 | 300 | -14 |
| 114 | 0.5 | 305 | +11 |
| 115 | 14 | 012 | -68 |
| 116 | 0.8 | 340 | -66 |
| 117 | 4776 | 144 | +30 |
| 118 | 27 | 007 | -67 |
| 119 | 44 | 023 | -64 |
| 121 | 9.6 | 035 | +78 |
| 122 | 4.9 | 308 | +76 |
| 123 | 1.1 | 121 | -71 |

TABLE 15
(continued)

MEAN NRM VECTORS OF TRAVERSE VIII SAMPLES

| Site/DDH depth | Intensity (microgauss) | Declination | Inclination |
|----------------|---------------------------|-------------|-------------|
| 124 | 0.4 | 355 | -12 |
| 125 | 7.3 | 346 | -15 |
| 126 | 0.9 | 063 | +79 |
| 127 | 0.1 | 331 | +61 |
| 128 | 15 | 231 | +27 |
| 129 | 0.7 | 045 | -46 |
| 130 | 0.5 | 124 | +35 |
| 131 | 31 | 214 | +35 |
| 132 | 185 | 188 | -31 |
| 133 | 9320 | 132 | -04 |
| 134 | 1.0 | 342 | -27 |
| 135 | 136 | 271 | -47 |
| 136 | 0.07 | 044 | -30 |
| ----- | | | |
| 98-107 | 0.6 | 087 | -38 |
| ----- | | | |
| 108-117 | 481 | 147 | +32 |
| ----- | | | |
| 118-127 | 7.3 | 012 | -53 |
| ----- | | | |
| 128-130, 136 | 3.5 | 230 | +27 |
| ----- | | | |
| 131-135 | 1870 | 134 | -05 |
| ----- | | | |

TABLE 16
 SUSCEPTIBILITIES AND KOENIGSBERGER RATIOS FOR TRAVERSE IX SAMPLES

| Site | Lithology | Stratigraphic position | k | Q |
|------|-----------|------------------------|------|------|
| 137 | a | Bp? | 93 | 0.03 |
| 138 | BG | Bp? | 32 | 0.01 |
| 139 | BG | Bp? | 26 | 0.04 |
| 140 | Lq | Bf? | 4 | 0.21 |
| 141 | rm-rLq? | Bf? | 7530 | 4.2 |
| 142 | Lq | Bf? | 3 | 0.09 |
| 143 | a | Bf? | 29 | 0.04 |

TABLE 17

MEAN NRM VECTORS OF TRAVERSE IX SAMPLES

| Site/DDH depth | Intensity (microgauss) | Declination | Inclination |
|----------------|---------------------------|-------------|-------------|
| 137 | 1.6 | 047 | -71 |
| 138 | 0.3 | 316 | -62 |
| 139 | 0.7 | 286 | -45 |
| 140 | 0.5 | 357 | -47 |
| 141 | 18310 | 232 | +72 |
| 142 | 0.2 | 019 | -30 |
| 143 | 0.6 | 350 | -39 |

TABLE 18
 SUSCEPTIBILITIES AND KOENIGSBERGER RATIOS FOR DDH NR1, DDH BMX1
 AND DDH TH2 SAMPLES

| Sample | Lithology | Stratigraphic position | k | Q |
|--------------|----------------|------------------------|------|------|
| NR1-92 m | bif/BG | Bp | 4210 | 0.27 |
| NR1-111 m | SE (+ mt, po) | Bp | 200 | 0.05 |
| NR1-160 m | a-ag | Bp | 87 | 0.00 |
| BMX1-150 m | qm(+po) in FSM | Tt? Tc? | 8590 | 0.19 |
| BMX1-159.5 m | M-qm(+po) | Tt? Tc? | 1290 | 0.57 |
| BMX1-180 m | FSM (+po) | Tt? Tc? | 75 | 0.40 |
| BMX1-197 m | FSM (+g) | Tt? Tc? | 35 | 0.16 |
| TH2-35 m | E(+po) | Tc | 49 | 0.00 |
| TH2-96 m | SM(+po) | Tc | 30 | 0.09 |
| TH2-150 m | S(+po) | Tc | 14 | 0.36 |
| TH2-175 m | S(+po) | Tc | 1640 | 0.26 |
| TH2-203.5 m | Bm-BG | Tc | 75 | 0.00 |

TABLE 19

MEAN NRM VECTORS OF DDH NR1, DDH BMX1 AND DDH TH2 SAMPLES

| Site/DDH depth | Intensity (microgauss) | Declination | Inclination |
|----------------|---------------------------|-------------|-------------|
| NR1-92 m | 665 | 227 | +02 |
| NR1-111 m | 6.1 | 194 | -74 |
| NR1-160 m | 0.1 | 248 | -55 |
| BMX1-150 m | 941 | 028 | -59 |
| BMX1-159.5 m | 430 | 281 | -61 |
| BMX1-180 m | 18 | 241 | +11 |
| BMX1-197 m | 3.3 | 076 | -03 |
| TH2-35 m | 0.1 | 258 | +36 |
| TH2-96 m | 1.5 | 347 | -71 |
| TH2-150 m | 2.9 | 311 | -53 |
| TH2-175 m | 250 | 050 | -62 |
| TH2-203 m | 0.1 | 110 | +12 |

TABLE 20

MAGNETIC STRATIGRAPHY OF THE RISE AND SHINE AREA

| Stratigraphic position | Magnetic signature | |
|---|------------------------|------------------------|
| Lower(?) Sundown Group (not basal) | (15 km; 1 km; 1100nT) | |
| | WESTERN LODE | EASTERN LODE |
| Hores Gneiss (middle to upper, but below top) | (>6 km; 500 m; 250 nT) | (300 m; 300 m; 100 nT) |
| Freyers Metasediments | (300 m; 300 m; 100 nT) | - |
| Parnell Formation (adjacent to lode horizon) | (>6 km; 400 m; 250 nT) | (>5 km; 800 m; 100 nT) |
| Thackaringa Group | (>3 km; 1 km; 450 nT) | (>5 km; 300 m; -80 nT) |

Magnetic signatures are characterised by: (total strike length of magnetic feature; typical strike length of individual anomalies; maximum anomaly amplitude).

TABLE 21

MAGNETIC STRATIGRAPHY OF THE RUPEE TREND AREA

| Stratigraphic position | Magnetic signature |
|--|--------------------------------------|
| Lower (?) Sundown Group (not basal) | (15 km; 5 km; 600 nT) |
| Hores Gneiss | non-magnetic |
| Freyers Metasediments | (15 km; 0.5-3.5 km; 100 nT) |
| Parnell Formation | (15 km; 0.5-2.5 km; 250 nT) |
| Allendale Metasediments | non-magnetic |
| Rasp Ridge Gneiss | non-magnetic |
| Cues Formation | (20 km; 2 km; 2000 nT) |
| Alma Gneiss | non-magnetic |
| Thorndale Composite Gneiss | (>12 km; 0.5-2.5 km; 250 nT) |
| Clevedale Migmatite | moderately to strongly magnetic zone |

APPENDIX I - SAMPLES COLLECTED FROM THE BROKEN HILL AREA

1. NORTHERN LEASES AREA (NORTH BROKEN HILL PTY LTD) - collected March, 1981

| Site Nos. | No. of samples | Lithology | Stratigraphic position | Locality (see Fig. 1) |
|------------------------|----------------|-----------------|------------------------|--|
| 1-9 [Traverse I] | 20 | BG ₁ | Bh | Mine antiform east of Thompson shaft; traverse from hinge of F ₂ structure to NW limb |
| 10-18 [Traverse II] | 19 | BG ₂ | Tr | Hanging Wall Synform defined by Lord's Hill granite gneiss |
| 19 | 3 | ax | Tc | SE limb of Round Hill Synform, SW of Round Hill Shaft |
| 20-21 | 3 | M+FM | S | F ₂ synform SE of Silver Peak shaft |
| 22 | 2 | rm | B? (Retrogressed) | Globe-Vauxhall shear zone at Silver Peak shaft |
| 23 | 8 | bif | Bp | SE of Imperial Ridge |

2. REDAN-FARMCOTE AREA (NBH LTD) - collected July 1979

| Site Nos. | No. of samples | Lithology | Stratigraphic position | Locality |
|-----------|----------------|-----------|------------------------|---|
| 24-1 | 7 | qf | T? | 2 km N of Byron Tank (EL 780) |
| 24-2 | 5 | qf-fe | T? | Fence gossan, line 1800E drill section 1070N (EL 780) |
| 24-3 | 3 | qm | T? | The Tors (Farmcote, EL 1067) |
| 24-4 | 5 | Pl(+mt) | T? | "Magnetic Redan Gneiss", north of the Tors (EL 1067) |
| 24-5 | 5 | a | tg? | 4.5 km NE of Farmcote homestead (EL 1067) |
| 24-6 | 4 | Czf | - | Haematite ferricrete, 1.5km ESE of Farmcote homestead (EL 1067) |
| 24-7 | 6 | qm | T? | NE of Mulculca homestead (Farmcote EL 1067) |
| 24-8 | 4 | Czf | - | SW of Edna's Tank (EL 1070) |
| 24-9 | 6 | Pl | T? | "Non-magnetic Redan Gneiss" 1km E of Oak's Tank (EL 1067) |

3. RISE AND SHINE PROSPECT (ABERFOYLE LTD) - collected October 1985

| Site Nos. | No. of samples | Lithology | Stratigraphic position | Locality (see Fig. 10) |
|-----------|----------------|-----------------|---------------------------------|---|
| 25-40 | 25 | - | Broken Hill Group (Bh→B→Bp)? | Traverse III through Broken Hill Group, adjacent to DDH PT1 |
| 25 | 2 | FE | Bh? (or S??) | 11510E, 31275N |
| 26 | 1 | FE | Bh? (or S??) | 11525E, 31260N |
| 27 | 1 | M | Bh? (or S??) | 11540E, 31245N |
| 28 | 2 | EM | Bh? (orS??) | 11545E, 31240N |
| 29 | 1 | M | Bh? | 11565E, 31230N |
| 30 | 2 | rm | Bh? | 11575E, 31215N |
| 31 | 1 | E | Bf? | 11600E, 31220N |
| 32 | 1 | M | Bf? | 11650E, 31205N |
| 33 | 1 | E | Bf? | 11605E, 31210N |
| 34 | 1 | S-M | Bf? | 11630E, 31190N |
| 35 | 1 | E | Bf? | 11700E, 31270N |
| 36 | 2 | ES | Bf? Bp? | 11725E, 31295N |
| 37 | 3 | EM/Lf? | Bf? Bp? | 11740E, 31300N |
| 38 | 2 | E | Bh? (or S??) | 11535E, 31240N (btwn 26,27) |
| 39 | 2 | ag | Bp? | 11620E, 30740N |
| 40 | 2 | bif | Bp? | 11660E, 30840N |
| DDH PT1 | 18 | - | (Bh→Bf→Bp)? | Adjacent to Traverse III |
| 10 m | 1 | BG ₂ | Bh? | |
| 17 m | 1 | P-FEM | Bh? | |
| 47 m | 1 | rm | Bh? | |
| 74 m | 1 | FEMg | Bf? | |
| 90 m | 1 | FEMg | Bf? | |
| 100 m | 1 | FEMg | Bf? | |
| 120 m | 1 | FSMg | Bf? | |
| 125 m | 1 | E-SE | Bf? | |
| 130 m | 1 | E-SE | Bf? | |
| 140 m | 1 | EM | Bf? | |
| 155 m | 1 | SE-E | Bf? | |
| 175 m | 1 | SE-E | Bf? | |
| 200 m | 1 | (F)EMg | Bf? | |
| 230 m | 1 | SE | Bf? | |
| 245 m | 1 | SE | Bf? | |
| 260 m | 1 | FSE | Bf? | |
| 272 m | 1 | ag | Bp? | |
| 290 m | 1 | rEM | Bp? | |
| 41-53 | 18 | | (Bh→S)? | Traverse IV through Broken Hill Group into Sundown Group |
| 41 | 2 | Lf | Bh? | 10370E, 30800N |
| 42 | 1 | FM-FS | Bh? | 10375E, 30820N |

| Site Nos. | No. of samples | Lithology | Stratigraphic position | Locality (see Fig. 10) |
|-----------|----------------|-----------|------------------------|---|
| 43 | 1 | a | Bh? | 10400E, 30815N |
| 44 | 1 | a | Bh? | 10405E, 30800N |
| 45 | 1 | a | Bh? | 10415E, 30800N |
| 46 | 1 | rE | Bh? | 10430E, 30800N |
| 47 | 1 | a | Bh? | 10455E, 30800N |
| 48 | 2 | M | S? | 10490E, 30825N |
| 49 | 1 | E-M | S? | 10500E, 30820N |
| 50 | 1 | E | S? | 10485E, 30815N |
| 51 | 1 | M | S? | 10500E, 30775N |
| 52 | 1 | M | S? | 10505E, 30780N |
| 53 | 4 | Lq | Bh? | 10400E, 30790N (btwn 42,43) |
| 54-76 | 47 | | Ba→Bs→ S→Bh | Traverse V (grid W-E, along ~28200N) |
| 54 | 2 | M | Ba? | ~9830E |
| 55 | 2 | M | Ba? | ~9870E |
| 56 | 2 | M | Ba? Bs? | ~9880E |
| 57 | 2 | FE | Bs? | ~9900E |
| 58 | 2 | M-E | Bs? | ~9960E |
| 59 | 2 | E | Bs? | ~10000E |
| 60 | 2 | E | Bs? | ~ 415 m W of tramway (~10050E) |
| 61 | 2 | G | - | ~360 m W of tramway |
| 62 | 2 | M | Bs? | ~330 m W of tramway |
| 63 | 2 | EM | Bs? | ~295 m W of tramway |
| 64 | 2 | Lf | Bh? | ~250 m W of tramway |
| 65 | 1 | E | S? | ~165 m W of tramway |
| 66 | 2 | E | S? | ~155 m W of tramway |
| 67 | 2 | S-M | S? | ~145 m W of tramway |
| 68 | 2 | EM | S? | ~135 m W of tramway |
| 69 | 2 | E | S? | ~115 m W of tramway |
| 70 | 2 | E | S? | ~95 m W of tramway |
| 71 | 2 | rm | S? | ~80 m W of tramway |
| 72 | 2 | BG? Lq? | Bh? | ~40 m W of tramway |
| 73 | 2 | M | Bh? | ~30 m W of tramway |
| 74 | 2 | FM-M | Bh? | ~20 m W of tramway |
| 75 | 3 | FM-M | Bh? | ~2 m W of tramway (10465E, 28220N) |
| 76 | 3 | FM-M | Bh? | ~10 m E of tramway |
| 77-85 | 19 | | (Bh→S)? | Traverse VI through Broken Hill Group (grid W-E along ~29400N) |
| 77 | 2 | M | Bh? | ~10500E, 29440N |
| 78 | 3 | Lf | Bh? | ~10550E, 29430N |
| 79 | 2 | ae | Bh? | ~10400E, 29400N |
| 80 | 3 | rFE | Bh? | ~10590E, 29400N |

| Site Nos. | No. of samples | Lithology | Stratigraphic position | Locality (see Fig. 10) |
|-----------|----------------|-----------|------------------------|---|
| 82 | 2 | (F)M | Bh? S? | ~10610E, 29400N |
| 83 | 2 | M(g) | Bh? S? | ~10630E, 29400N |
| 84 | 3 | (F)EMg | S? | 10800E, 29395N |
| 85 | 1 | (F)M | S? | 10800E, 29380N |
| 86-97 | 13 | | Broken Hill Group | Traverse VII W-E along ~32500N, from percussion holes in lode horizon towards Silver City highway |
| 86 | 1 | rM | Bp? | ~10050E, 32525N |
| 87 | 1 | E | Bp? | ~10120E |
| 88 | 1 | rE-rM | Bp? | ~10180E |
| 89 | 1 | E-M | Bp? | ~10240E |
| 90 | 1 | M | Bf? | ~10300E |
| 91 | 1 | M | Bf? | ~10400E |
| 92 | 1 | E | Bf? | ~10500E, 32380N |
| 93 | 1 | S | Bf? | ~10580E, 32380N |
| 94 | 1 | M | Bf? | ~10710E, 32420N |
| 95 | 1 | E-M | Bf? | ~10800E |
| 96 | 1 | rE-rM | Bf? | ~10900E |
| 97 | 1 | S | Bf? | ~11000E |

| Site Nos. | No. of samples | Lithology | Stratigraphic position | Locality (see Fig. 17,18) |
|-----------|----------------|--------------|------------------------|-------------------------------|
| 137 | 1 | a | Bf? Bp? | ~4075W, 12800N |
| 138 | 1 | BG | Bp | ~4150W |
| 139 | 1 | BG | Bp | ~4250W |
| 140 | 1 | Lq | Bf | ~4250W |
| 141 | 1 | rm-rLq? | Bf | ~4400W |
| 142 | 1 | Lq | Bf | ~4790W |
| 143 | 1 | a | Bf | ~4500W, 12300N |
| DDH NR1 | 3 | - | Bp | 3795W, 12200N (Rupee grid) |
| 92 m | 1 | bif-BG | | |
| 111 m | 1 | SE (+ mt,po) | | |
| 160 m | 1 | a-ag | | |

5. BMX PROSPECT, RUPEE TREND (BILLITON LTD.)

| Site Nos. | No. of samples | Lithology | Stratigraphic position | Locality (see Fig. 17,18) |
|-----------|----------------|-----------------|------------------------|--|
| DDH BMX1 | 4 | - | Tt? Tc? | 1355W, 1400N (Rupee grid ~ 4.25 km NE of airport) |
| 150 m | 1 | qm (+po) in FSM | | |
| 159.5 m | 1 | M-qm(+po) | | |
| 180 m | 1 | FSM(+po) | | |
| 197 m | 1 | FSM(+g) | | |

6. THORNDALE PROSPECT, RUPEE TREND (BILLITON LTD)

| Site Nos. | No. of samples | Lithology | Stratigraphic position | Locality (see Fig. 17,18) |
|-----------|----------------|-----------|------------------------|--|
| DDH TH2 | 5 | - | Tc | 525W, 1600S (Rupee grid, ~1.75 km E of airport) |
| 35 m | 1 | E(+po) | | |
| 96 m | 1 | SM(+po) | | |
| 150 m | 1 | S(+po) | | |
| 175 m | 1 | S(+po) | | |
| 203.5 m | 1 | Bm-BG | | |

APPENDIX II - STRATIGRAPHIC INDEX (ABRIDGED)

| Formation/Subgroup/Group | Description | Symbol |
|--------------------------|--|--------|
| Williyama Supergroup | Folded Lower Proterozoic metasedimentary and metaigneous rocks. | W |
| Sundown Group | "Pelite Suite": predominantly pelitic to psammopelitic metasediments, with calc-silicate nodules. Basic and felsic gneisses and lode horizon rocks absent. | S |
| Broken Hill Group | "Mine Sequence Suite": predominantly pelitic to psammopelitic/psammitic metasediments intercalated with felsic and basic gneisses. A basal metasediment unit (Ba) is overlain by the Purnamoota Subgroup. | B |
| Purnamoota Subgroup | Metasediment sequence with intercalated basic gneisses, garnet-rich felsic gneisses and lode horizon rocks (quartz-gahnite, garnet-quartz rocks). Subdivided into Parnell Formation (basal), Freyers Metasediments and Hores Gneiss (top). | Bs |
| Hores Gneiss | Mainly garnet-bearing felsic gneisses (BG) with metasediments, lode horizon rocks and bif. | Bh |
| Freyers Metasediments | Mainly pelitic-psammopelitic/psammitic schists, with rare basic gneiss, tourmaline-bearing and lode horizon rocks. | Bf |
| Parnell Formation | Extensive bodies of basic gneiss, lenticular masses of garnet-bearing felsic gneiss, and lode horizon rocks, bif and tourmaline-bearing rocks intercalated with pelitic to psammopelitic/psammitic metasediments. | Bp |

| | | |
|----------------------------|---|----|
| Allendale Metasediments | Mainly pelitic to psammopelitic/psammitic metasediments | Ba |
| Thackaringa Group | "Quartzofeldspathic Suite": predominantly quartz-feldspar-biotite gneisses and leucocratic plagioclase-quartz rocks. Subdivided into Lady Brassey Formation/Alma gneiss (basal lateral equivalents), Alders Tank Formation/Cues Formation, and Himalaya Formation/Rasp Ridge gneiss (lateral equivalents at top). | T |
| Rasp Ridge Gneiss | Typically a medium to fine-grained quartz-K feldspar-plagioclase-biotite ("granite") gneiss, with leucocratic quartz-feldspar phases and thin basic gneiss bodies. | Tr |
| Cues Formation | Mainly psammopelitic to psammitic composite gneisses or metasediments, with intercalated bodies of basic gneiss and stratiform horizons of garnet-quartz ± magnetite rocks and quartz-magnetite rocks. | Tc |
| Alders Tank Formation | Mainly psammitic to psammopelitic composite gneisses. Basic and quartzofeldspathic gneisses absent. | Tt |
| Alma Gneiss | Mainly medium to fine-grained quartz-feldspar-biotite ± garnet gneisses with K-feldspar or plagioclase megacrysts. | Ta |
| Thorndale Composite Gneiss | Predominantly metasedimentary quartz-feldspar-biotite-sillimanite ± garnet ± cordierite composite gneiss. | tg |
| Clevedale Migmatite | Basal exposed unit in Willyama Supergroup. Mainly migmatite to migmatitic composite gneiss which is often leucocratic. | cm |

APPENDIX III - Lithological/Mineralogical Index

| Category | Symbol | Description |
|---|---|--|
| <u>Metasediments</u> | | |
| | E | pelite [pelitic schist: (sillimanite/ andalusite + mica) > (quartz + feldspar)] |
| | S | psammite (psammitic quartz + feldspar rock with minor biotite, garnet and/or sillimanite) |
| | M | psammopelite (medium to coarse grained psammopelitic quartz + biotite + sillimanite ± feldspar ± garnet ± cordierite schist, gneiss or rock). |
| | EM | pelite/psammopelite-rich unit |
| | SM | psammite/psammopelite-rich unit |
| | SE | psammite/pelite rich unit. |
| <u>Metasedimentary Composite Gneisses</u> | | |
| | FS, FE, FM etc. | S, E, M etc. (50-90%), intimately intermixed with granitic/pegmatitic segregations. |
| | FS ₁ , FSM ₁ etc. | with garnet |
| | FS ₂ , FSM ₂ etc. | without garnet |
| <u>Quartzo-feldspathic Composite Gneiss</u> | | |
| | F1 | composite gneiss with leucocratic layers and abundant cordierite. |
| <u>Quartzo-feldspathic Gneisses</u> | | |
| | Bm | Medium to coarse-grained quartz + feldspar rich gneiss with >5% mafic minerals (biotite, garnet, magnetite, cordierite). |
| | Bm ₁ | Bm with rare garnet poikiloblasts |
| | Bm ₂ | Bm with coarse garnet poikiloblasts and K- feldspar megacrysts. |
| | Bc | As for Bm, with abundant very coarse K-feldspar megacrysts (Bc ₁) or lensoids (Bc ₂) ("augen gneiss"). |
| | BG | Medium to fine-grained quartz + feldspar + biotite gneiss with abundant, very coarse garnet. |

| Category | Symbol | Description |
|--|-----------------|--|
| | BG ₁ | BG with garnet porphyroblasts ("Potosi Gneiss") |
| | BG ₂ | BG with garnet poikiloblasts and feldspar augen. |
| | BS | medium to fine-grained quartz + feldspar + biotite + sillimanite gneiss. Gneissosity poorly developed (BS ₁) to well-developed (BS ₂). |
| <u>Leucocratic Quartzo-feldspathic Rocks</u> | | |
| | P | pegmatite (coarse to very coarse-grained K-feldspar-rich) |
| | Lq | leucocratic K-feldspar-rich coarser grained quartz + feldspar rock with 20-80% pegmatite |
| | Lf | leucocratic medium-grained quartz + K-feldspar ± plagioclase ± biotite gneiss or rock with <20% pegmatite. |
| | Pl | sodic plagioclase + quartz ± K-feldspar ± biotite rock with saccharoidal texture. |
| <u>Amphibolites/Basic Granulites</u> | | |
| | a | hornblende + plagioclase + quartz amphibolite |
| | ag | garnet amphibolite: similar to a, with garnet |
| | ae | epidote amphibolite: similar to a, with epidote |
| | ax | orthopyroxene + hornblende granulite |
| <u>Zinc, Manganese or Iron-rich Rocks</u> | | |
| | qg | quartz + gahnite ± feldspar ± garnet rock |
| | gs | fine-grained garnet ± quartz rock ("garnet sandstone") |
| | gq | medium to coarse-grained quartz + garnet rock ("garnet quartzite") |
| | bif | Broken Hill-type banded-iron formation (finely layered magnetite + garnet ± quartz ± apatite rock). |
| | qm | layered quartz-magnetite rock |
| | qf | quartz + secondary iron oxide (after iron sulphides) rock |
| | fe | ferruginous gossan |

| Category | Symbol | Description |
|---|-------------|--|
| | ts | tourmaline ± quartz ± mica schist |
| | lh | "lode horizon" rocks, e.g. qg, gs, gq, ts |
| <u>Retrograde Rocks</u> | | |
| | rE, rM etc. | retrogressed E, M etc. |
| | rm | micaceous schist (sericite + quartz ± chlorite schist) |
| <u>Post-folding Granitic Intrusives</u> | | |
| | G | granite |
| <u>Cainozoic Rock Units</u> | | |
| | Czf | ferricrete |
| <u>Minerals</u> | | |
| | g | garnet |
| | mt | magnetite |
| | hm | haematite |
| | mhm | maghaemite |
| | po | pyrrhotite |

Fig. 1. Geology and sampling localities in the Northern Leases

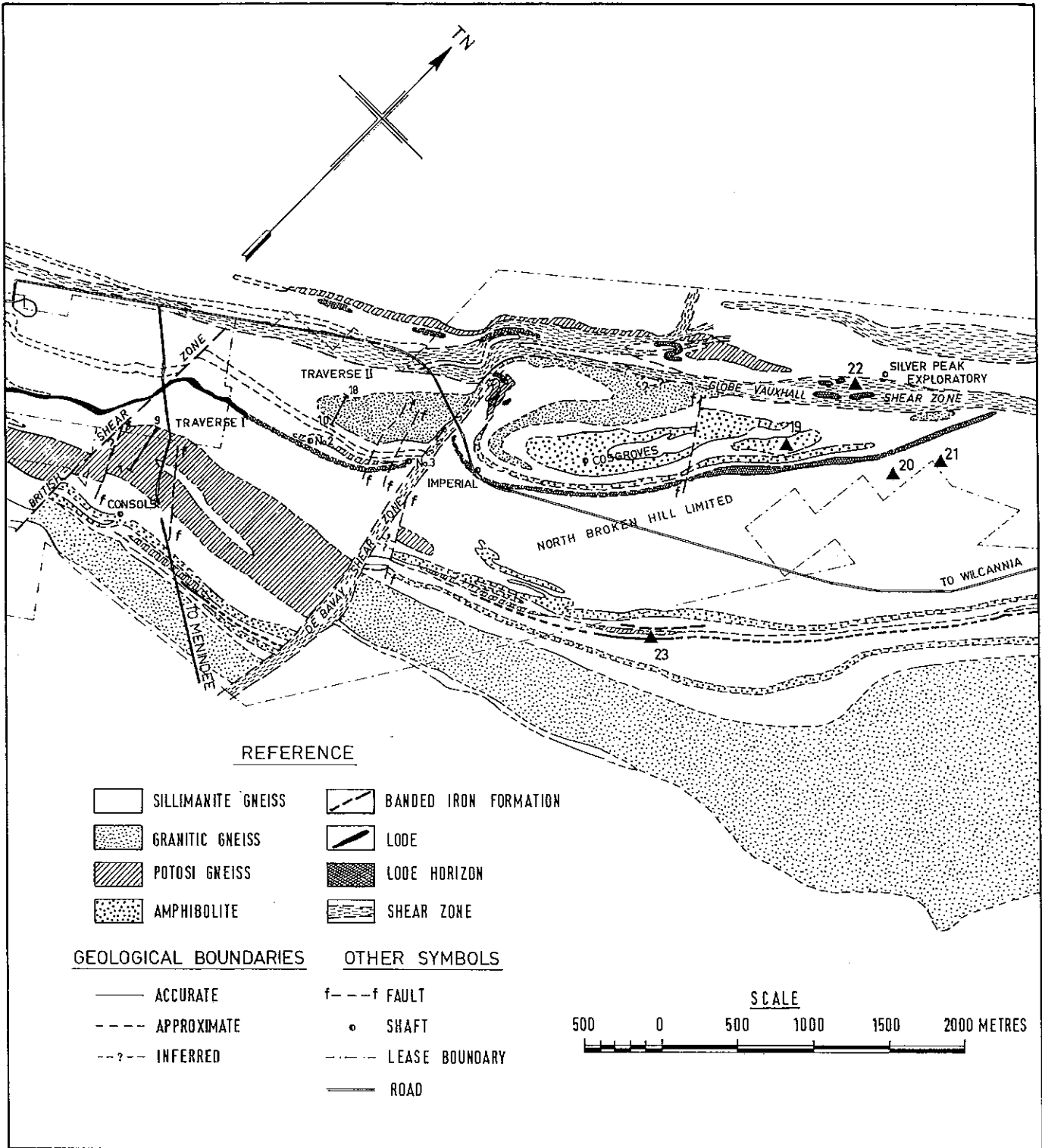


FIG. 1

Fig. 2. Magnetic fabric of sites 1-4. Major susceptibility axes (magnetic lineations) are represented by squares, intermediate axes are represented by triangles (sometimes omitted for clarity) and minor susceptibility axes are represented by dots. Estimated schistosity planes, their corresponding poles (represented by asterisks), mesoscopic lineations and fold axis plunges are also indicated.

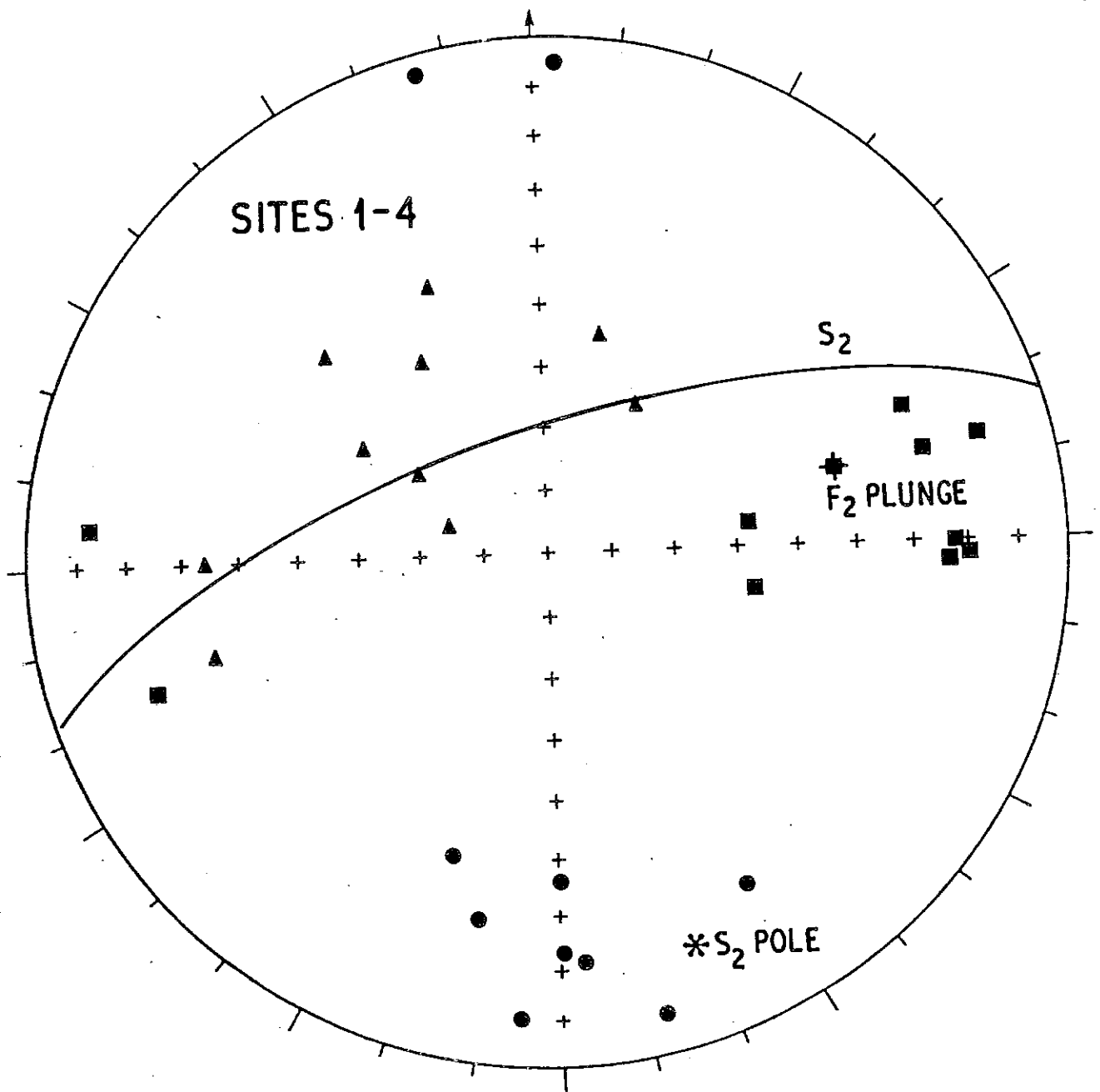


FIG. 2

Fig. 3. Magnetic fabric of sites 5-9. Symbols as for Fig.2.

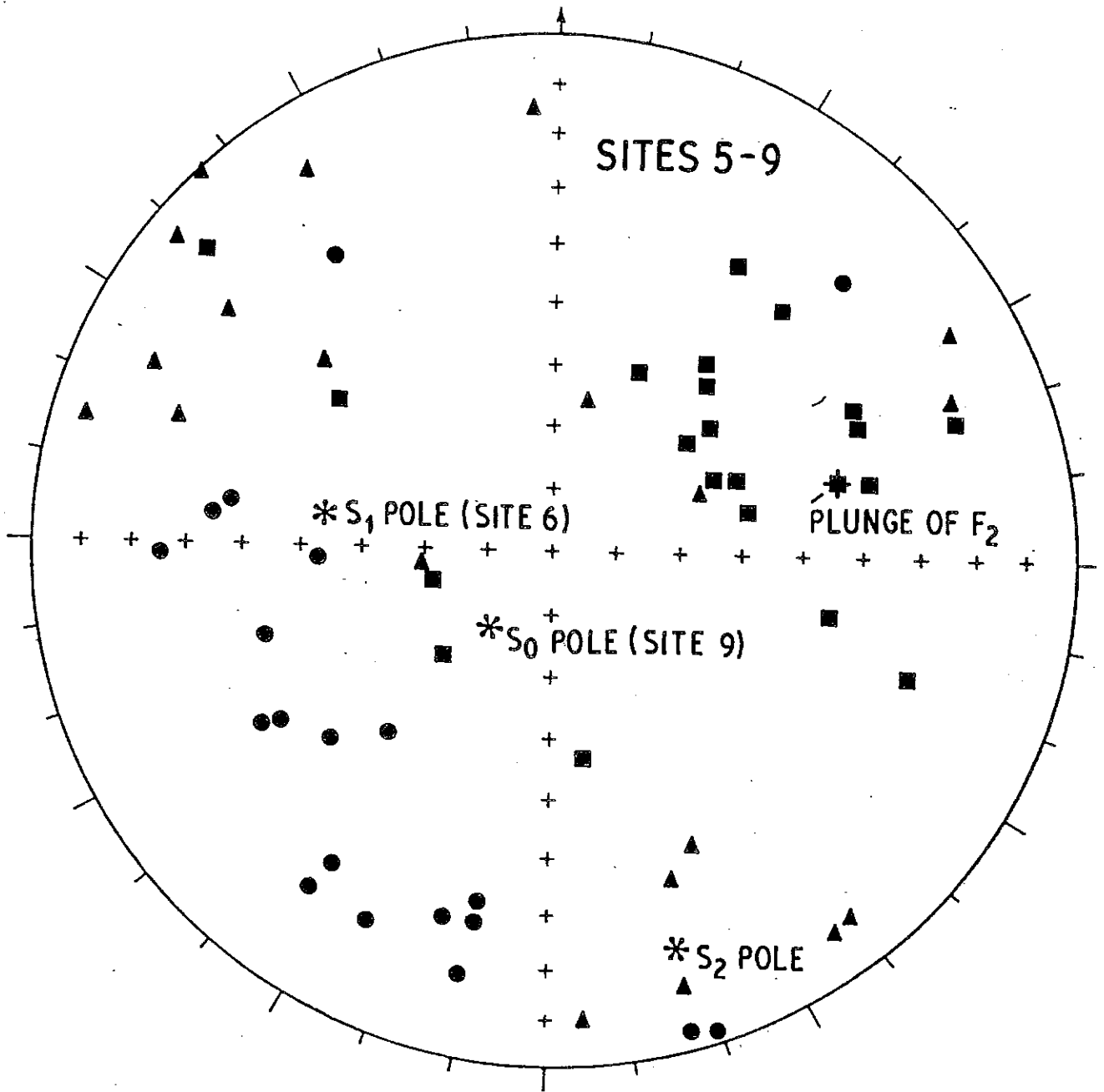


FIG. 3

Fig. 4. Magnetic fabric of sites 10-18. Magnetic lineations from specimens with prolate susceptibility ellipsoids and magnetic foliations from specimens with oblate ellipsoids are plotted. Symbols as for Fig.2.

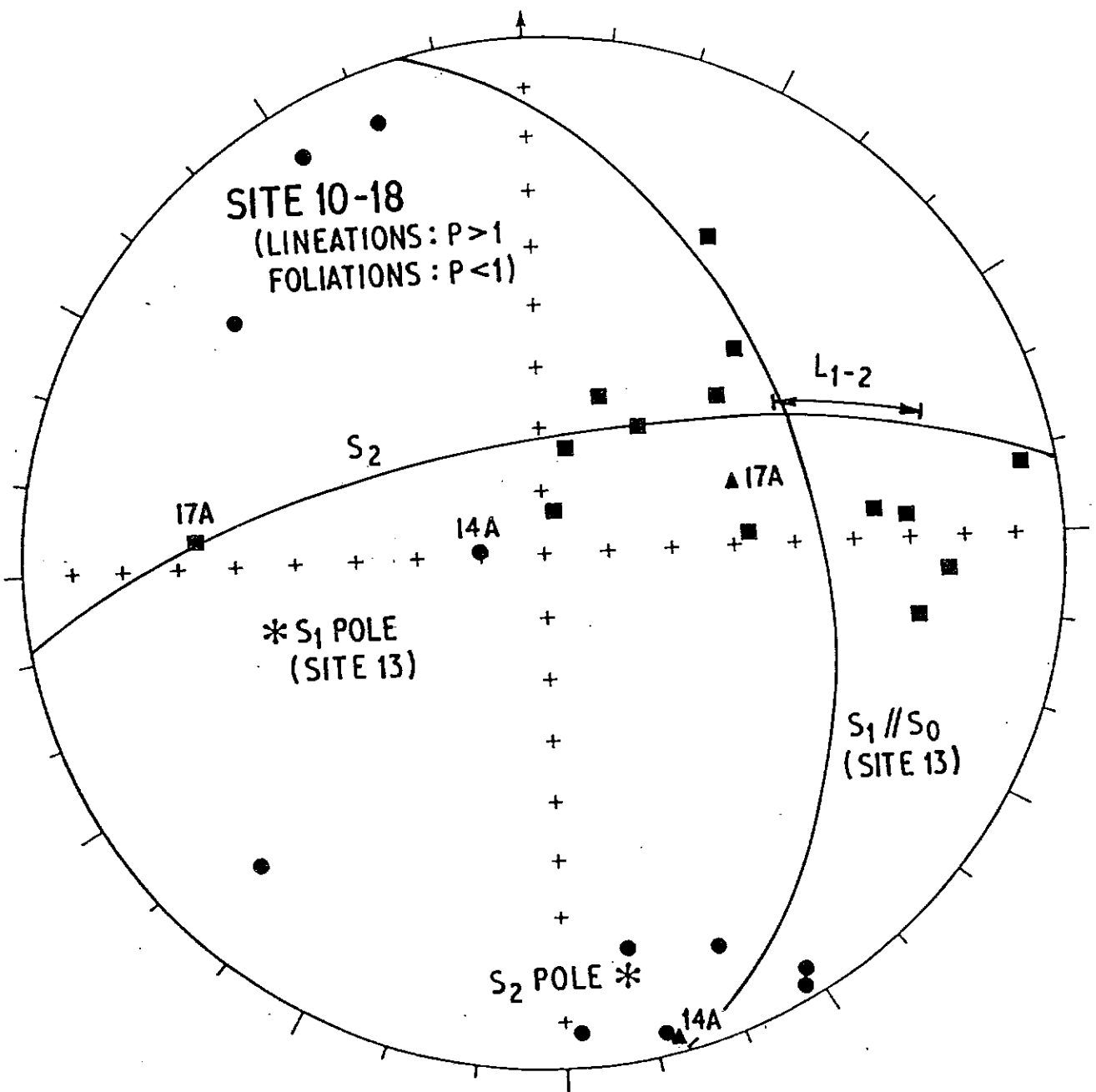


FIG.4

Fig. 5. Magnetic fabric of site 19. Symbols as for Fig.2.

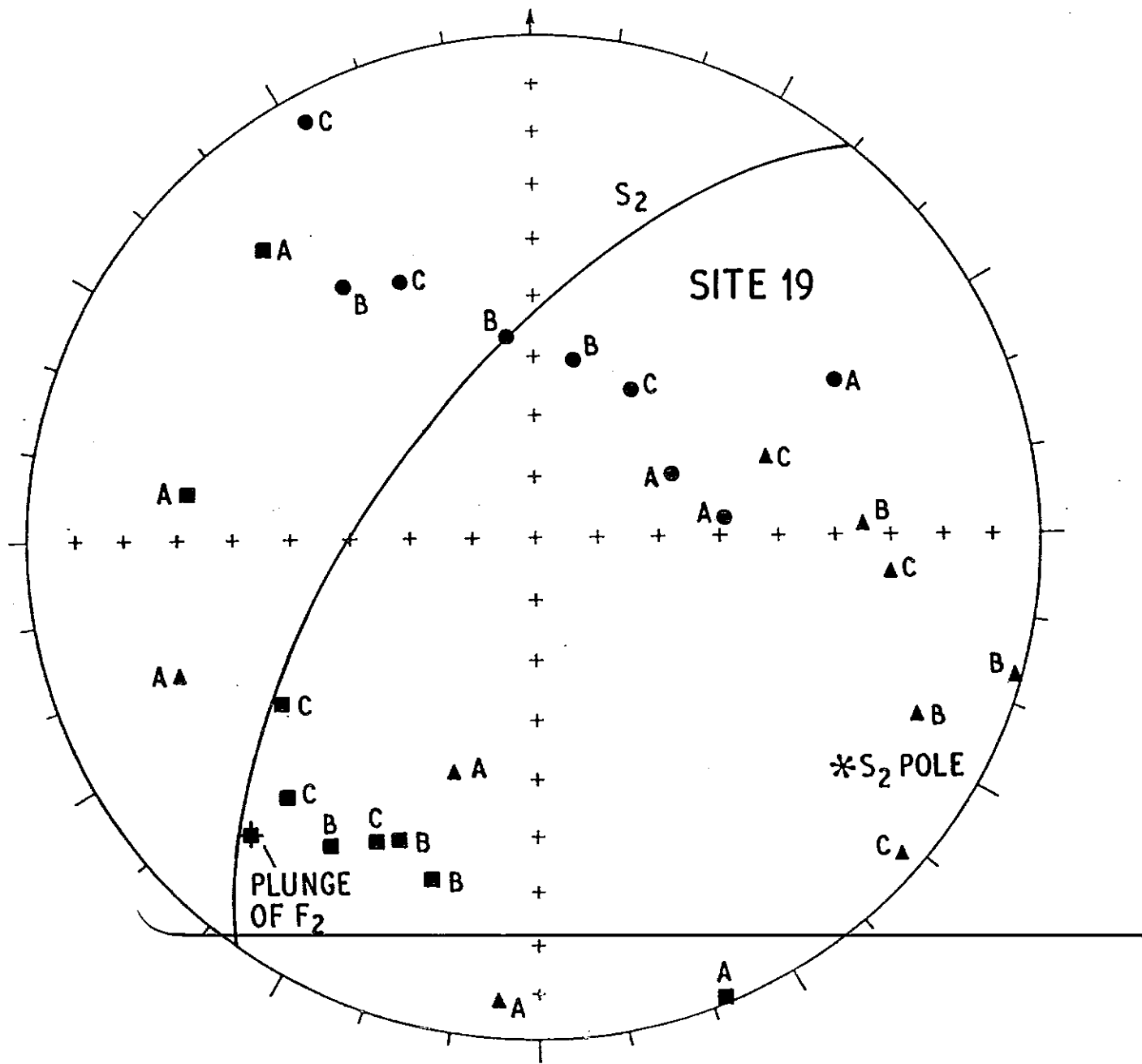


FIG.5

Fig. 6. Magnetic fabric of site 20. Symbols as for Fig.2.

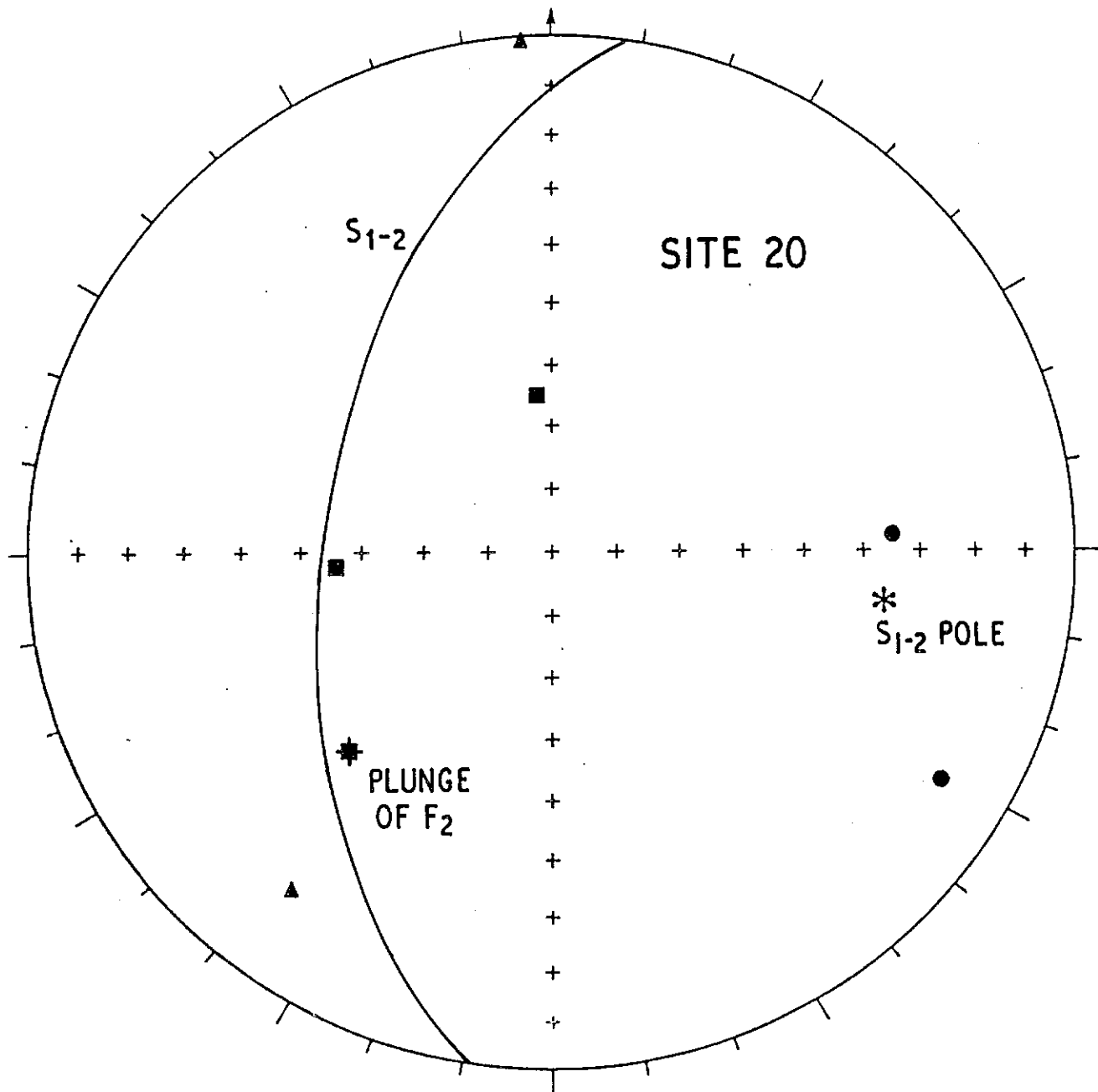


FIG.6

Fig. 7. Magnetic fabric of site 21. Symbols as for Fig.2.

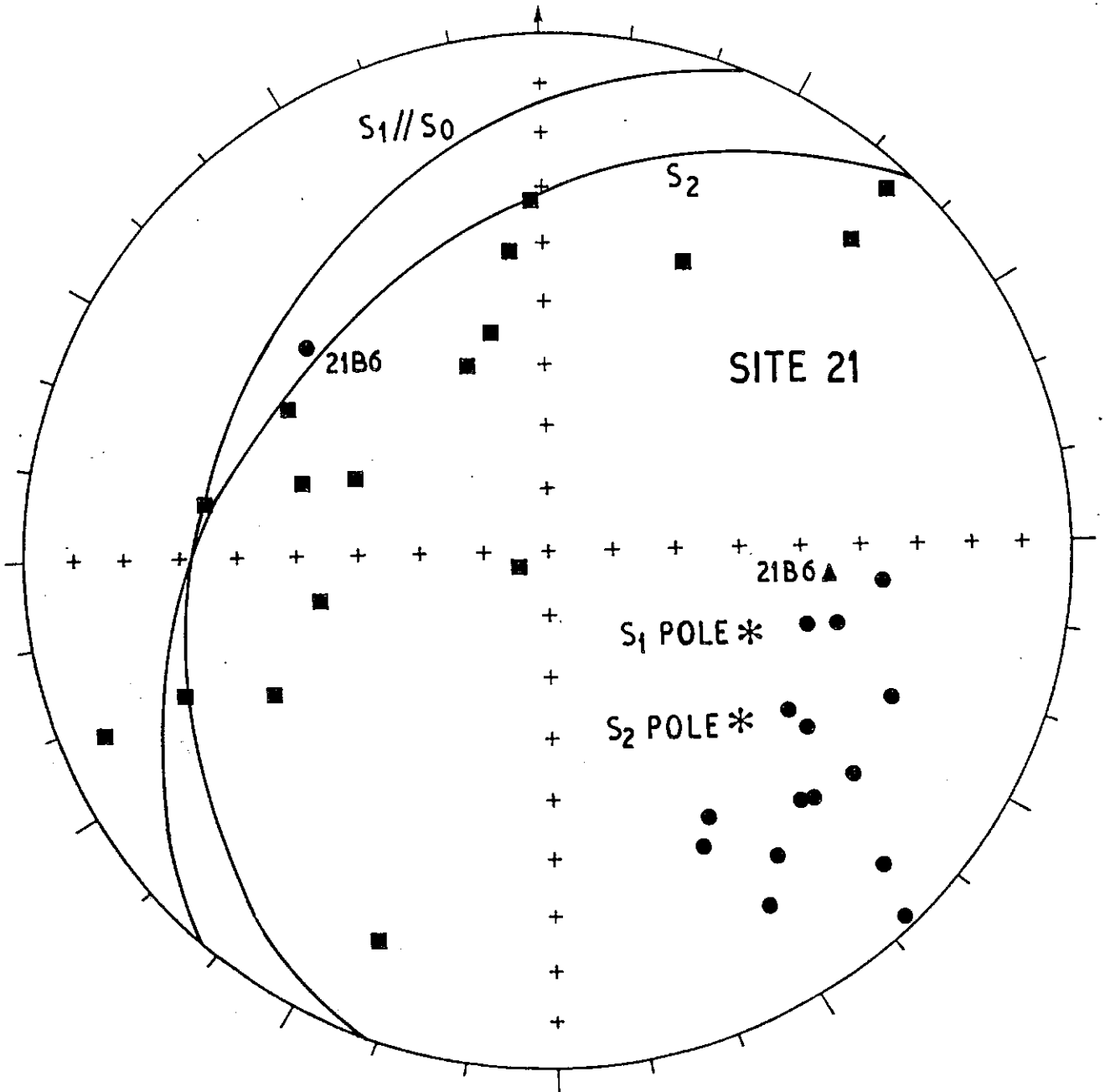


FIG.7

Fig. 8. Magnetic fabric of all specimens from site 22.
Symbols as for Fig.2.

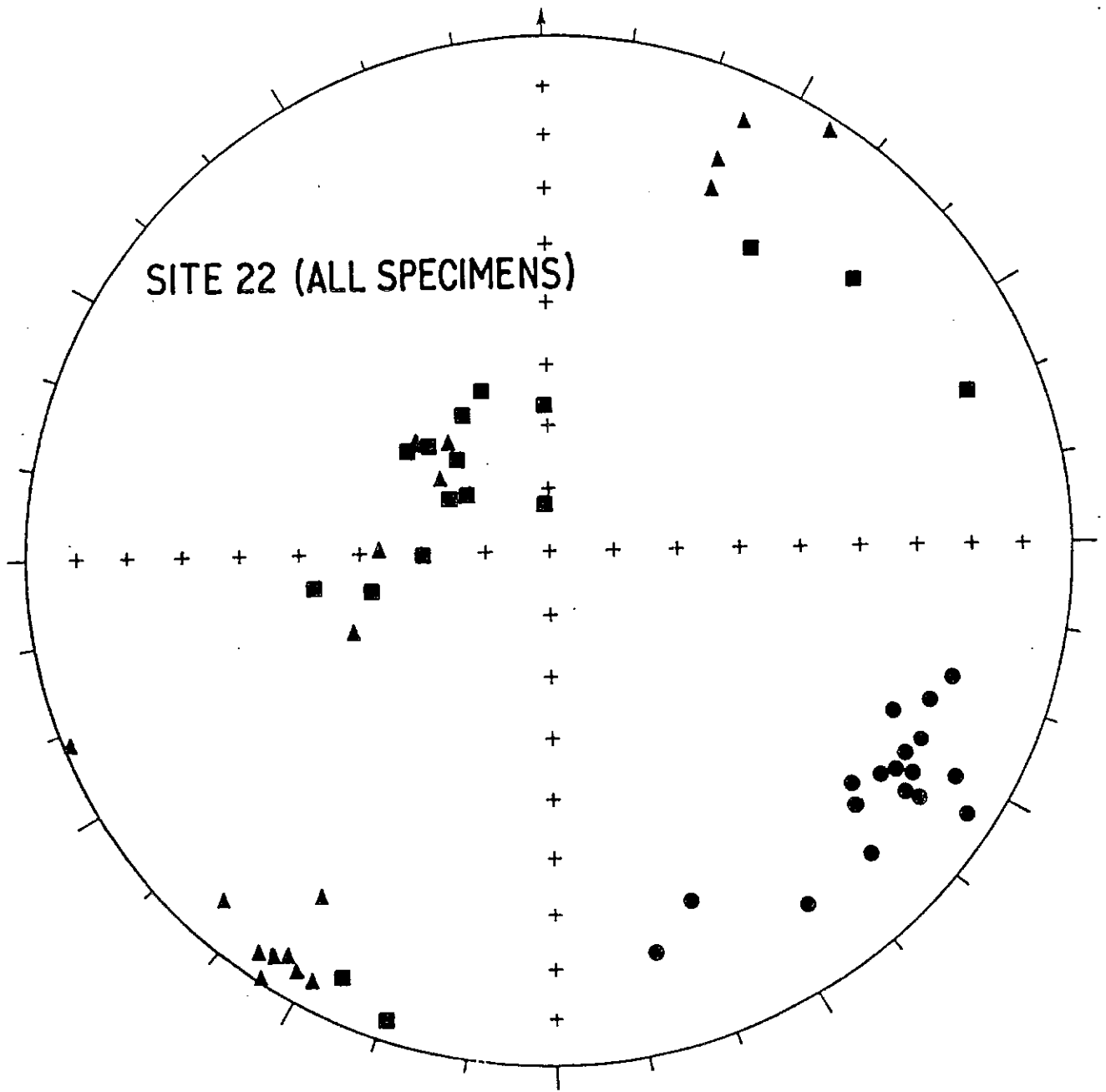


FIG.8

Fig. 9. Magnetic lineations of specimens with $L > 1.02$, magnetic foliation poles of specimens with $F > 1.02$ (site 22). Symbols as for Fig.2.

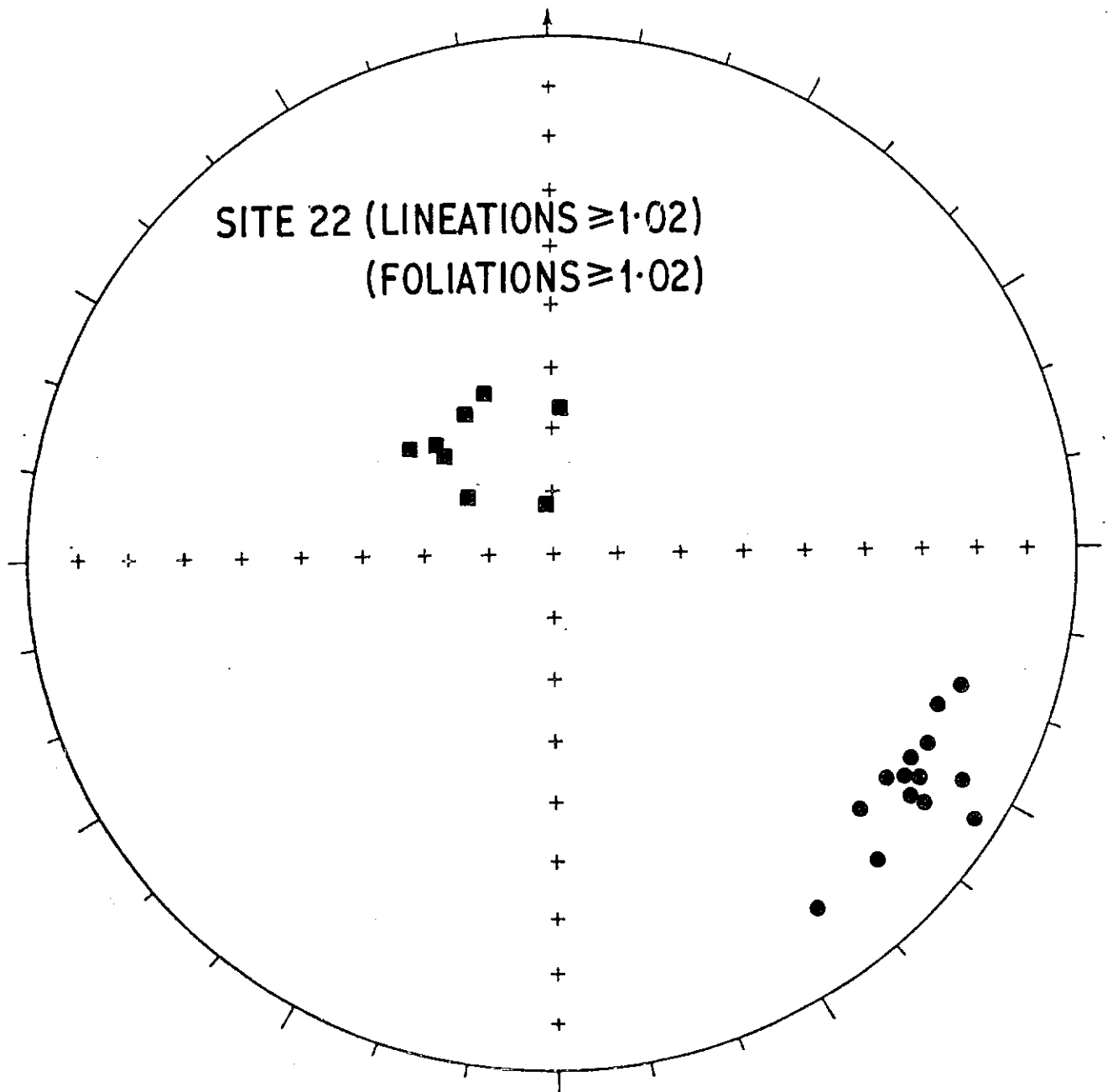


FIG.9

Fig.10. Geology and sampling localities of the Rise and Shine area.

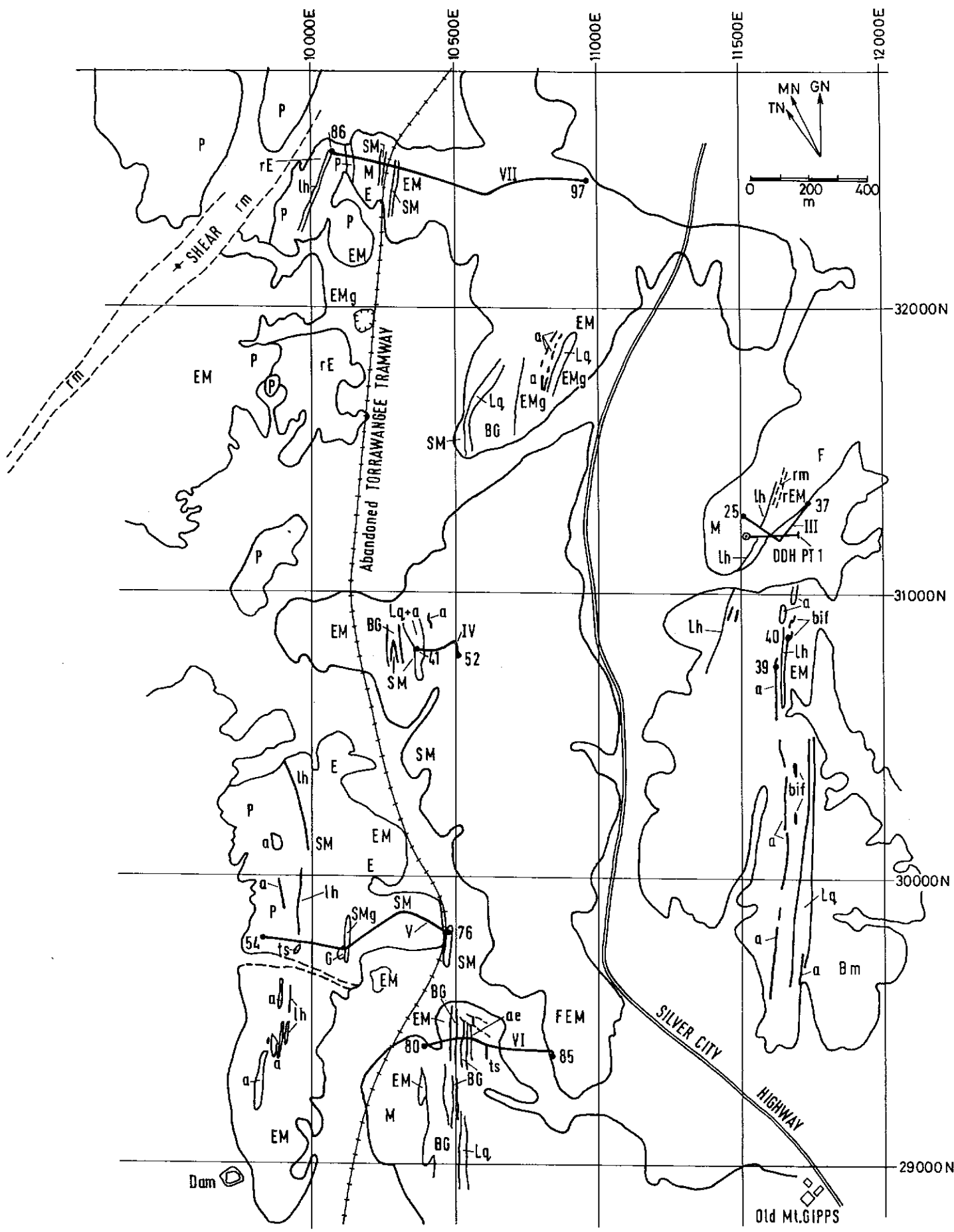


FIG.10

Fig.11. Peppertree Prospect (Rise and Shine) - geology and magnetics.

Fig.12. Magnetic fabric of the Peppertree Prospect DDH PT1 samples.
Symbols as for Fig.2.

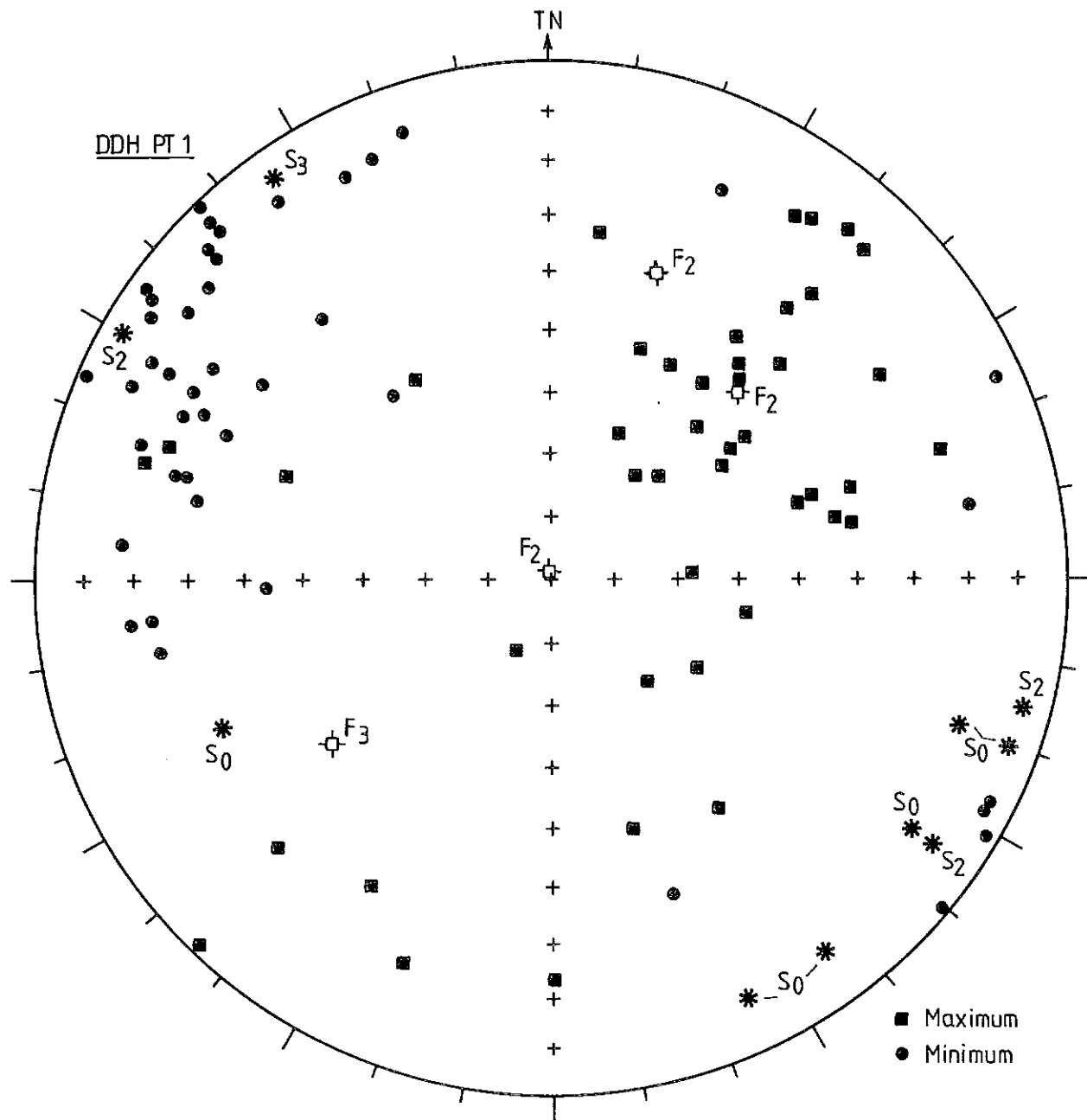


FIG.12

Fig.13. Magnetic fabric of the Traverse IV samples.
Symbols as for Fig.2.

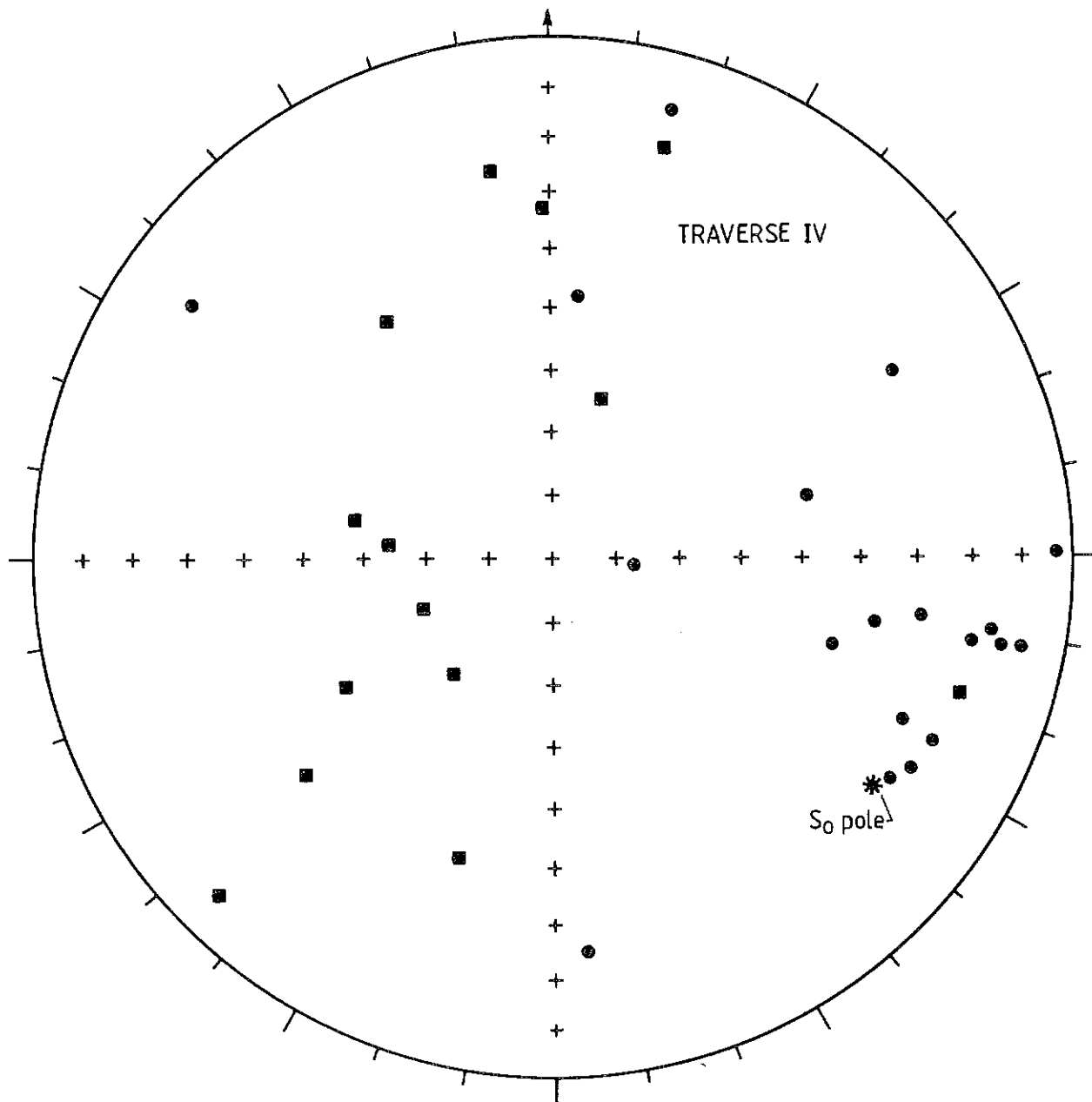


FIG.13

Fig.14. Magnetic fabric of the Traverse V samples.
Symbols as for Fig.2.

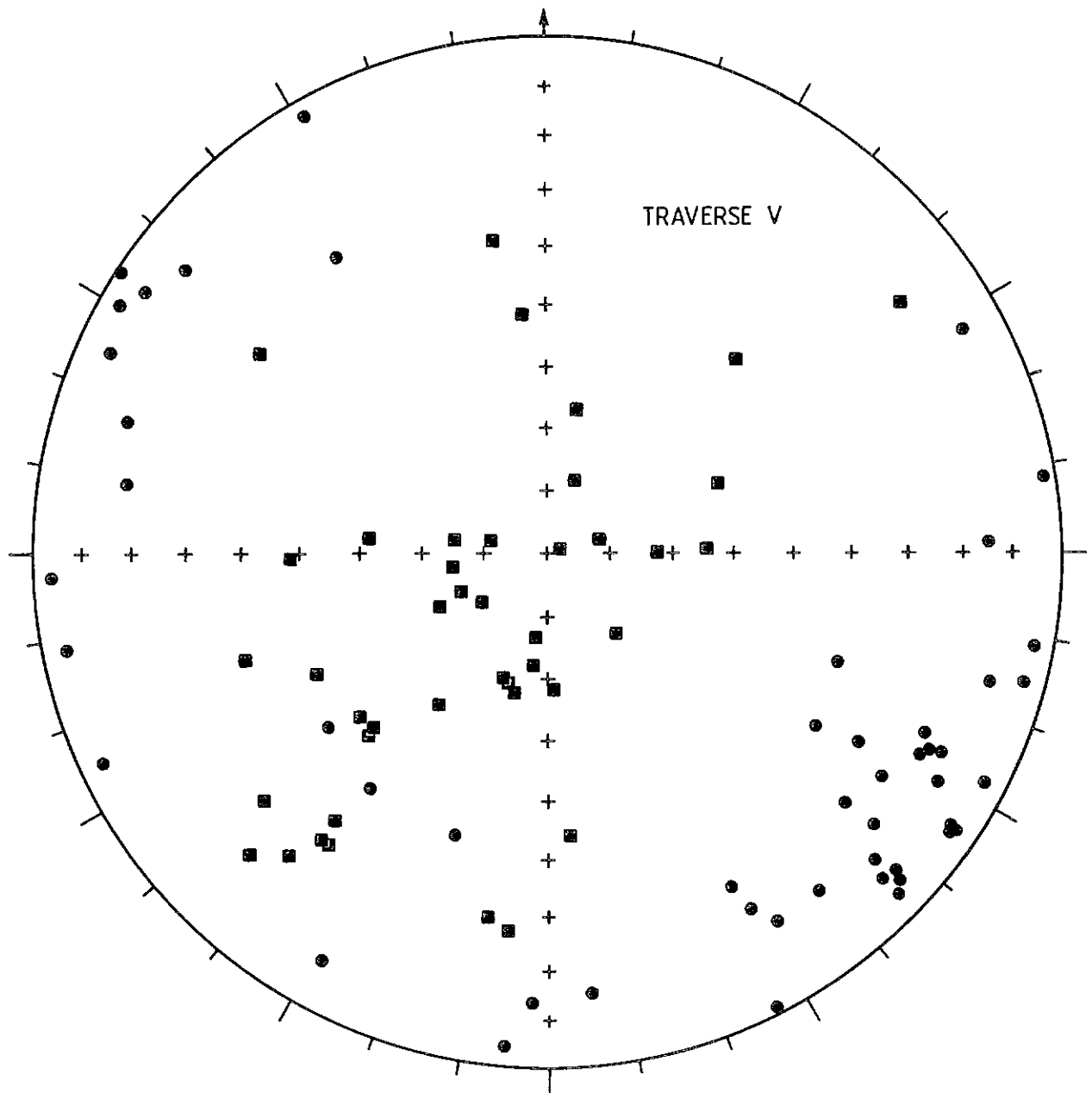


FIG.14

Fig.15. Magnetic fabric of the Traverse VI samples.
Symbols as for Fig.2.

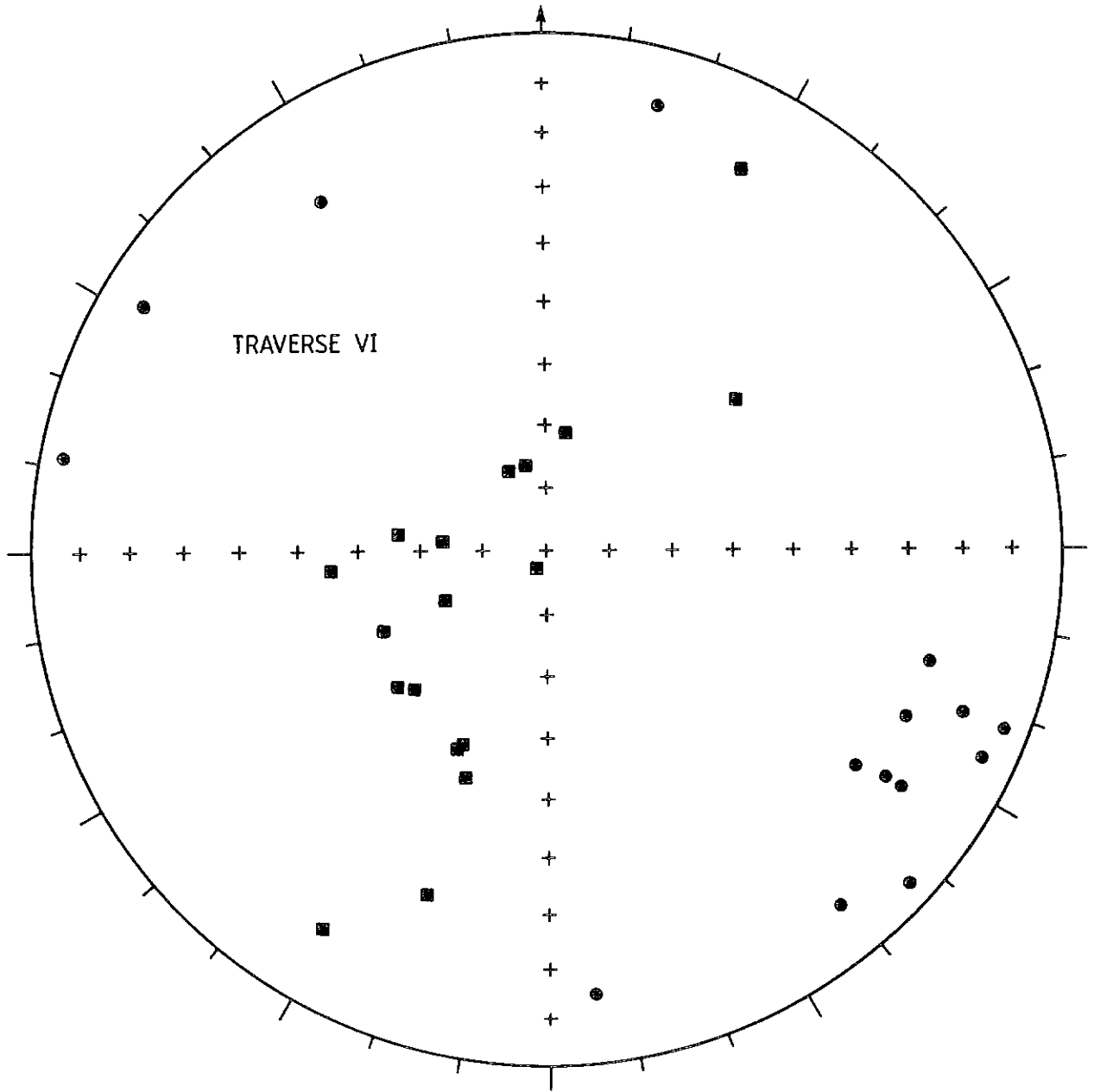


FIG.15

Fig.16. Magnetic fabric of the Traverse VII samples.
Symbols as for Fig.2.

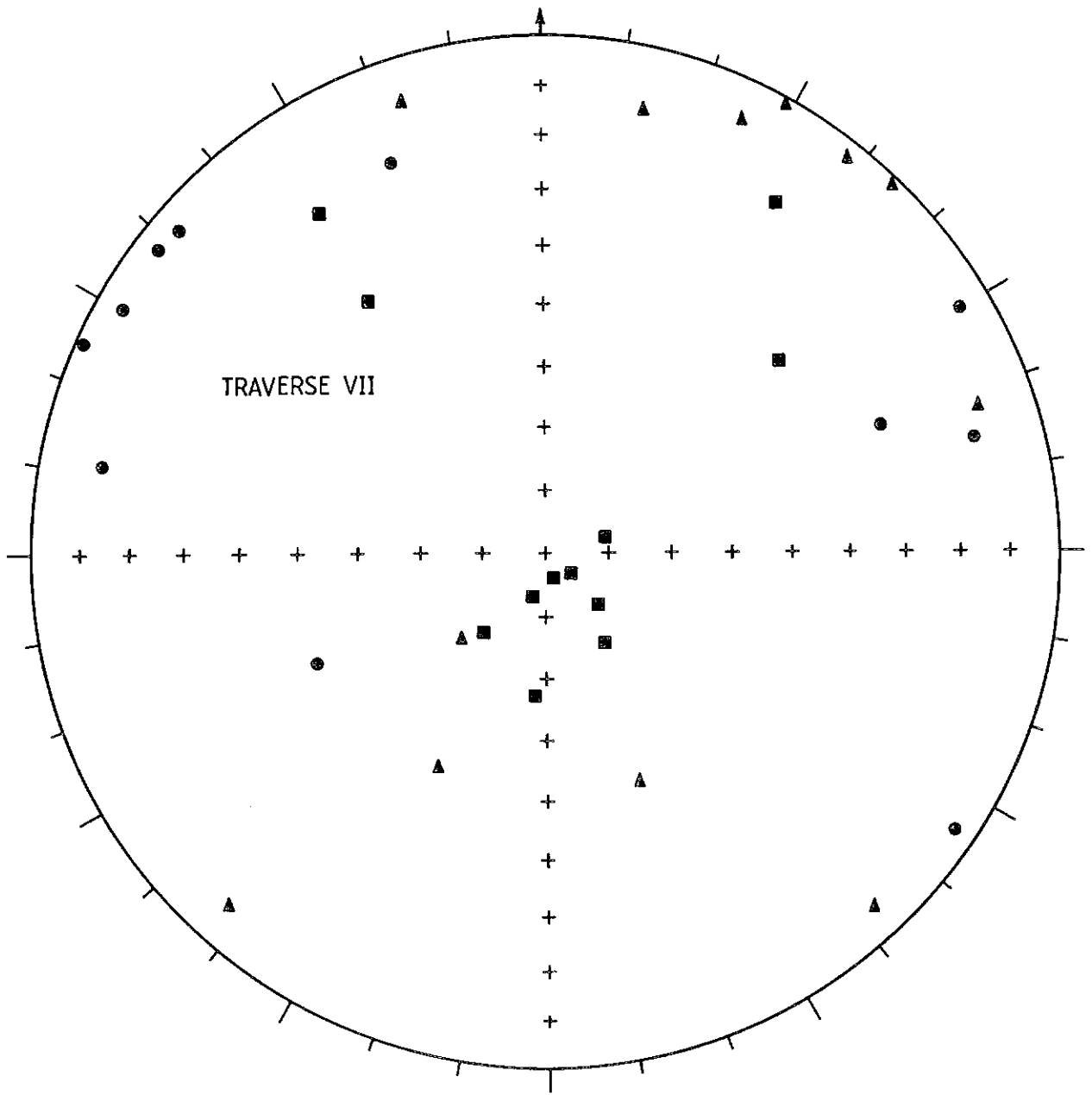
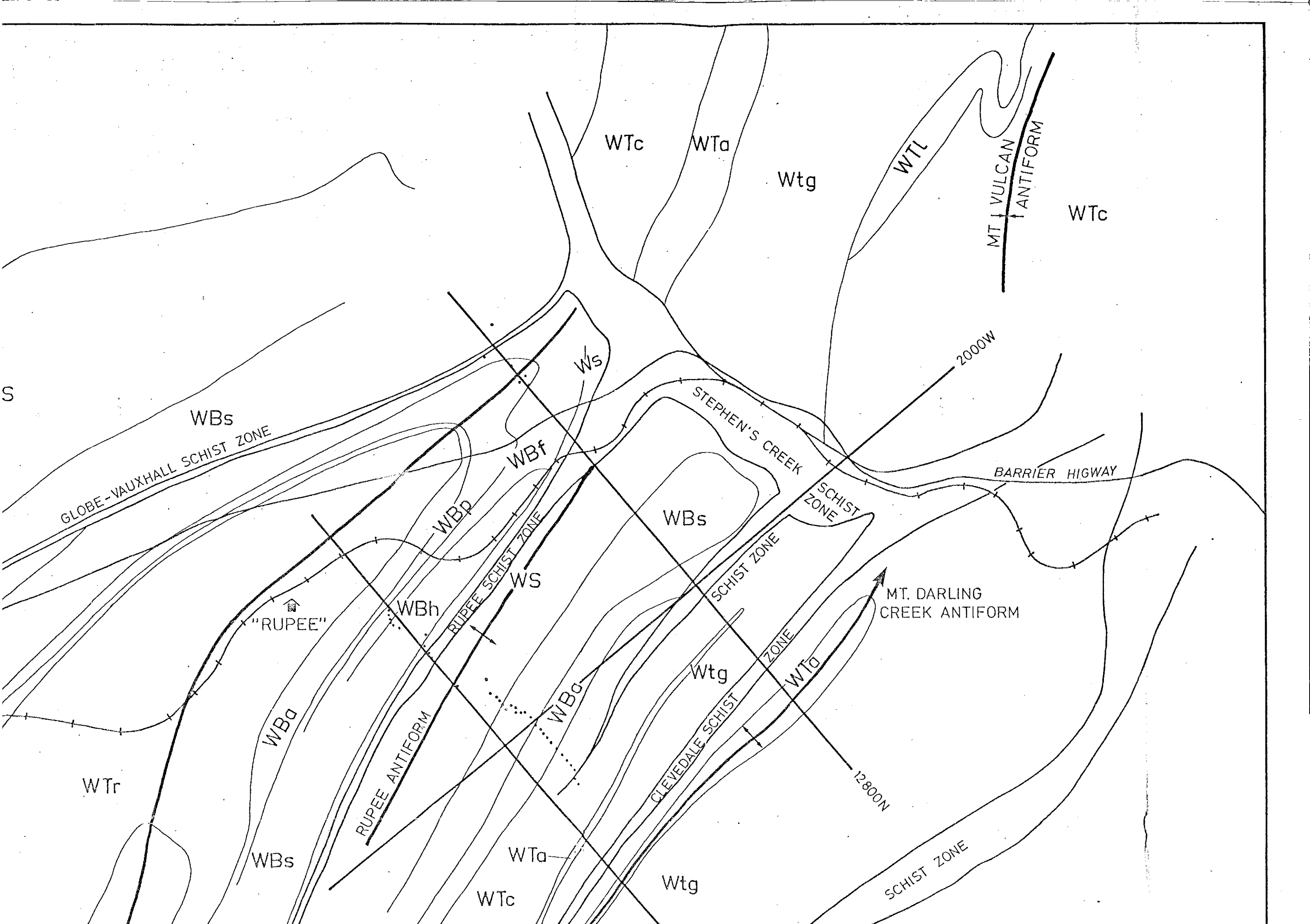
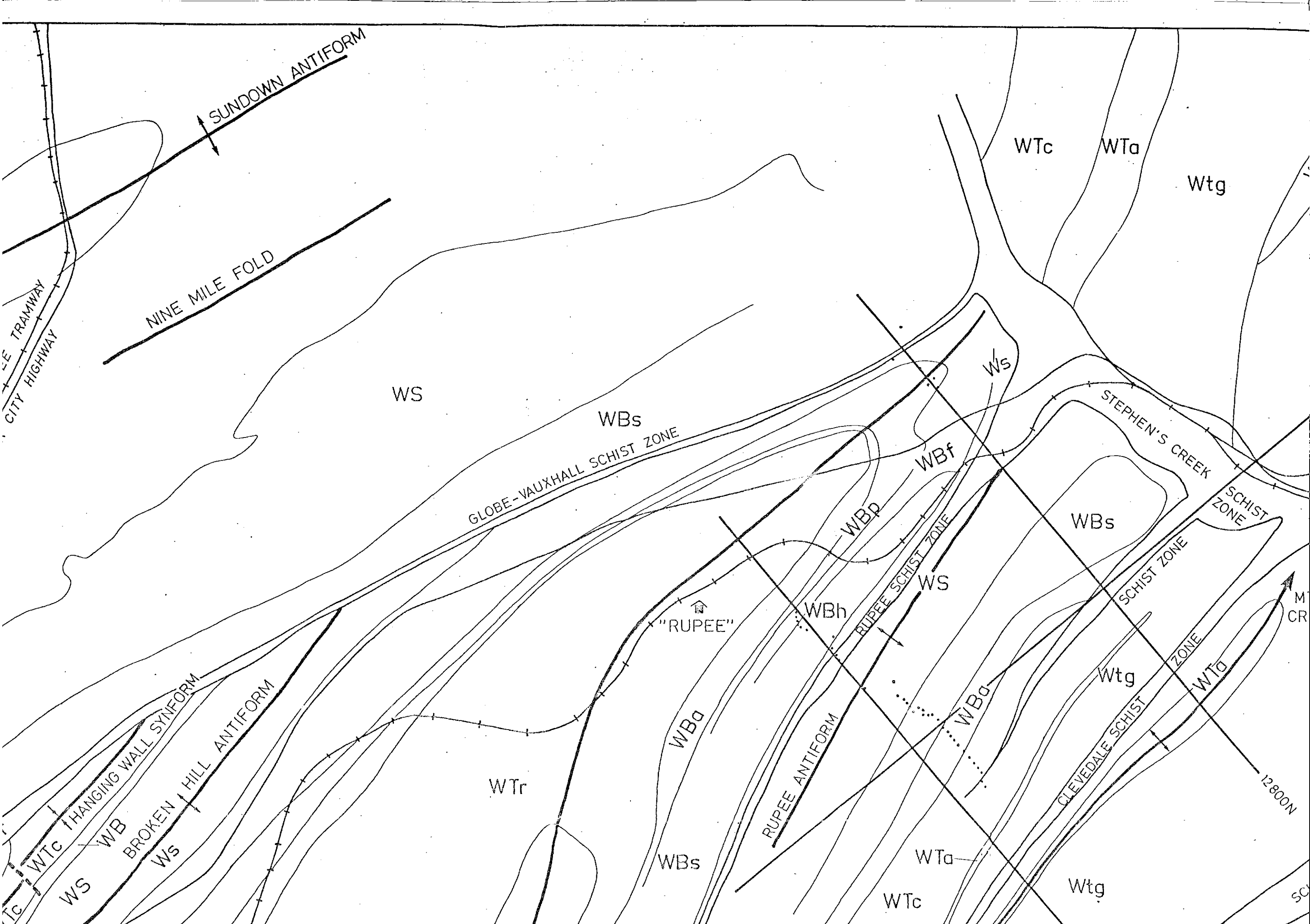
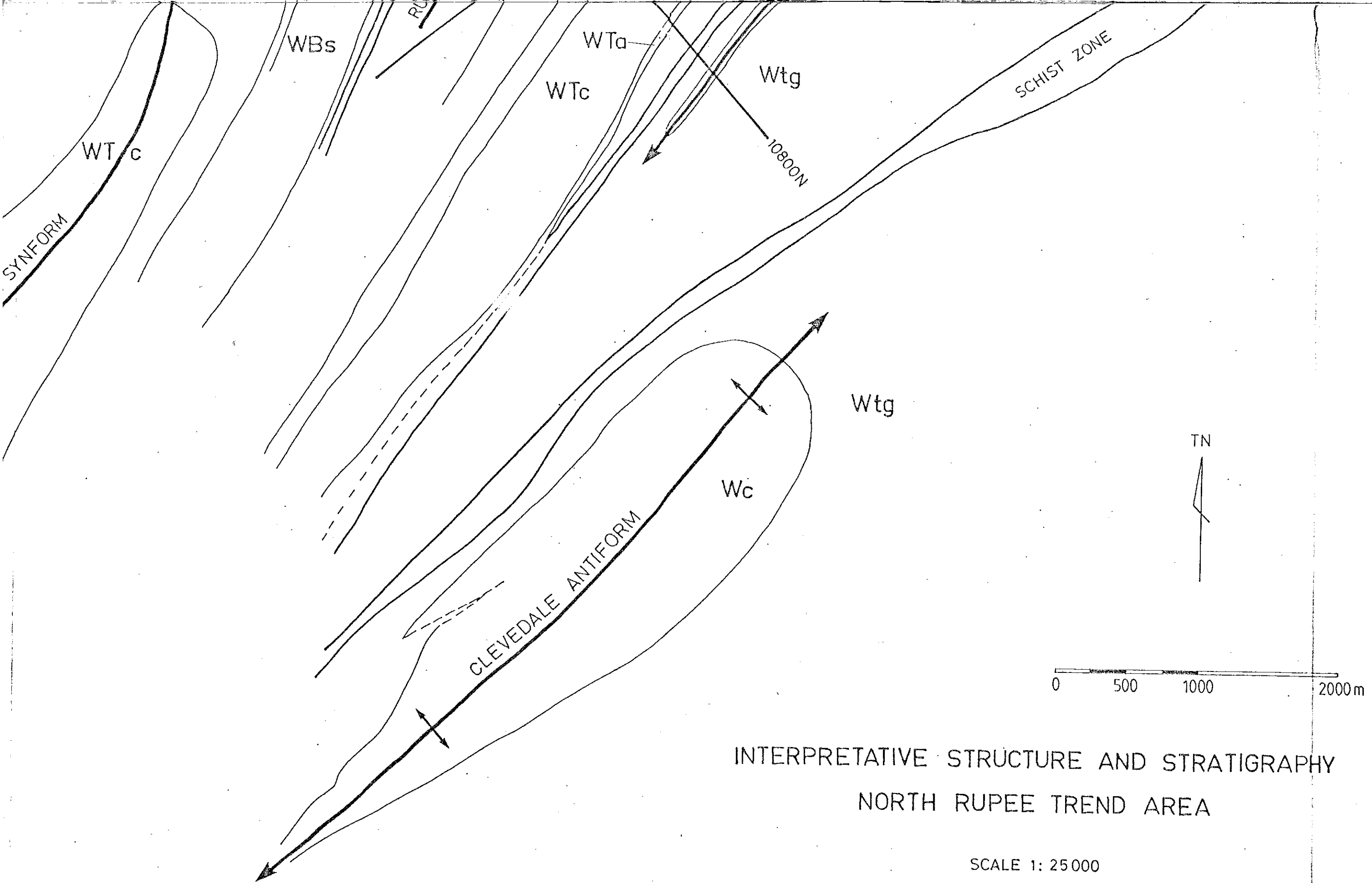


FIG.16

Fig.17. Simplified 1:25000 geology and sampling localities,
northern Rupee Trend area (back pocket).







INTERPRETATIVE STRUCTURE AND STRATIGRAPHY
NORTH RUPEE TREND AREA

SCALE 1: 25 000

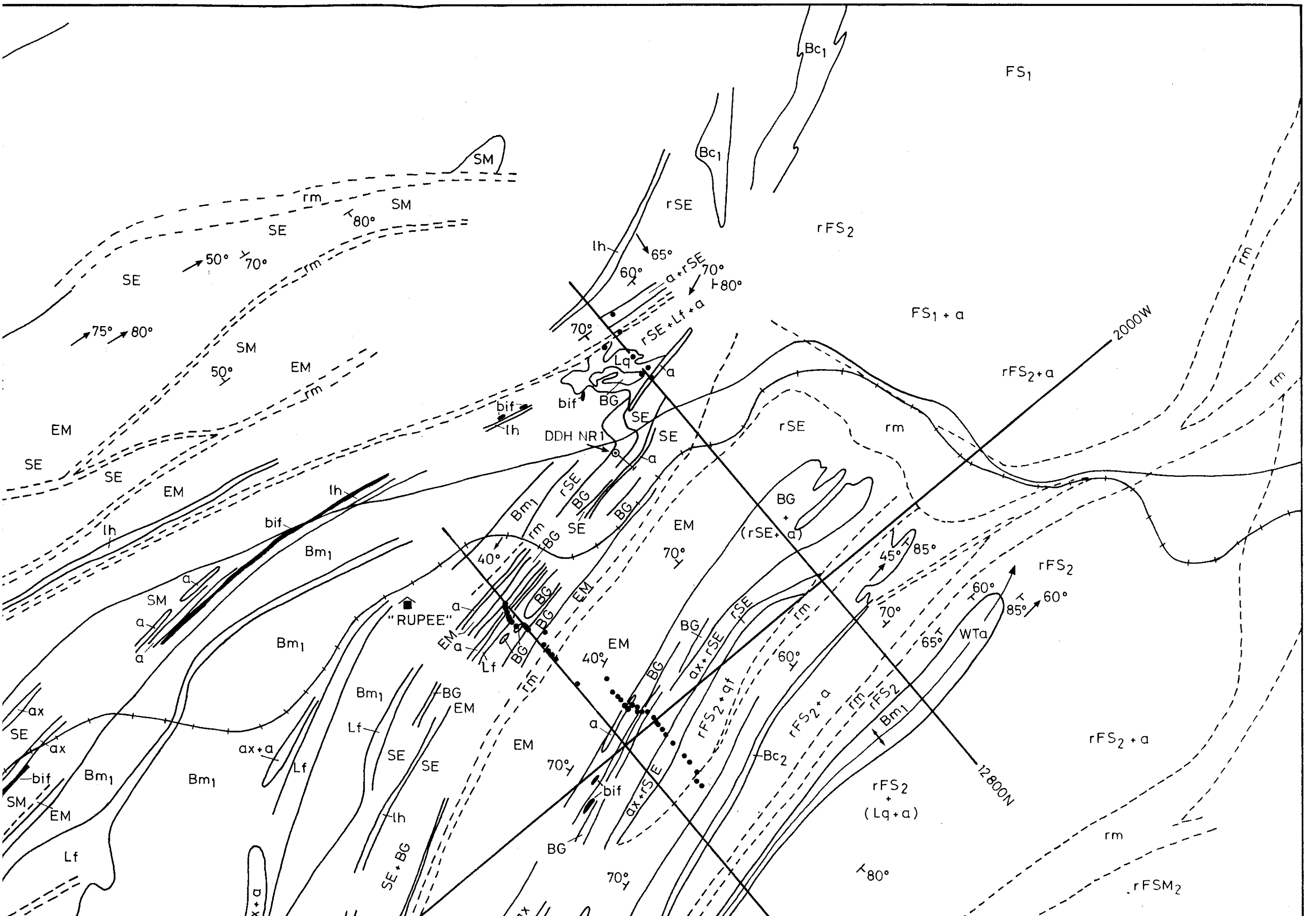


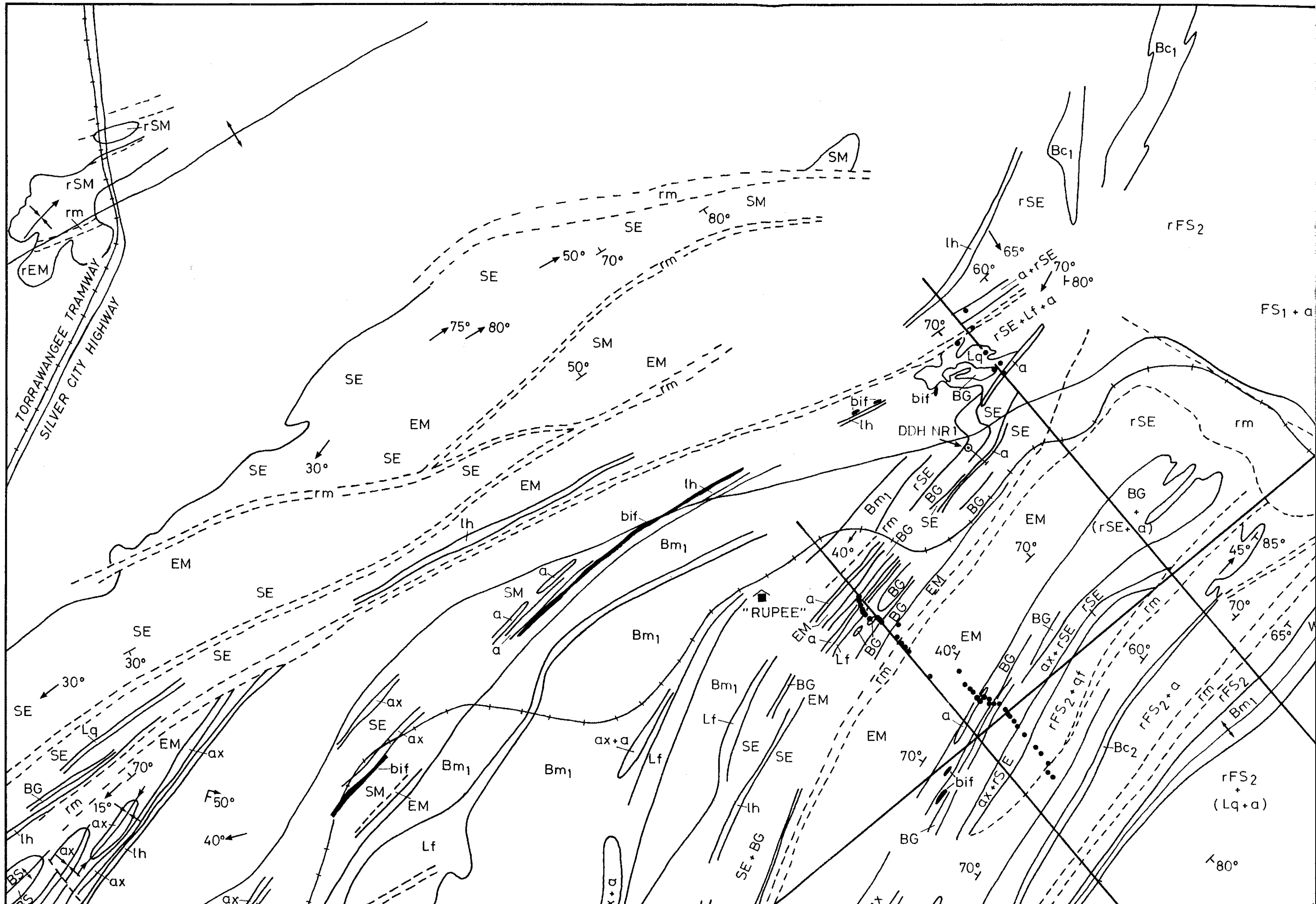
INTERPRETATIVE STRUCTURE

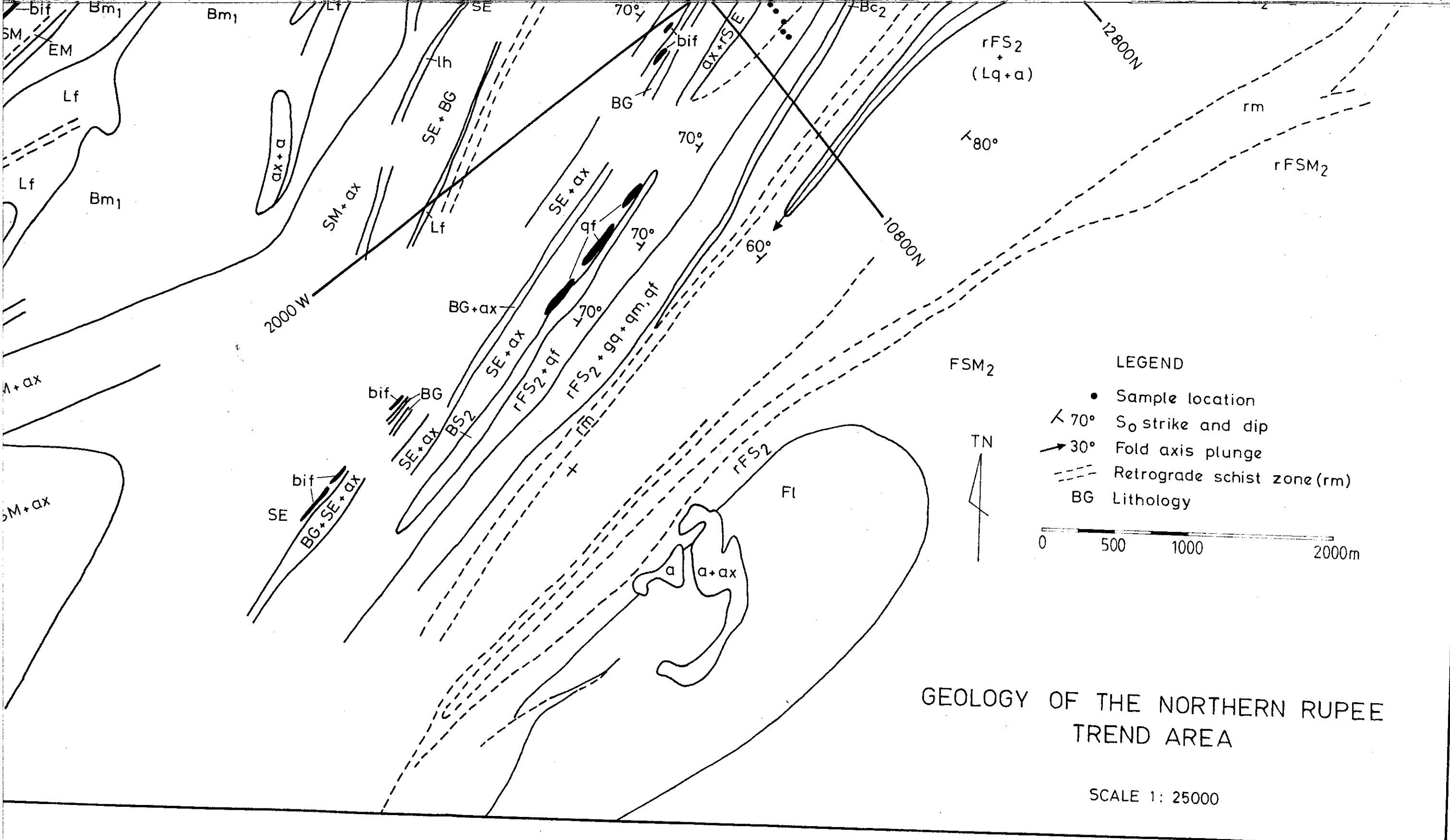
NORTH RUPERT

SCALE

Fig.18. Structural and stratigraphic interpretation, northern
Rupeo Trend area (back pocket).



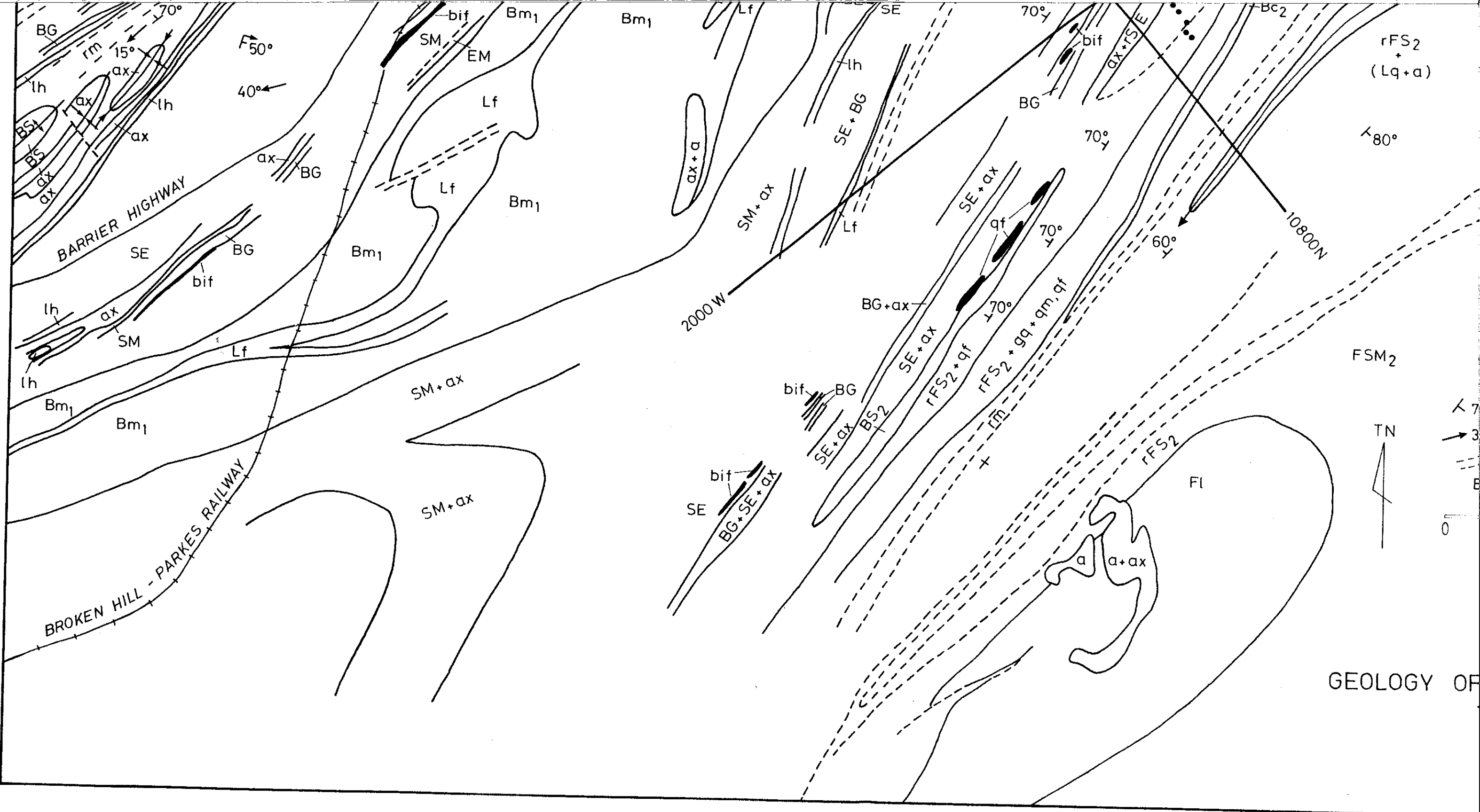




GEOLOGY OF THE NORTHERN RUPEE
TREND AREA

SCALE 1: 25000

13249 m



GEOLOGY OF

Fig.19. Magnetic profile, geology and susceptibility
along Traverse VIII (10800N, Rupee grid).

Fig.20. Magnetic fabric of sites 98-107 (Purnamoota Subgroup),
Traverse VIII. Symbols as for Fig.2.

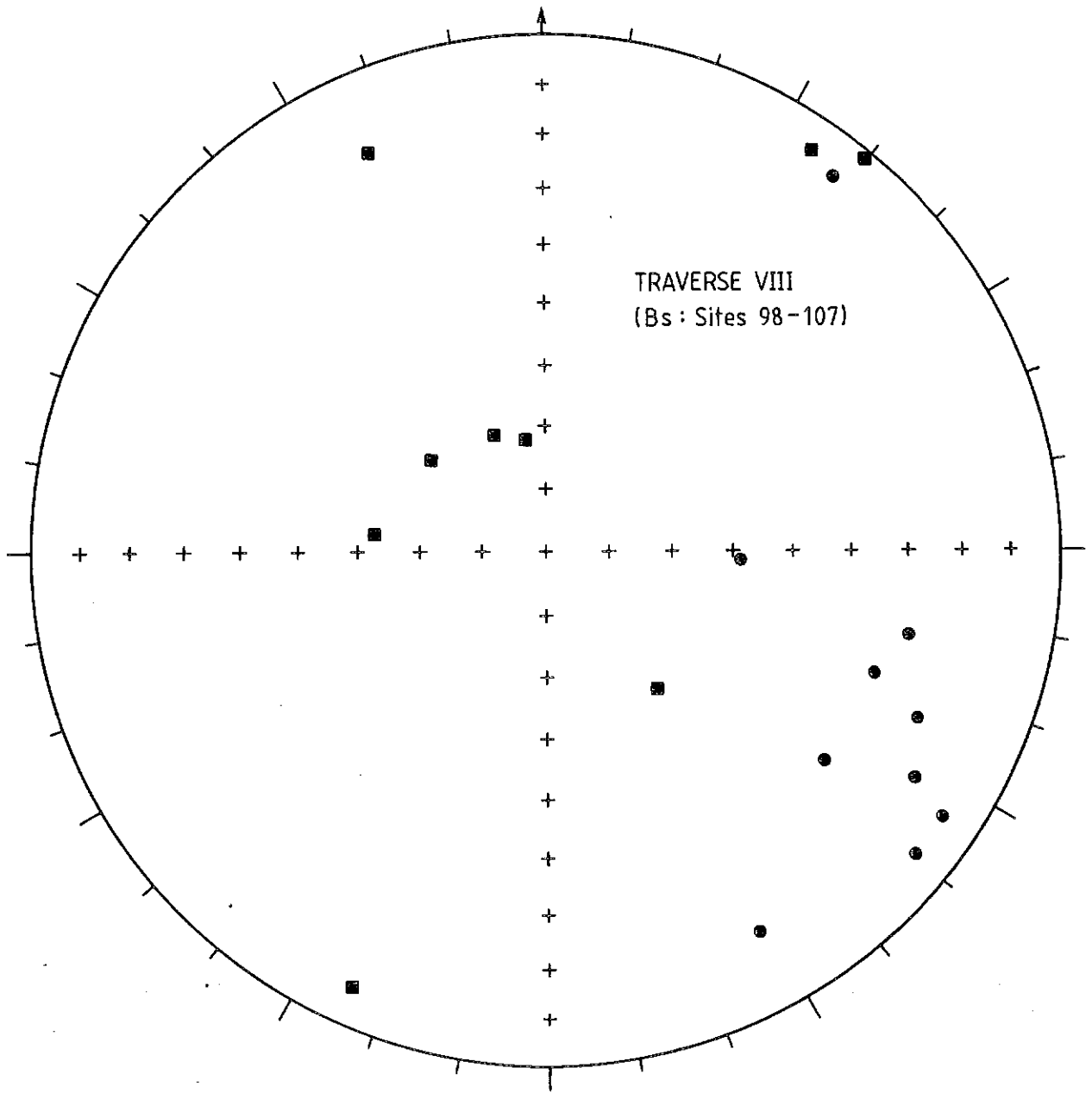


FIG.20

Fig.21. Magnetic fabric of sites 108-117 (Sundown Group),
Traverse VIII. Symbols as for Fig.2.

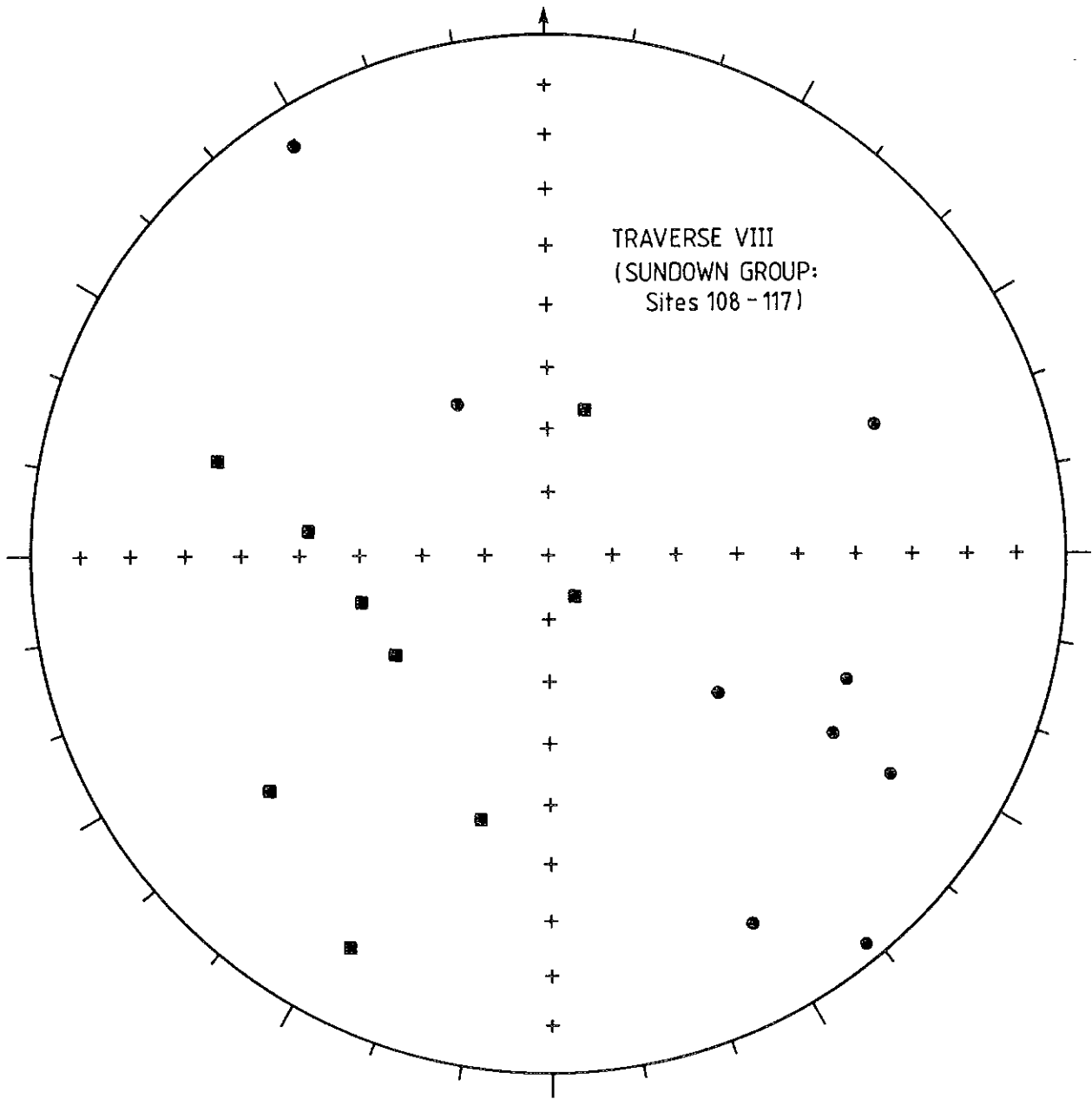


FIG.21

Fig.22. Magnetic fabric of sites 118-130 (Broken Hill Group),
Traverse VIII. Symbols as for Fig.2.

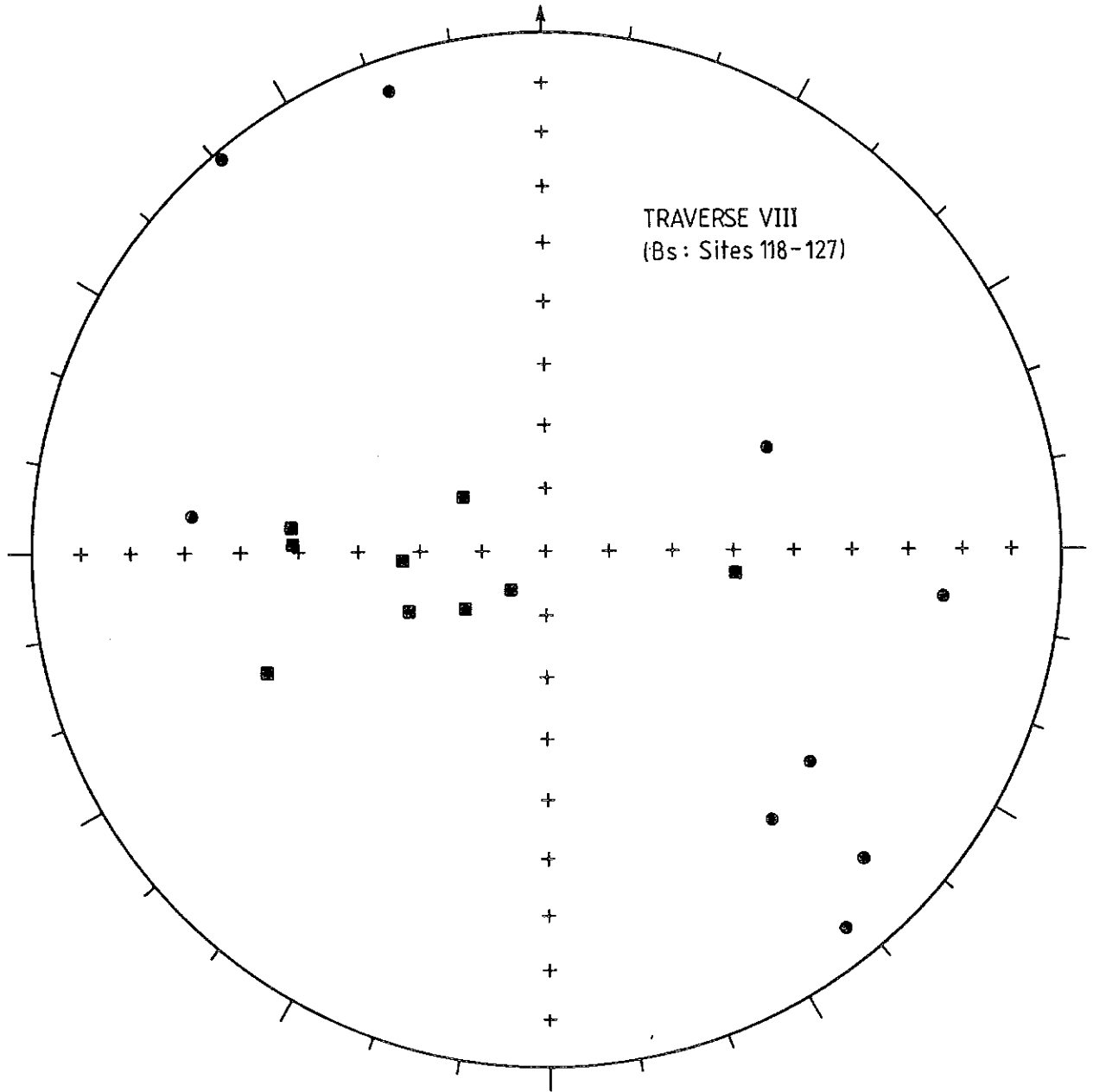


FIG.22

Fig.23. Magnetic fabric of sites 131-135 (Cues Formation),
Traverse VIII. Symbols as for Fig.2.

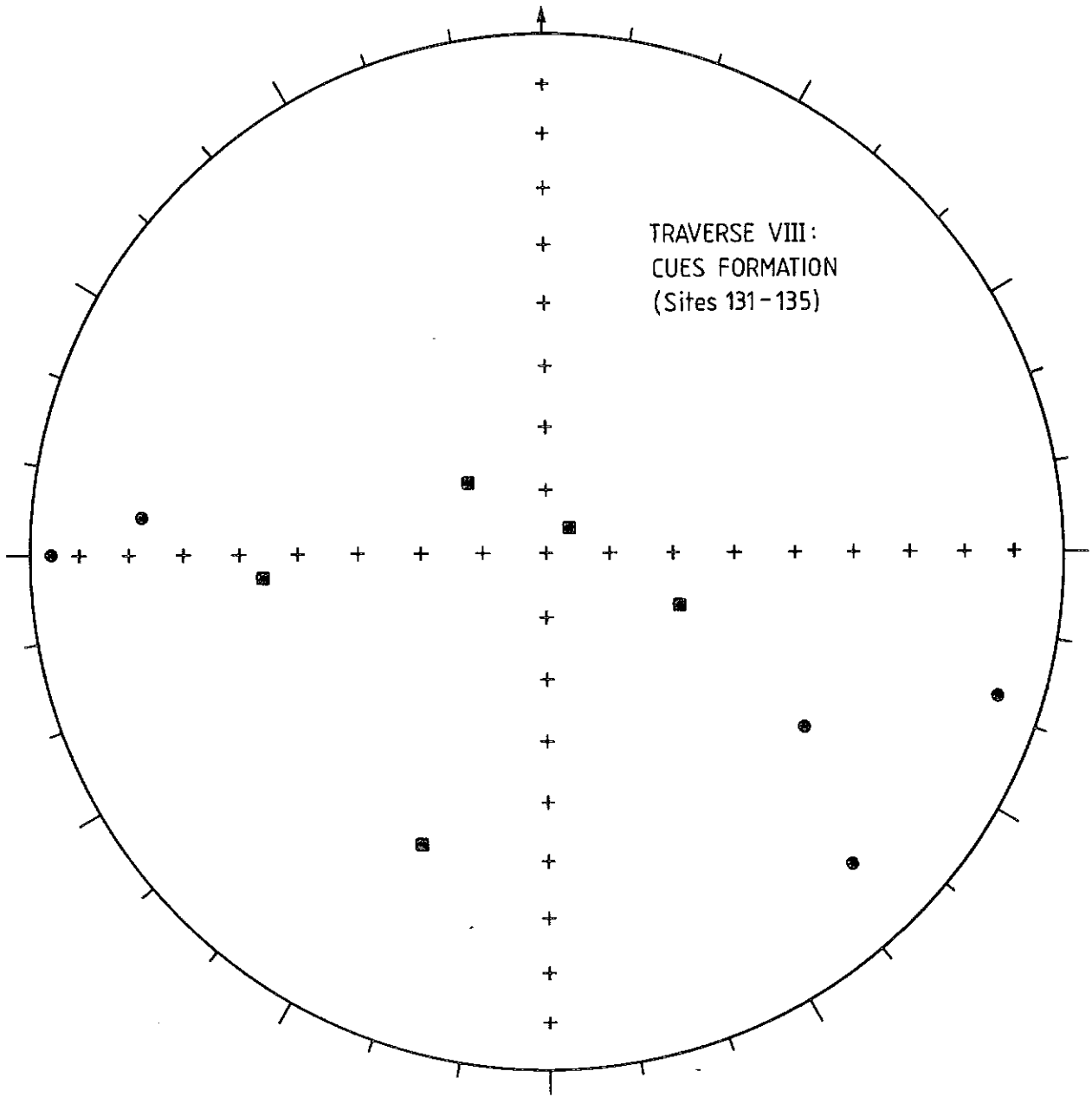


FIG.23

Fig.24. Magnetic stratigraphy of the Rise and Shine
and northern Rupee Trend areas.

MAGNETIC STRATIGRAPHY

RISE AND SHINE

RUPEE TREND

Western Lode

Eastern Lode

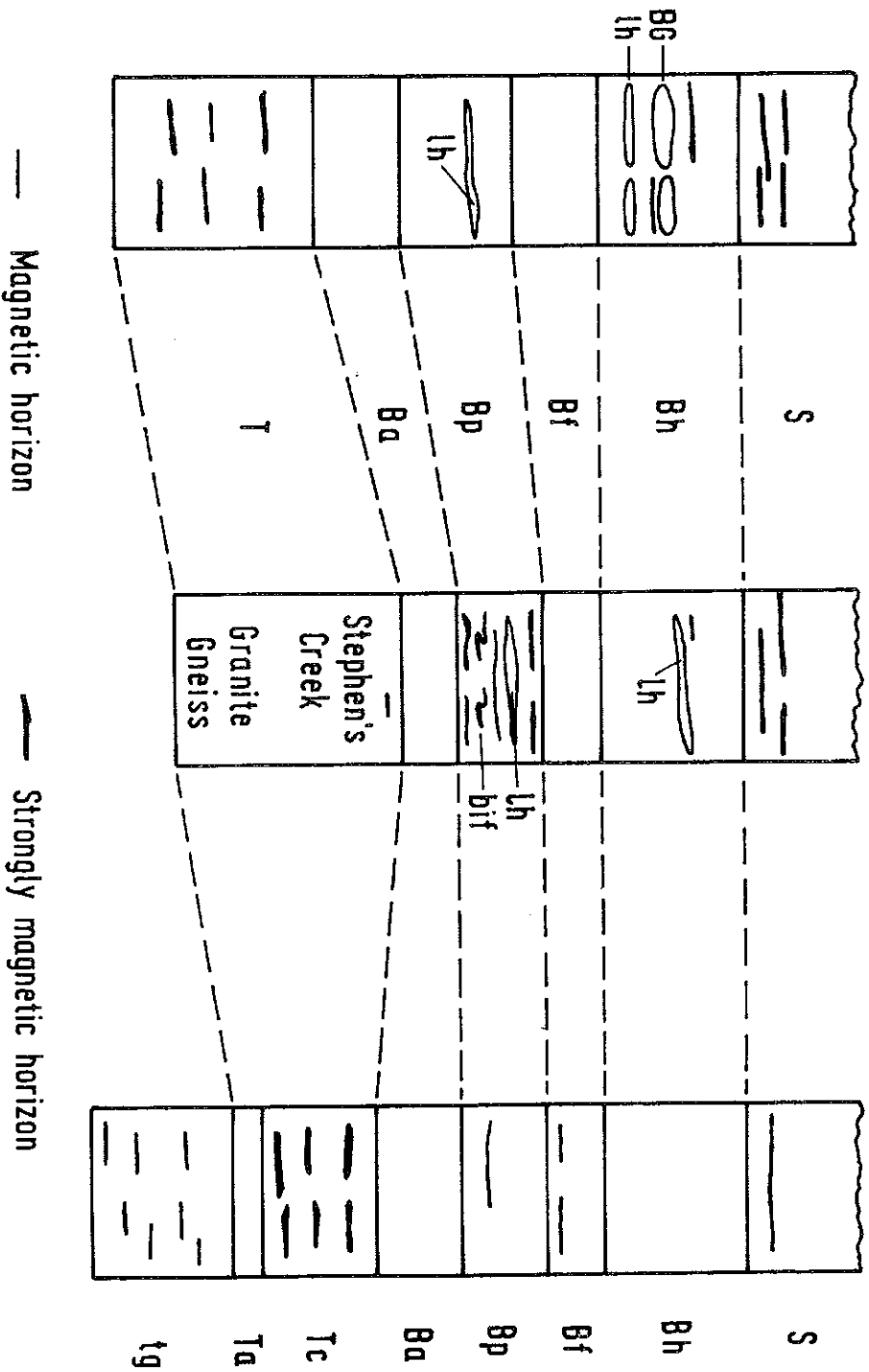


FIG.24